

Lehrstuhl für Phytopathologie  
der Technischen Universität München

## The action of the bacterial effector protein harpin on *Arabidopsis thaliana*

Maren Livaja

Vollständiger Abdruck der von der Fakultät Wissenschaftszentrum Weihenstephan  
für Ernährung, Landnutzung und Umwelt der Technischen Universität München  
zur Erlangung des akademischen Grades eines

Doktors der Naturwissenschaften (Dr. rer. nat.)

genehmigten Dissertation.

Vorsitzender: Univ.-Prof. Dr. Gerhard Wenzel

Prüfer der Dissertation: 1. Priv.-Doz. Dr. Jörg Durner  
2. Univ.-Prof. Dr. Siegfried Scherer

Die Dissertation wurde am 08.08.2005 bei der Technischen Universität München eingereicht und durch die Fakultät Wissenschaftszentrum Weihenstephan für Ernährung, Landnutzung und Umwelt am 23.11. 2005 angenommen.

Parts of this thesis are already published, or publication is in progress, respectively.

**Krause, M.**, and Durner, J.: Harpin inactivates mitochondria in *Arabidopsis* suspension cells. *MPMI* Vol.17, No.2, 2004, pp.131-139

**Livaja, M.**, Zeidler, D., von Rad, U., and Durner, J.: The *Arabidopsis* response to the bacteria-derived PAMPs harpin and lipopolysaccharide (submitted)

**Livaja M.**, and Durner, J.: Genomic, proteomic and metabolomic analyses of harpin-affected mitochondria of *Arabidopsis* (submitted)

## Index

Summary .....	1
I. Animal and plant innate immunity – An introduction .....	2
1. Attack of a pathogen - the type III secretion pathway .....	2
2. Pathogen recognition.....	4
2.1. The gene-for-gene interaction .....	4
2.2. General elicitors – PAMPs.....	4
3. Signaling in innate immunity.....	5
4. Programmed cell death and apoptosis .....	7
5. MLO as modulator of defense and cell death .....	9
6. The harpin experimental system .....	9
7. Aims of the study and research strategy .....	10
II. Results .....	12
1. Effect of harpin on <i>Arabidopsis</i> plants and <i>Arabidopsis</i> suspension cells .....	12
1.1. Recombinant harpin induces cell death in <i>Arabidopsis</i> suspension cells .....	12
1.2. Impact of harpin on plant growth .....	13
1.3. Enhanced resistance to <i>Pseudomonas syringae</i> pv. <i>tomato</i> DC3000.....	14
1.4. Harpin induces the formation of reactive oxygen species and nitric oxide.....	15
2. Mitochondria mediated apoptosis in <i>Arabidopsis</i> suspension cells .....	17
2.1. Mitochondrial formation of reactive oxygen species .....	17
2.2. Decrease of mitochondrial transmembrane potential $\Delta\Psi_m$ .....	17
2.3. Loss of intracellular ATP.....	18
2.4. Respiratory oxygen uptake.....	19
2.5. Induction of alternative oxidase .....	20
2.6. Cytochrome c release from mitochondria .....	21
2.7. Nuclear translocation of cytochrome c.....	22
2.8. Analysis of the mitochondrial transcriptome .....	23
2.9. Analysis of the mitochondrial proteome.....	28
2.10. Activity of citric acid cycle related enzymes.....	31
2.11. Intermediates of the citric acid cycle.....	31
3. The <i>Arabidopsis</i> transcriptome analysis of harpin induced apoptosis .....	33
3.1. Two tiers of innate immune response: The transcriptome in response to harpin and LPS.....	33
3.2. Global changes in transcriptional programs of LPS and harpin treated <i>Arabidopsis</i> .....	33
3.3. Majority of transcription factor genes are expressed in response to harpin.....	35
3.4. Genes involved in cell wall biogenesis and organization .....	37
3.5. Different effects on cell rescue and defense.....	38
3.6. Cellular communication and signal transduction .....	41
3.7. <i>Discussion of the chapter</i> .....	44
4. Studies with <i>Arabidopsis Mlo</i> knockout mutants.....	47
4.1. Induction of transcript accumulation of <i>AtMlo</i> genes and <i>AtMlo</i> co-regulated calmodulin- encoding genes by harpin .....	47
4.2. Infections with the fungus <i>Alternaria alternata</i> .....	49
4.3. Salicylic acid accumulation in <i>Mlo</i> knockout mutants .....	52
4.4. <i>Discussion of the chapter</i> .....	55
5. Uptake and fate of harpin .....	58
III. Discussion .....	60
1. Harpin induces ROS and NO .....	60
2. Decrease of mitochondrial transmembrane potential $\Delta\Psi_m$ and loss of ATP .....	62
3. Cytochrome c release from mitochondria .....	62
4. Alternative respiration through AOX pathway.....	63
5. Induction of genes encoding mitochondrial proteins.....	64
6. Harpin activates mitochondrial enzymes .....	65

\* For a better structure of the text the discussion of chapter 3 and 4 is separated from the general discussion.

IV. Methods .....	69
1. Harpin.....	69
1.1. Preparation of harpin protein.....	69
1.2. Purification by FPLC.....	69
1.3. Fluorescence labeling.....	70
2. Plant material .....	70
2.1. Maintenance of <i>Arabidopsis</i> cell culture and treatment with harpin.....	70
2.2. Growth conditions of <i>Arabidopsis</i> plants and treatment with harpin.....	71
2.3. Fractionation of <i>Arabidopsis</i> suspension cells.....	71
2.4. Preparation of protoplasts .....	73
3. Cell death assay.....	74
4. Nucleic acid based techniques.....	74
4.1. DNA isolation from <i>Alternaria alternata</i> infected plants.....	74
4.2. RNA isolation.....	74
4.3. Semi-quantitative RT-PCR.....	74
5. Microarrays.....	76
5.1. Microarray experiments.....	76
5.2. Target synthesis and array hybridization.....	77
5.3. Data collection, analysis and gene classification.....	78
6. Northern blotting.....	79
6.1. Sample preparation.....	79
6.2. Gel run and RNA transfer.....	79
6.3. Preparation of DIG labeled DNA probes.....	79
6.4. Hybridization, washing and detection.....	80
7. Proteome analysis.....	81
7.1. Protein sample preparation and 2-D gel electrophoresis.....	81
7.2. MALDI-TOF Mass Spectrometry for peptide fingerprint analysis.....	81
8. Western blotting.....	82
8.1. Cytochrome c in cytosolic fractions.....	82
8.2. Cytochrome c in nuclear fractions.....	82
9. Measurement of intracellular ATP.....	83
10. Determination of mitochondrial transmembrane potential $\Delta\psi_m$ .....	83
11. Respiratory oxygen uptake.....	83
12. Activity of tricarboxylic acid cycle enzymes.....	83
12.1. Citrate synthase.....	84
12.2. Aconitase.....	84
12.3. Isocitrate dehydrogenase.....	85
12.4. Fumarase.....	85
12.5. Malate dehydrogenase.....	85
13. Quantification of tricarboxylic acid cycle metabolites.....	86
13.1. Citrate.....	86
13.2. Isocitrate.....	87
13.3. 2-oxoglutarate.....	87
13.4. Malate.....	87
13.5. Oxaloacetate.....	88
14. Fluorescence microscopy.....	88
15. Fluorescence microscopy immunolabeling.....	89
16. NO and ROS quantification.....	89
17. Determination of Salicylic acid content.....	89
18. Studies with pathogens.....	90
18.1. <i>Alternaria alternata</i> .....	90
18.2. <i>Pseudomonas syringae</i> pv. <i>tomato</i> DC3000.....	91
V. Materials.....	93
1. Plant materials.....	93
2. Bacteria and fungi.....	93
3. Chemicals.....	93
4. Molecular biological reagents, enzymes and kits.....	95
5. Consumables.....	96
6. Buffers, solutions and media.....	97

## Abbreviations

aa-dUTP	Aminoallyl labeled Deoxyuridine triphosphate
abs	Absorbance
ADP	Adenosine diphosphate
AOX	Alternative oxidase
ATP	Adenosine triphosphate
BIOP	Institute for Biochemical Plant Pathology
BSA	Bovine serum albumin
c	Concentration
cDNA	Complementary DNA
CDPK	Calcium-dependent protein kinase
cfu	Colony forming units
CL	Citrate lyase
cm	Centimeter
cm <sup>2</sup>	Square centimeter
CoASH	Coenzyme A
CV	Column Volume
d	Deposit thickness
DIG	Digoxygenin
DNA	Deoxyribonucleic acid
dNTP	Deoxyribonucleoside triphosphate
dsDNA	Double-stranded DNA
ETC	Electron transport chain
ε	Extinction coefficient
F	Fluorescence
FITC	Fluorescein isothiocyanate
FPLC	Fast protein liquid chromatography
g	Gram
g	Gravitation constant
GIDH	Glutamate dehydrogenase
h	Hours
HPLC	High-performance liquid chromatography
HR	Hypersensitive response
HSP	Heat shock protein
ICDH	Isocitrate dehydrogenase
IEF	Isoelectric focusing
kDa	Kilodalton
KVh	Kilovolt hour
LDH	Lactate dehydrogenase
ln	Natural logarithm
LPS	Lipopolysaccharide
M	Molar
mA	Milliampere
MALDI-TOF	Matrix-assisted laser desorption/ionization time of flight mass spectrometry
MAPK	Mitogen-activated protein kinase
MAPKK	Mitogen-activated protein kinase kinase
MAPKKK	Mitogen-activated protein kinase kinase kinase

MDH	Malate dehydrogenase
mg	Milligram
min	Minute
MJ	Methyl jasmonate
ml	Milliliter
mm	Millimeter
mM	Millimolar
µg	Microgram
µl	Microliter
µm	Micrometer
µmol	Micromol
N	Normal
NAD	Nicotinamide adenine dinucleotide
NADH	Nicotinamide adenine dinucleotide, reduced form
NADP	Nicotinamide adenine dinucleotide phosphate
NADPH	Nicotinamide adenine dinucleotide phosphate, reduced form
NBT	Nitroblue tetrazolium
ng	Nanogram
NL	Netherlands
nm	Nanometer
NO	Nitric Oxide
OADC	Oxaloacetate decarboxylase
ORF	Open reading frame
PAMPs	Pathogen-associated molecular patterns
PCD	Programmed cell death
PCR	Polymerase chain reaction
pg	Picogram
pH	Potential of hydrogen
pI	Isoelectric point
PTP	Permeability transition pore
RLK	Receptor like kinase
RNA	Ribonucleic acid
ROS	Reactive oxygen species
rpm	Rounds per minute
RT-PCR	Reverse transcriptase polymerase chain reaction
SA	Salicylic acid
SAR	Systemic acquired resistance
SD	Standard deviation
sec	Second
sHSP	Small heat shock protein
SOD	Superoxide dismutase
TCA	Tricarboxylic acid
TMV	Tobacco mosaic virus
U	Unit
UV	Ultra violet light
V	Volume
v/v	Volume per volume
w/v	Weight per volume

## Figures

Figure 1: Protein secretion systems in Gram-negative bacteria. ....	3
Figure 2: Signaling cascade in innate immunity of insects, mammals, and plants.....	6
Figure 3: Major molecular events leading to apoptosis in animal cells. ....	8
Figure 4: Time course study of harpin-induced cell death and pH.....	12
Figure 5: Effect of harpin treatment on <i>Arabidopsis</i> plant growth. ....	13
Figure 6: Harpin causes enhanced disease resistance against <i>Pst</i> DC3000. ....	14
Figure 7: Timecourse analysis of ROS and NO generation in <i>Arabidopsis</i> suspension cells. ....	15
Figure 8: Fluorescence staining for NO and ROS detection in <i>Arabidopsis</i> suspension cells. ....	16
Figure 9: Cytological detection of mitochondrial ROS. ....	17
Figure 10: Implication of harpin on mitochondrial transmembrane potential $\Delta\Psi_m$ . ....	18
Figure 11: ATP levels in <i>Arabidopsis</i> suspension cells after exposure to 50 $\mu\text{g/ml}$ harpin. ....	19
Figure 12: Respiratory $\text{O}_2$ uptake of isolated mitochondria after harpin treatment. ....	20
Figure 13: AOX1a gene expression in <i>Arabidopsis thaliana</i> suspension cells. ....	21
Figure 14: Cytochrome c release from mitochondria in response to harpin treatment.....	22
Figure 15: Harpin induces nuclear translocation of cytochrome c. ....	23
Figure 16: Changes in transcript accumulation of genes encoding mitochondrial proteins in <i>Arabidopsis</i> . ....	23
Figure 17: Comparison of mitochondrial and global gene expression dynamics during harpin treatment. ....	24
Figure 18: Transcript abundance of genes encoding proteins of the citric acid cycle. ....	25
Figure 19: Induction of genes encoding proteins of the electron transport chain and oxidative phosphorylation. ....	26
Figure 20: Two-dimensional separations of mitochondrial fractions from <i>Arabidopsis thaliana</i> . ....	29
Figure 21: Enzyme activity in <i>Arabidopsis</i> mitochondria after harpin stress. ....	31
Figure 22: Levels of TCA metabolites in <i>Arabidopsis</i> cell extracts during harpin treatment. ....	32
Figure 23: Gene expression in functional categories after LPS and harpin treatment. ....	34
Figure 24: Expression patterns of six important transcription factor families regulated by LPS and harpin. ....	36
Figure 25: Clustering of <i>Arabidopsis</i> gene expression after treatment with LPS and harpin. ....	38
Figure 26: Heat shock protein gene expression in <i>Arabidopsis</i> after LPS and harpin treatment. ....	40
Figure 27: Harpin induces <i>AtMlo</i> gene induction in <i>Arabidopsis thaliana</i> . ....	47
Figure 28: <i>Arabidopsis</i> leaf inoculation with <i>Alternaria alternata</i> . ....	49
Figure 29: Macroscopic symptoms on plants infected with <i>Alternaria alternata</i> . ....	50
Figure 30: Quantification of fungal DNA in pathogen-challenged <i>Arabidopsis</i> wild-type and <i>AtMlo</i> mutant plants.....	51
Figure 31: Accumulation of free salicylic acid in <i>Arabidopsis</i> plants after harpin treatment.....	52
Figure 32: Accumulation of conjugated SA in <i>Arabidopsis</i> plants after harpin treatment.....	53
Figure 33: Salicylic acid accumulation in untreated <i>Atmlo</i> mutants. ....	54

Figure 34: Time course analysis of constitutive SA accumulation in untreated <i>mlo2-6-12</i> mutants.....	54
Figure 35: Cytological detection of fluorescence labeled harpin protein.....	58
Figure 36: Fluorescence microscopy immunolabeling of harpin in <i>Arabidopsis</i> leaves.....	58
Figure 37: Immunodetection of harpin in <i>Arabidopsis</i> leaves.....	59
Figure 38: Relative timing of mitochondria-associated parameters after harpin treatment.....	64
Figure 39: Overview of mitochondrial events in harpin induced PCD.....	68

## Tables

Table 1: Transcriptional analysis of mitochondrial carrier proteins in <i>Arabidopsis thaliana</i> .....	27
Table 2: Transcriptional analysis of the mitochondrial protein import apparatus.....	28
Table 3: Identification of 2-D separated proteins from <i>Arabidopsis</i> mitochondria.....	30
Table 4: Comparison of already known LPS and harpin caused events in plants.....	33
Table 5: Summary of LPS and harpin induced transcription factor genes.....	35
Table 6: Comparison of AtWRKY genes differentially regulated during different stress treatments in <i>Arabidopsis</i> .....	37
Table 7: Transcriptional analysis of genes associated with ROS generation and/or redox-balance...	39
Table 8: Receptor-like kinases (subfamilies) induced by the treatment with LPS or harpin.....	41
Table 9: Transcriptional analysis of genes involved in cellular communication and signaling.....	43
Table 10: AtMlo gene induction after harpin treatment.....	47
Table 11: Agilent Arabidopsis 2.0 microarray analysis of calmodulin and calmodulin-related transcripts.....	48



## Summary

The presented thesis is concerned with plant defense responses to harpin from *Pseudomonas syringae* pv. *syringae* that can elicit the hypersensitive response (HR) in plants. In nature, harpin protein secreted by *Erwinia* spp., and *Pseudomonas* spp. via type III secretion system causes fire blight in apples and pears as well as soft-rot that affect a wide range of plants including several economically important crops.

The aim of this work was to identify and characterize molecular components of the activation of natural defense mechanisms induced by harpin in *Arabidopsis thaliana*, and to gain insights in immune responses that are analogous to that in animals.

Given the importance of mitochondria in the mediation and regulation of programmed cell death (PCD) in animal systems, the effect of harpin from *Pseudomonas syringae* on mitochondrial functions in *Arabidopsis* suspension cells was investigated in detail. Fluorescence microscopy studies suggested a co-localization of mitochondria and generation of reactive oxygen species (ROS). Among the early responses a decrease of the mitochondrial membrane potential  $\Delta\Psi_m$  and as a direct consequence a decline of ATP pool size, were observed. Moreover, treatment of *Arabidopsis* cells with harpin induced a rapid cytochrome c release from mitochondria into the cytosol and a partially nuclear translocation of the cytochrome c, which is regarded as a hallmark of PCD or apoptosis in animals. Northern and DNA array analyses showed strong induction of protecting and/or scavenging systems such as alternative oxidase (AOX) and small heat shock proteins, components that are known to be associated with cytochrome c decay.

Transcriptional profiling of *Arabidopsis* genes behind harpin and LPS induced defense responses revealed some interesting parallels, such as high similar pattern of induced genes associated with cell rescue and general stress responses. Harpin and LPS induced an overlapping array of genes involved in cell wall biogenesis and strengthening, cellular communication and signaling. In contrast, a remarkably difference was observed regarding some of the most prominent, central components of plant defense such as WRKY transcription factors, receptor kinases, and oxidative burst-associated genes, whose expression became apparent only after treatment with harpin.

The influence of harpin on transcript abundance of genes encoding mitochondrial proteins revealed a total of 199 transcripts that changed significantly during harpin treatment. It mainly concerned genes encoding mitochondrial proteins associated with metabolism, with transport mechanisms such as mitochondrial protein import apparatus, and with energy budget affecting processes like electron transport chain and citric acid cycle. The effect of harpin on all citric acid cycle related enzyme complexes was partially recovered at proteomic and metabolomic level, and confirmed by studying the activities of appropriate enzymes.

In sum, the presented work demonstrates that *Arabidopsis thaliana* possess a cell death pathway that is activated by the bacterial effector protein harpin and mediated dependently on mitochondria. There is strong evidence that, despite the differences, plants and animals share conserved mechanisms during the PCD process.

## I. Animal and plant innate immunity – An introduction

Different cellular structures and lifestyles of animals and plants would suggest that very different strategies for defense responses would have emerged during evolution. But have they? Obviously, plants do not possess the principle of somatic gene rearrangement, and they do not dispose of specialized defense cells as animals do. It is also true that plants survive in a hostile environment, defending themselves effectively against all kinds of attacking pathogens.

A surprising implication of researches in animal and plant diseases was the discovery of pathogens that can attack both, plants and animals. Examples for these cross-kingdom pathogens are *Erwinia* spp., which cause a variety of wilt diseases in plants such as bacterial fire blight on apple and pears, and have been isolated from wounds and abscesses in mammalian too. *Burkholderia cepacia*, the causal agent of soft rot in onion, can cause life-threatening infections in immuno-compromised and Cystic Fibrosis patients. The probably best-studied cross-kingdom pathogen is *Pseudomonas aeruginosa* which has been shown to cause disease in hosts as mammals, insects, amoeba, worms, fungi, and plants (Guttman, 2004).

Long time the immune system of animals has been considered as unique and complete different from anything found in plants. However, beside the strong and real differences, in recent studies a series of similarities between the innate immune response of plants and animals was discovered. Innate immunity constitutes the first line of defense against a pathogen attack. Like animals, plants possess an innate immune system enable them to recognize pathogen-associated molecular patterns (PAMPs). Striking similarities were found regarding the molecular mode of PAMP-perception in both kingdoms. This includes the disclosure of plant receptors akin to mammalian Toll-like receptors or leucine-rich repeat (LRR) proteins. Furthermore, animals and plants common share molecular building blocks of PAMP-induced signaling cascades leading to the transcriptional activation of immune response genes. Nitric oxide (NO) as well as mitogen-activated protein kinase (MAPK) cascade has been implicated in triggering innate immunity responses (Nurnberger et al., 2004).

The following chapters will endeavor to highlight the current state of innate immunity research in plants, to accent the similarities between the molecular organization of animal and plant systems for pathogen perception and defense, and clarify the aim of this work.

### 1. Attack of a pathogen - the type III secretion pathway

Bacterial pathogens of animals and plants have evolved elaborate strategies to infect and colonize their eukaryotic hosts. Under appropriate environmental conditions, plant pathogenic bacteria enter the leaf mesophyll tissue through natural stomatal openings, hydathodes, or wounds, thus making their first contact with internal host cells. Phytopathogenic bacteria multiply in the intercellular spaces (apoplast) and remain extracellular. This is in contrast to many animal bacterial pathogens that gain entry into their host cells and then multiply intracellularly. Bacterial colonization of a host often depends on extracellular proteins which are active transported across the bacterial membranes (Staskawicz et al., 2001). Up to now, six major protein secretion systems were identified (Fig. 1).

Three classes of secretion systems, the type I, type III, and the type IV, have been implicated in virulence, and are widely distributed and highly conserved among pathogens of plants and humans (Guttman, 2004). Gram-negative bacteria use different protein secretion systems to transport proteins across the inner and outer membrane. Many gram-negative pathogenic bacteria are secreted and translocated directly across the eukaryotic cell membrane into the host cell cytosol where they can interfere with cellular processes and suppress host defenses. Bacterial proteins that are delivered by a type III secretion system presumably pass through the eukaryotic cell membrane via a proteinaceous transmembrane channel known as type III secretion translocon, which is of bacterial origin. This specialized protein secretion system is required for pathogenesis in a wide range of human pathogens (e.g. *Escherichia coli*, *Pseudomonas aeruginosa*, *Salmonella enterica*, *Shigella* spp., and *Yersinia* spp.) and plant pathogens (e.g. *Pseudomonas syringae*, *Xanthomonas* spp., and *Erwinia* spp.). The type III secretion system is a complex apparatus that spans both bacterial membranes and is associated with an extracellular filamentous structure. It is encoded by at least 20 genes, many of which are highly conserved among both plant and human pathogens. These genes are typically clustered in a so called pathogenicity island on the bacterial genome or an accessory plasmid (Buttner and Bonas, 2002a; Guttman, 2004).

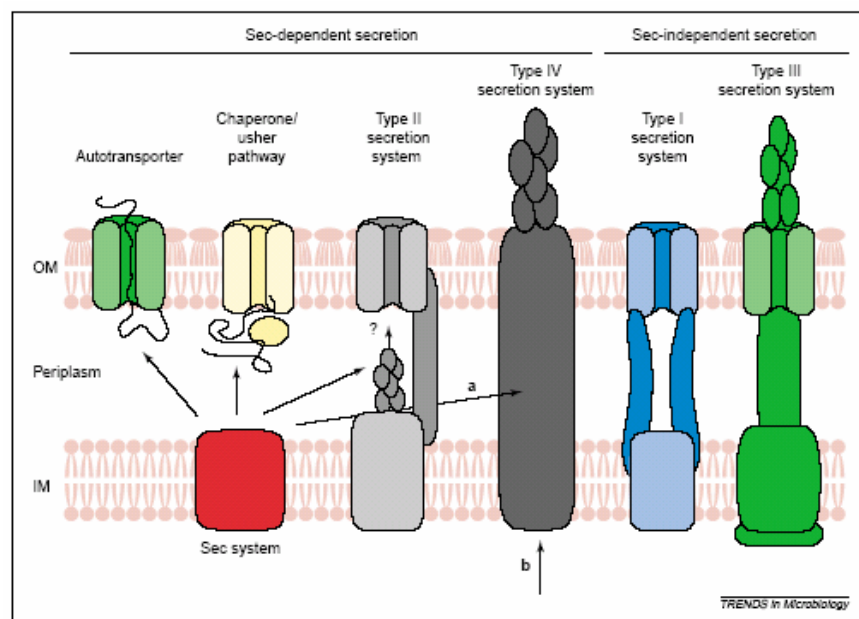


**Figure 1:** Protein secretion systems in Gram-negative bacteria. (Figure is adapted from Buttner and Bonas, 2002b).

Among the model organisms for the molecular and genetic characterization of host-plant interaction and the functional analysis of the type III secretion system are *Erwinia amylovora* and pathovars (pv.) of *Pseudomonas syringae*. Both gram-negative species secrete the harpins, the first proteins known to be secreted by the type III secretion system. Harpins are small, heat-stable glycine-rich proteins that lack cysteines and elicit a necrosis-like reaction when infiltrated into non-host plants. Harpin from *Pseudomonas syringae* (HrpZ) was found to bind to the plant plasma membrane and to form ion-conducting pores in artificial lipid bilayers. The role of harpins is not well understood, a contribution to bacterial virulence could not be demonstrated (Buttner and Bonas, 2002a).

## 2. Pathogen recognition

### 2.1. The gene-for-gene interaction

Once released into plant apoplasts or directly into plant cells via the type III secretion system, effector proteins are recognized directly or indirectly by plant resistance (R) proteins. In this role, pathogen-encoded effectors are called avirulence (Avr) proteins. The recognition is typically race-specific, meaning that a given R protein recognizes the Avr proteins from one or very few pathogen isolates. This *R-avr* genetic interaction initiates what is referred to as gene-for-gene resistance. If either the pathogen or the host lacks the corresponding *avr* or *R* gene, then the plant-pathogen interaction results in disease. R proteins are either transmembrane or intracellular proteins that are presumed to initiate signal transduction cascades upon ligand binding. Five classes of mostly structurally conserved R proteins have been identified: intracellular proteins with a nucleotide-binding site (NBS), a leucine-zipper motif and a leucine-rich repeat (LRR) domain; intracellular NBS-LRR proteins with a region of similarity to the cytoplasmic domain of the mammalian IL-1 receptor and *Drosophila* Toll proteins (TIR domain); intracellular protein kinases (PKs); proteins with a leucine-rich repeat (LRR) domain that encodes membrane-bound extracellular proteins; and receptor-like kinases (RLKs) with an extracellular LRR domain (Cohn et al., 2001; Holt et al., 2003).

In contrast to R proteins, no or only a low homology was found between Avr proteins (Nimchuk et al., 2001; Bonas and Lahaye, 2002). Because plants have no specialized and distinct immune system, each cell has the ability to respond to a pathogen attack. This defense capacity is maintained by a very large repertoire of rapidly evolving *R* genes that constitute the innate immune system of plants (Dangl and Jones, 2001).

### 2.2. General elicitors – PAMPs

In addition to the R proteins which recognize pathogen-derived race-specific effectors (Avr proteins), plants dispose of further receptors with broad range specificity which recognize many related molecular structures called PAMPs (pathogen-associated molecular patterns). In contrast to what the term suggests, PAMPs are not unique to pathogens, and are produced by many microorganisms, pathogenic or not. Among these general elicitors are essential polysaccharides and polynucleotides, which are not found in host plant and differ slightly from pathogen to pathogen. The most important PAMPs are conserved cell-surface structures like flagellin, lipopeptides (LP), peptidoglycans (PG) and lipopolysaccharides (LPS) which are unique to bacteria (Nurnberger et al., 2004). LPS are major parts of Gram-negative bacteria cell surfaces, composed of a hydrophobic lipid A, a covalently linked non-repetitive core oligosaccharide, divided into inner and outer core, and the O-antigen of oligosaccharide-repeating units. Various structural elements of LPS are potent inducers of plant defense reactions (Newman et al., 2002).

The flg22, a highly conserved fragment of flagellin and the main building block of eubacterial flagellae, triggers plant-defense associated reactions in *Arabidopsis* and tomato plants (Felix et al., 1999). In *Arabidopsis* the perception of flagellin occurs by recognition of flg22, and depends on the

LRR-type receptor kinase FLS2 (flagellin sensing 2), which leads to an activation of a downstream mitogen-activated protein kinase cascade, composed of AtMKK4/AtMKK5 and AtMPK3/AtMPK6 (Zipfel et al., 2004). Flagellin is also recognized as a PAMP in mammals, by the way of Toll-like receptor TLR5 from both Gram-positive and Gram-negative bacteria. Activation of the TLR5 receptor mobilizes the nuclear factor NF- $\kappa$ B and stimulates the tumour necrosis factor- $\alpha$  formation (Hayashi et al., 2001).

It appears that plants recognize patterns similar to those reported to activate innate defense reactions in mammals and *Drosophila*. Likewise the animal innate immune system recognizes PAMPs, in this case by an array of the so called pattern recognition receptors (PRRs). The binding of PAMPs to these receptors results in an activation of immune response genes and the production of antimicrobial compounds. One such PRR-PAMP complex is formed between the mammalian Toll-like receptor 4 (TLR4) -MD2-CD14 complex and LPS. Lipid A is the sole portion of LPS recognized by TLR4. Many regulated lipid A modifications are required for bacterial virulence. For example, lipid A modifications promote virulence in a variety of pathogens including *Salmonella enterica* serovar typhimurium, *Legionella pneumophila*, *Bordetella bronchiseptica*, the insect pathogen *Photobacterium luminescens*, and the plant pathogen *Erwinia carotovora*. In many cases, lipid A modifications promote bacterial resistance to killing by antimicrobial peptides. Different lipid A structures exhibit differential recognition by TLR4. Recognition of lipid A is in part determined by extracellular variable domains in TLR4 and MD2. There is evidence for positive selection in these domains across different species, which supports the hypothesis that variability in innate immune recognition determines infectious disease outcome (Miller et al., 2005).

### 3. Signaling in innate immunity

The *Drosophila* Toll protein, mammalian Toll-like receptors (TLR) TLR4 and TLR5, *Arabidopsis* FLS2, and the plant *R* genes Cf9 from tomato and Xa21 from rice exemplify transmembrane receptors for the perception of PAMPs or Avr signals, respectively (Fig. 2). LPS and flagellin, both stimulate the innate immunity in mammals. Upon recognition by the LPS binding protein (LBP), a complex with LRR proteins CD14 and TLR4 is formed. Flagellin recognition occurs by TLR5. In *Drosophila melanogaster*, peptidoglucans of Gram-positive bacteria initiate a proteolytic cascade, upon which the Toll-ligand Spätzle is generated. Toll / TLRs interact with protein kinases Pelle / IRAK using adapter proteins dMyD88-Tube / MyD88. Pelle / IRAK share homology with kinase domains of receptor-like kinases such as FLS2 or Xa21. Subsequently, protein kinases including mitogen-activated protein kinases (MAPKs) mediate the activation of the transcription factors Dif/Dorsal / NF- $\kappa$ B/I $\kappa$ B and expression of immune response genes.

In tomato, Avr9 protein, which is structurally similar to *Drosophila* Spätzle, is recognized by a high-affinity binding site; this complex interacts with Cf9 and activates at least two MAPKs. The rice Xa21 and the *Arabidopsis* FLS2 are likely to transduce the pathogen signal through their cytosolic protein kinase domain. Flg22 directly binds to FLS2 and activates the MAPKs AtMPK3, and AtMPK6.

Intracellular perception of pathogen-derived molecules occurs in plants as well as in mammals. The intracellular recognition of LPS in mammals is mediated by the NBS-LRR receptors, nucleotide-binding oligomerization domain NOD1/2, whereas intracellular PAMP-perception in plants has not been observed until now. NOD1/2 possess of an additional caspase recruitment domain (CARD), while plant intracellular NBS-LRR proteins are linked to Coiled-coil (CC) or Toll-Interleukin1-receptor-like (TIR) domains (Nurnberger et al., 2004).

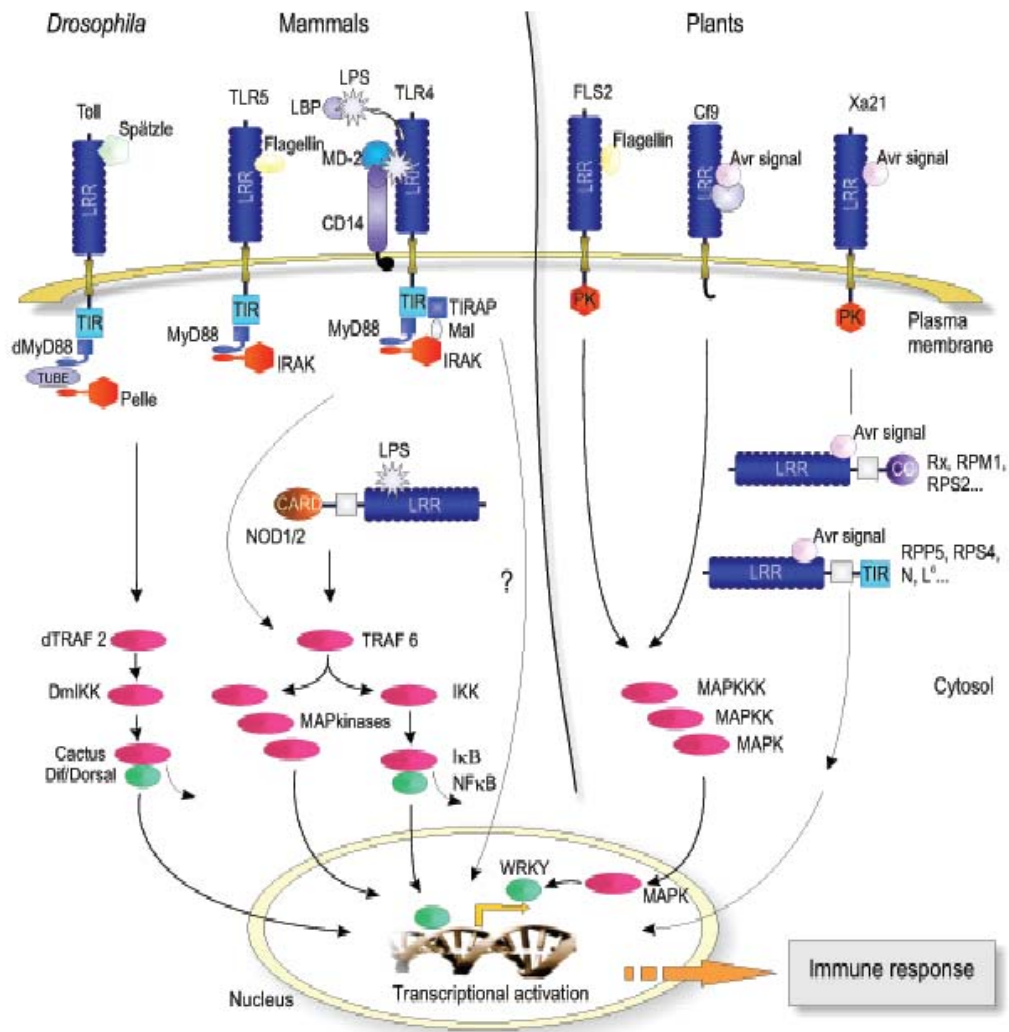


**Figure 2:** Signaling cascade in innate immunity of insects, mammals, and plants.

Pathogen recognition by the innate immune system relies on interactions between pathogen-derived molecules and corresponding host receptor molecules. Signaling pathways leading to activation of defense response genes in insects, mammals and plants share common components. More detailed information can be found in the text (Figure is adapted from Nurnberger 2004).

#### 4. Programmed cell death and apoptosis

Plants dispose of a wide array of defense strategies against pathogenic microorganisms. The hypersensitive response (HR) of plants is an induced defense mechanism and has been defined as programmed cell death at the sites of infection with the pathogen. It is manifested in the formation of dry, necrotic lesions, and restriction of pathogen growth and spread. With infection levels typically encountered in natural environment, the HR produces individual dead plant cells that are scattered within successfully defended healthy tissue. In this manner plants use apoptosis to save their own survival. HR is induced as a reaction to biotic and abiotic stimuli, and is initiated by host recognition of race specific (e.g. Avr proteins) or non-specific molecules such as glycoproteins, small peptides, and oligosaccharides. The HR is associated with the induction of defense related genes which play important roles in containing pathogen growth either indirectly, by helping to reinforce the plant cell walls, or directly, by producing antimicrobial enzymes and phytoalexins (Dixon et al., 1994; Goodman and Novacky, 1994; Osbourn, 1996).

In plants, the HR is the best studied model for programmed cell death (PCD). Characteristic features are cell shrinkage, chromatin condensation, DNA fragmentation (laddering), and activation of various proteases. A further prominent feature is a sustained oxidative burst, a massive increase in formation of reactive oxygen species (ROS) which precedes and accompanies the lesion-associated host cell death. ROS such as superoxide radical ( $O_2^{\cdot-}$ ) and hydrogen peroxide ( $H_2O_2$ ) appear to play key roles in early and later stages of plant defense response against pathogens. Several sources of ROS are discussed. At least in tobacco and *Arabidopsis* a NADPH oxidase (respiratory oxidative burst homologues, rboh) seems to contribute to the pathogen-induced oxidative burst. In addition, mitochondria have the capacity to produce high fluxes of ROS (Alfano and Collmer, 1997; Moller and McPherson, 1998; Scheel, 1998; Dangl and Jones, 2001; Mettraux and Durner, 2004).

Several strands of evidence support the notion that mitochondria are involved intimately in mediating HR cell death in animals. Elevated  $Ca^{2+}$  and oxidative stress, both contribute to the opening of the mitochondrial permeability transition pore (PTP), which depolarizes the mitochondria and leads to mitochondrial swelling and subsequent release of cytochrome c from the intermembrane space (Goldstein et al., 2000).

Cytochrome c normally functions as part of the respiratory chain; however, when released into the cytosol, as a result of the PTP opening, it becomes a critical component of the apoptosis execution machinery, where it activates caspases (cysteine aspartate proteinases) and, if ATP is available causes apoptotic cell death (Thornberry and Lazebnik, 1998). Caspases are inactivated by interacting with the suppressor protein Bcl-2 and also Apaf-1. Activation e.g. by oxidative stress involves cytochrome c release from the mitochondrion which initiates an ATP-driven conformational change in Apaf-1 to activate the caspase. Caspases digest Bcl-2 (which can suppress cytochrome c release) and the degradation product, BAX, forms further pores in the mitochondrion, resulting in a further release of cytochrome c and thus the apoptotic cascade is initiated (Fig. 3).



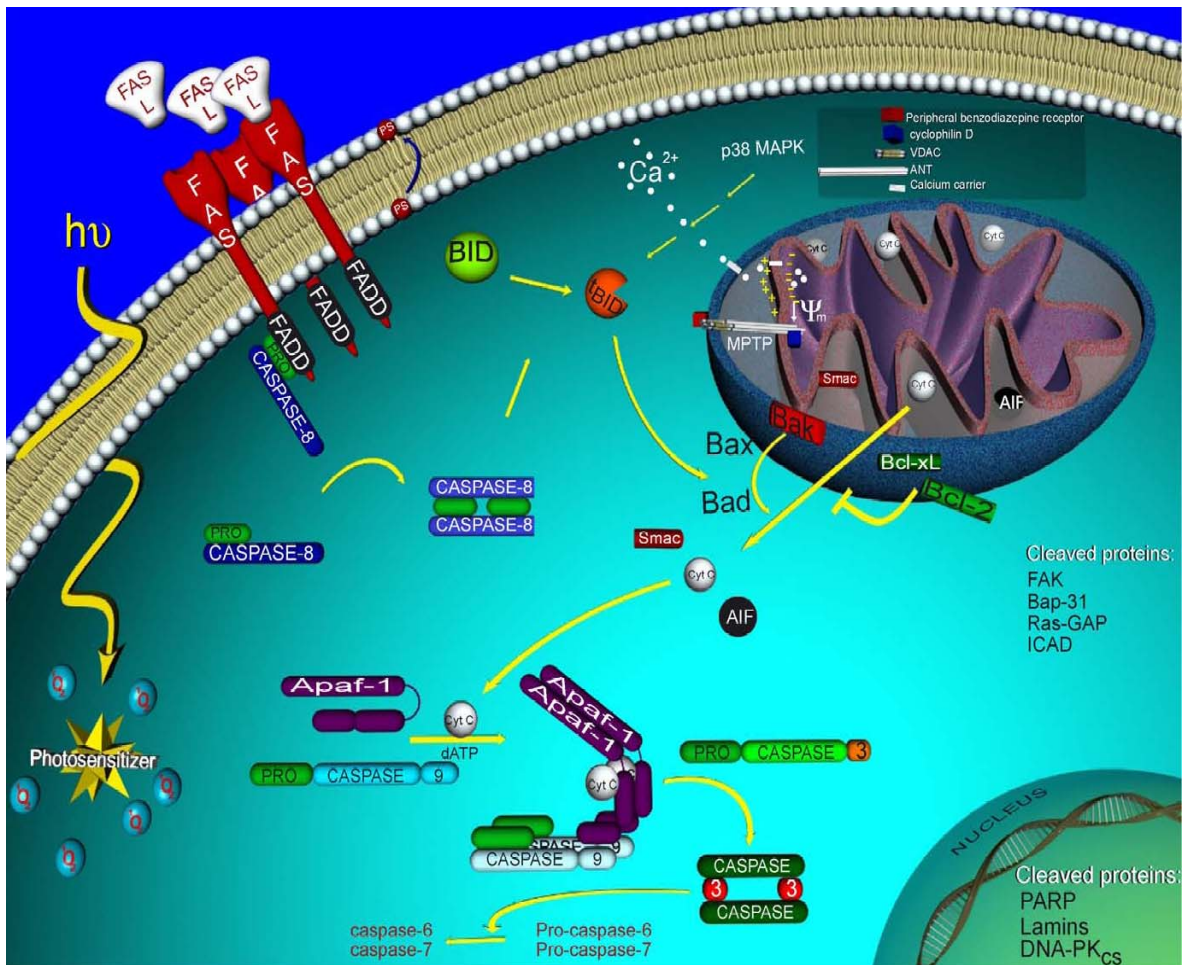


**Figure 3:** Major molecular events leading to apoptosis in animal cells.

The two major apoptotic pathways, the death receptor-mediated, or extrinsic pathway, and the mitochondria-mediated-pathway are represented. (Figure is adapted from Almeida et al., 2004).

In plants, the involvement of mitochondria in pathogen-induced defense responses and cell death has been demonstrated. In tobacco, mitochondria are implicated in salicylic acid (SA)- induced plant resistance to viral pathogens (Chivasa and Carr, 1998). Cyanide, an inhibitor of mitochondrial cytochrome c- dependent respiration, but also of other heme-containing enzymes, induced formation of DNA laddering in cowpea (Ryerson and Heath, 1996). In *Arabidopsis* spp., nitric oxide (NO) induced activation of alternative respiration (Huang et al., 2002). In menadione treated tobacco as well as during *Agrobacterium*-induced apoptosis in maize, cytochrome c release has been associated with cell death (Sun et al., 1999; Hansen, 2000). More recently, a possible role of mitochondrial-derived ROS has been suggested in controlling apoptotic cell death in oats (Yao et al., 2002). A review on plant mitochondria and oxidative stress also has been published (Moller, 2001). It was shown that harpin induced a decrease of ATP-pool size in tobacco cell cultures (Xie and Chen, 2000).



## 5. MLO as modulator of defense and cell death

Genetic analysis of barley resistance responses to the compatible fungal pathogen *Blumeria graminis* f.sp.*hordei* (Bgh) revealed two major pathways: dominantly or semi-dominantly inherited race-specific resistance triggered by single *R* gene products, a subset of which requires the signaling genes *Rar1* and *Sgt1*; and broad-spectrum powdery mildew resistance controlled by recessive, loss-of-function mutations in a single gene, *Mlo* (Jorgensen, 1994). The *Mlo* gene encodes a plant-specific integral membrane protein that contains seven transmembrane domains (Devoto et al., 1999). The protein is thought to mediate defense suppression to *Blumeria graminis* f.sp.*hordei* attack via direct  $Ca^{2+}$ -dependent interaction with calmodulin. MLO appears to function as a negative regulator of cell death. Loss-of-function mutations at this locus confer resistance to powdery mildew *via* blockage of host cell entry by fungal sporelings at the cell wall. Enhanced mesophyll cell death reminiscent of premature senescence and spontaneous callose deposition in unchallenged plants are pleiotropic effects of barley *mlo* mutants (Wolter et al., 1993; Eckardt, 2002; Elliott et al., 2002; Piffanelli et al., 2002). In *Arabidopsis* 15 distinct *Mlo* family members were identified. These homologs can be grouped in at least 4 distinct phylogenetic clades what potentially reflects a putative functional diversification of the protein family. The phylogenetic analysis based on amino acid sequence similarity further revealed that three AtMLO proteins (AtMLO2, AtMLO6, and AtMLO12) cluster together and define a subfamily which appears to be restricted to dicots or, alternatively, to *Arabidopsis*. But except for barley *Mlo*, no biological function has been assigned to any other *Mlo*-like gene to date (Devoto et al., 2003).

## 6. The harpin experimental system

In addition to effector Avr proteins, type III secretion systems of plant pathogenic bacteria secrete another class of proteins termed harpins. Harpin is a well known proteinaceous elicitor that can induce an oxidative burst and programmed cell death in various host plants. It is an acidic protein with a size between 35 and 44 kDa, depending on the secreting bacterium such as *Pseudomonas* spp., and *Erwinia* spp.. Harpin is glycine-rich, cysteine-lacking, water soluble, and heat stable up to 100°C for at least fifteen minutes.

Studying innate immunity in plants using harpin will contribute to the understanding of the general principles of innate immunity in plants and animals. The presence of type III secretion systems exclusively in bacteria with a pathogenic potential may provide a unique target for the development of therapeutic agents that may spare normal flora, Furthermore, modulating or harnessing the type III secretion system may provide a valuable tool for the development of novel vaccines and therapeutic approaches.

Treatment of plants with harpin from *Erwinia amylovora* effects plant growth and development, resulting in higher yields. It is reported that harpin treated plants exhibit accelerated growth, early flowering, fruit set, and increased fruit set. Furthermore, the observed effects on plant growth and development can lead to a shortened time to harvest (<http://www.edenbio.com>, (Dong et al., 2004).

The systemic acquired resistance (SAR) as a plant defense response, whose induction usually follows cell death resulting from HR and disease necrosis, is elicited in a variety of plants by harpin. It results in a defense gene expression such as the pathogenesis-related (PR) genes (Strobel et al., 1996; Lee et al., 2001a). It is reported that harpin-induced resistance is salicylic acid (SA) dependent but jasmonic acid (JA) independent (Dong et al., 1999).

In *Arabidopsis* suspension cells, harpin induced the expression of plant defense genes encoding enzymes such as phenylalanine ammonia-lyase (PAL) and anthranilate synthase (ASA1) (Desikan et al., 1998). Further it was shown that harpin activates the two mitogen-activated protein kinase (MAPK)-like enzymes AtMPK4 and AtMPK6 in *Arabidopsis*, the activation of AtMPK4 could be reduced by a MAPKK inhibitor (Desikan et al., 2001).

Elicitation of tobacco suspension cells with harpin leads to an alkalinization of the surrounding growth medium (Wei et al., 1992), potassium efflux, and membrane depolarization, which can be blocked by a protein kinase inhibitor (Popham et al., 1995). In tobacco BY-2 cells, harpin from *Pseudomonas* pv. *tomato* caused nuclear DNA fragmentation during apoptotic cell death, accompanied by a rapid generation of hydrogen peroxide (H<sub>2</sub>O<sub>2</sub>) (Ichinose et al., 2001). Unlike Avr proteins that need to be transferred into the plant cell to exert their function, the harpins can elicit the hypersensitive response (HR) when delivered to the surface of plant cells. Nürnbergers working group identified a non-proteinaceous binding site for harpin from *Pseudomonas syringae* pv. *phaseolicola* in tobacco plasma membranes, whereas the binding was specific, reversible, and saturable (Lee et al., 2001a). It was found that harpins are integrated into lipid bilayer membranes to form an ion-conducting channel *in vitro* (Lee et al., 2001b). They also report a harpin-mediated strong increase of cytosolic free calcium (Ca<sup>2+</sup>) in *Petroselinum crispum* suspension cells (Blume et al., 2000).

So far, no animal homologue of harpin has been reported. That does not implicate, that this class of type III secretion effector proteins does not exist in animal pathogens.

## 7. Aims of the study and research strategy

The general aim of this thesis is to elucidate the mode of action of the type III secretion protein harpin in plants by characterization of the activation of plant defense systems at the molecular level. The interaction between recombinant harpin from *Pseudomonas syringae* pv. *syringae* and *Arabidopsis thaliana* will be used as a model system to investigate how this protein can stimulate or interact with plant host cellular processes.

The basic morphological and biochemical features of PCD or apoptosis, respectively, are conserved between the animal and plant kingdoms. An important biological context of apoptosis is the host-pathogen interaction and immunity. Recent evidence points to the mitochondria as a key organelle in the regulation of cellular responses to stress. Given the demonstrated roles of mitochondria in animal apoptosis or PCD respectively, main emphasis of this work will be the investigation of the effect of harpin on mitochondrial function in *Arabidopsis thaliana* suspension cells. The effect of harpin regarding hallmarks of plant defense such as the formation of nitric oxide (NO) and reactive oxygen species (ROS), and the induction of cell death will be studied in detail. A further aspect of this work

will be the analysis of differential gene expression in *Arabidopsis thaliana* plants in response to harpin and the comparative transcriptional profiling of genes after treatment with other elicitors such as the PAMP lipopolysaccharide. Continuative experiments will be performed to discover whether the induction of plant defense systems by harpin leads to enhanced resistance against pathogens such as the bacterium *Pseudomonas syringae* and the fungus *Alternaria alternata*.

## II. Results

### 1. Effect of harpin on *Arabidopsis* plants and *Arabidopsis* suspension cells

#### 1.1. Recombinant harpin induces cell death in *Arabidopsis* suspension cells

It is long time known that programmed cell death is a key component of the hypersensitive disease resistance response of plants. To characterize the activation of plant defense systems by harpin at the molecular level, at first the effect of harpin on cell viability in *Arabidopsis* suspension cultures was analyzed. Following treatment with harpin cell death was monitored by counting dead and live cells after staining with Evans blue. No significant cell death was detected during the first 6 h of incubation (Fig. 4a). Substantial cell death induced by harpin occurred 8 h after treatment. As described earlier for tobacco BY-2 cell suspension cultures, after 24 h already 30% of the cells were dead (Andi et al., 2001; Ichinose et al., 2001). Beside the induction of cell death, treatment of suspension cells with harpin elicited an immediate increase in extracellular pH (Fig. 4b). Although the pH value of the growth medium was adjusted to pH 6.0, in 6-day-old suspension cultures the pH always was lowered to ~ pH 5.0. The harpin caused media alkalinization from ~ pH 5.0 to ~ pH 6.7 was found as nearly constant after 24 h. These data go along with already reported observations (Wei et al., 1992; Baker et al., 1993).

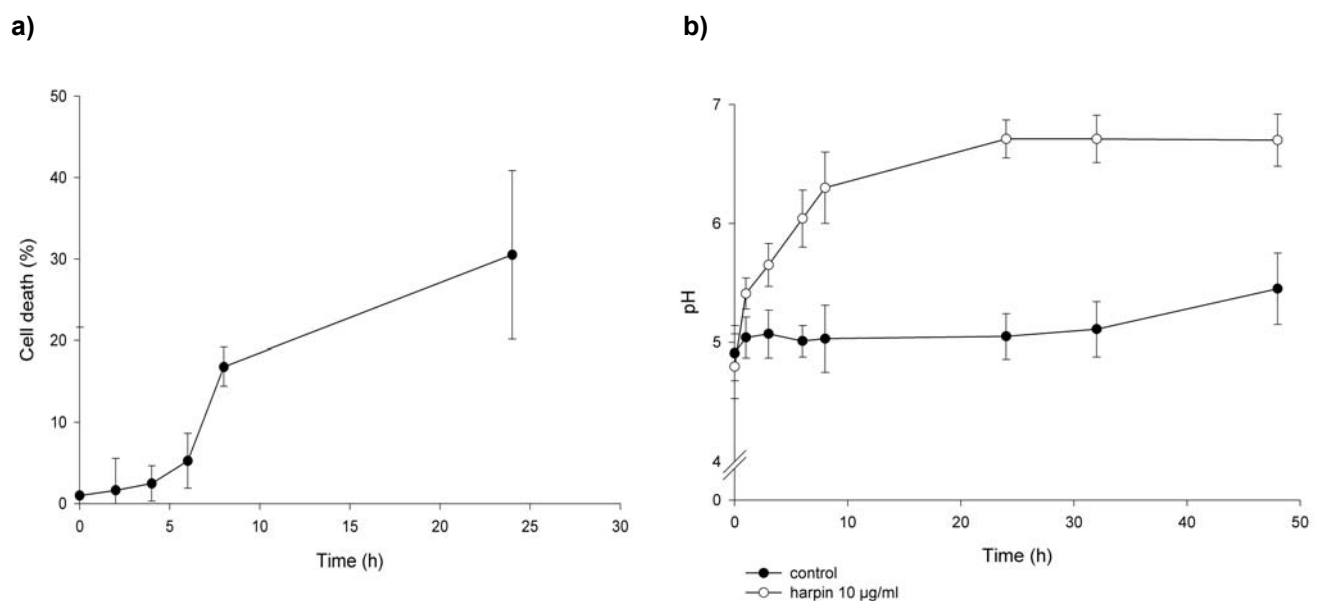


**Figure 4:** Time course study of harpin-induced cell death and pH.

**a)** *Arabidopsis* suspension culture was treated with harpin at 50 µg/ml final concentration. At indicated time points cell viability was estimated among 500 cells by Evans blue staining. Values represent mean ± SD from five independent experiments.

**b)** Changes in extracellular pH in *Arabidopsis* cell suspension treated with 10 µg/ml of harpin. Measurements were taken using a pH electrode; data are represented as means ± SD from 3 independent experiments.

## 1.2. Impact of harpin on plant growth

Treatments of plants with harpin from *Erwinia amylovora* as the active ingredient of the commercial plant activator messenger<sup>®</sup> have significant effects on plant growth and development, resulting in higher yields. It is reported that laboratory and field studies have shown that messenger<sup>®</sup> treated plants exhibit accelerated growth, early flowering; early fruit set, and increased fruit set. Beneath are to mention increased boll numbers in treated cotton, increased fruit yield in treated tomatoes, early fruit maturation in raspberry plants as well as enhanced growth of both root and aerial portions of *Arabidopsis* plants. Furthermore, the observed effects on plant growth and development can lead to a shortened time to harvest (<http://www.edenbio.com>, (Dong et al., 2004). Here, the impact of harpin from *Pseudomonas syringae* pv. *syringae* on growth and development of *Arabidopsis* plants in comparison with messenger<sup>®</sup> induced effects was observed. To ensure equal conditions, every two weeks the plants were treated either with water, messenger<sup>®</sup> or harpin at 12 µg/ml as final concentration, as specified from manufacturer (Eden Bioscience, Bothell, USA) for the commercial messenger<sup>®</sup>. The development status of treated plants after 10 weeks, as presented in Fig. 5, confirms the expected growth enhancing character of messenger<sup>®</sup>. Observably is that messenger<sup>®</sup> treated plants show increased growth in comparison to water sprayed controls whereas harpin treated plants are significant smaller and individual leaves appear almost complete necrotic. But, a difference in development was not confirmed, every six-pack of pots had breed exactly one flower (marked by circles) at this time point. However, in this study enhanced growth of *Arabidopsis* plants caused by harpin from *Pseudomonas syringae* pv. *syringae* was never observed. This was also not the case at lower concentrations, accompanied by a lower activity of the protein, which was supposed to be a possible reason for the contrary effects of both harpins.



**Figure 5:** Effect of harpin treatment on *Arabidopsis* plant growth.

Every 2 weeks, wild-type *Arabidopsis* plants were treated with 12 µg/ml of harpin, messenger<sup>®</sup>, or water respectively. Photos were taken after 10 weeks that means following 5 treatments, black circles mark existing flowers.

### 1.3. Enhanced resistance to *Pseudomonas syringae* pv. *tomato* DC3000

A disease resistance enhancing character of harpin proteins has already been monitored for different plant species. There are several reports which describe a protecting role of harpin such as an harpin induced resistance against *Penicillium expansum* (blue mold) in apple fruits, enhanced resistance against tobacco mosaic virus (TMV) in tobacco, and against *Peronospora parasitica* and *Erwinia carotovora* in *Arabidopsis* (de Capdeville et al., 2003; Kariola et al., 2003; Peng et al., 2003). Here, the extent of harpin-mediated protection against pathogens on *Arabidopsis* plants was assessed after inoculation with the virulent strain *Pseudomonas syringae* pv. *tomato* DC3000. Six week old wild-type *Arabidopsis* ecotype Columbia (Col-0) plants were inoculated with  $1 \times 10^6$  colony forming units/ml (cfu/ml) of *Pseudomonas syringae* pv. *tomato* DC3000 bacteria by syringe injection. The plants were pre-treated for 2 or 5 days by spraying water, harpin or messenger<sup>®</sup> onto the leaf surfaces. Bacterial growth on leaves was determined 5 days after inoculation of *Pst* DC3000 (Fig. 6).

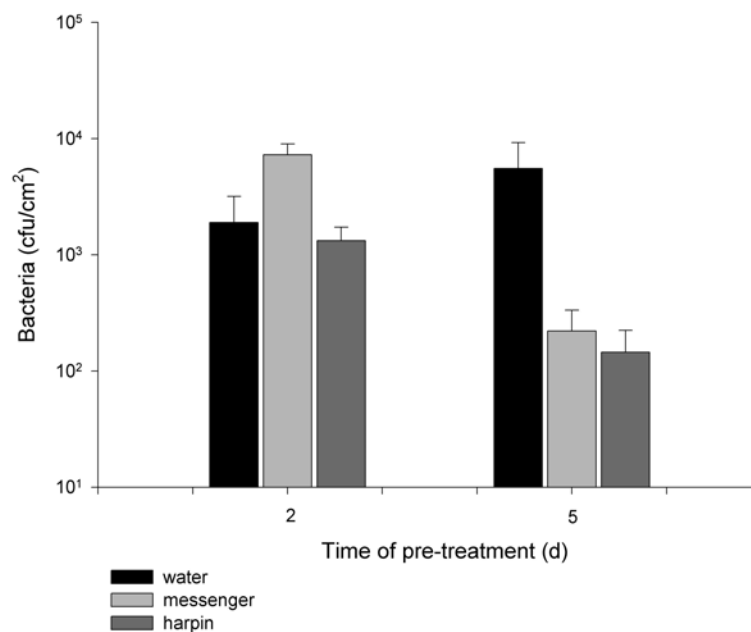


**Figure 6:** Harpin causes enhanced disease resistance against *Pst* DC3000.

Wild-type plants were pre-treated for 2 or 5 days with 12 µg/ml of harpin or messenger<sup>®</sup>, or water respectively. Bar graphs indicate the number of *Pst* DC3000 bacteria 5 days after inoculation, values represent mean ± SD from 3 independent experiments.

Under mentioned conditions, *Arabidopsis* plants which were pre-treated for 2 days with harpin did not show any increase in bacterial disease resistance. Moreover, the commercial messenger<sup>®</sup> containing harpin from *Erwinia amylovora*, apparently caused a stronger infection with *Pseudomonas* bacteria. But, 5 days water pre-treated controls showed significant stronger disease symptoms than harpin or messenger<sup>®</sup> treated, what correlated with higher numbers of bacteria. Thus, plants pre-treated for 5 days with harpin or harpin containing messenger<sup>®</sup> became less susceptible, or more resistant, to virulent *Pst* DC3000 bacteria as demonstrated by an at least 10-fold reduction in bacterial growth 5 days after inoculation.

#### 1.4. Harpin induces the formation of reactive oxygen species and nitric oxide

A characteristic feature of the hypersensitive response (HR) is a sustained increase of reactive oxygen species (ROS), the so called oxidative burst. ROS such as superoxide radical ( $O_2^-$ ) and hydrogen peroxide ( $H_2O_2$ ) appear to play key roles in early and later stages of the plant response against pathogens. Although ROS used to be regarded merely as toxic by-products of cellular metabolism, it is now recognized that they have a signaling role in many biological systems. ROS can serve as second messengers for the activation of defense gene expression (Alvarez et al., 1998). In addition, experimental data indicating that ROS can activate cell death programs, both in animal and plants. In plant tissue, not only pathogen attack, but various conditions lead to accelerated generation and/or accumulation of ROS and subsequent PCD, for example ozone ( $O_3$ ) fumigation, cold stress, UV radiation and senescence (Lam et al., 1999; Langebartels et al., 2000).

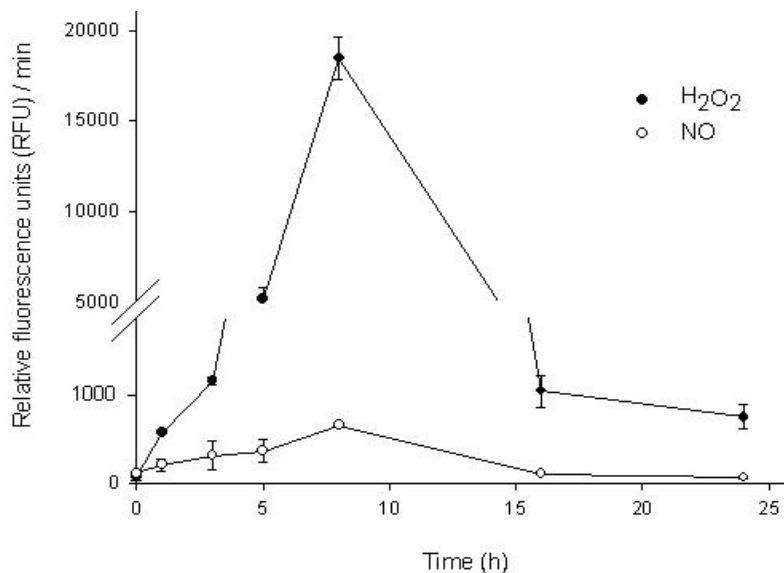


**Figure 7:** Timecourse analysis of ROS and NO generation in *Arabidopsis* suspension cells.

At indicated time points of incubation with 50  $\mu$ g/ml of harpin NO was determined by adding DAF-FM,  $H_2O_2$  concentration in culture medium was estimated by adding  $H_2DCF$ -DA, followed by immediately measuring of fluorescence intensities over a 20 min period with a Tecan multiwell plate reader. Data of Relative fluorescence units (RFU) are represented by 20 independent samples as means  $\pm$  SD.

Harpin induced generation of ROS has been reported for several plants including *Arabidopsis* and tobacco (Desikan et al., 1998; Xie and Chen, 2000). Here, photometrical measurement of  $H_2O_2$  using  $H_2DCF$ -DA as ROS-indicator in conjunction with a plate reader equipped with usual FITC excitation and emission filters confirmed fast ROS production after harpin treatment. Highest ROS accumulation was observed between 6-8 h after treatment (Fig. 7). This oxidative burst paralleled induction of cell death, which reached about 30% after 24 h (Fig. 4a).

Plant defense responses and/or cell death after pathogen attack (e.g. *Pseudomonas syringae* or tobacco mosaic virus) seem to be regulated by the concerted action of NO and ROS (Delledonne et al., 1998; Durner et al., 1998; Delledonne et al., 2001). So the question came up whether harpin

would induce NO, too. Here, cells were treated with harpin and analyzed for NO using the fluorescence dye DAF-FM at a fluorescence microscope. DAF has been used to visualize NO production in kalanchoe (Pedroso et al., 2000), barley (Beligni et al., 2002), mung bean (Lum et al., 2002) and tobacco (Foissner et al., 2000). The ability of diaminofluoresceins to specifically detect NO in biological systems has been confirmed (e.g. (Suzuki et al., 2002)). The basal fluorescence shown in Fig. 8 represents basal NO in untreated cells. Nevertheless, the difference to induced cells is significant. As a control, carboxy-2-phenyl-4,4,5,5-tetramethylimidazo-linone-3-oxide-1-oxyl (cPTIO) was applied, a NO scavenger that does not react with any ROS (Barchowsky et al., 1999) and which has been used to block NO production as well as NO-dependent cell death and defense gene activation in tobacco, soybean, *Arabidopsis* and barley (Delledonne et al., 1998; Durner et al., 1998; Foissner et al., 2000; Beligni et al., 2002). The cPTIO completely suppressed the elicited bursts of fluorescence. Timecourse analysis of NO-generation with a plate reader revealed that the NO generation roughly paralleled the oxidative burst, but was much weaker (Fig. 7). After 2 h, ROS production was increased more than 10-fold, while a significant rise in NO generation was observed only after 8 h. It is assumed that NO accumulation in harpin-treated *Arabidopsis* cells plays a minor role in cell death, and represents a consequence of cellular decay.

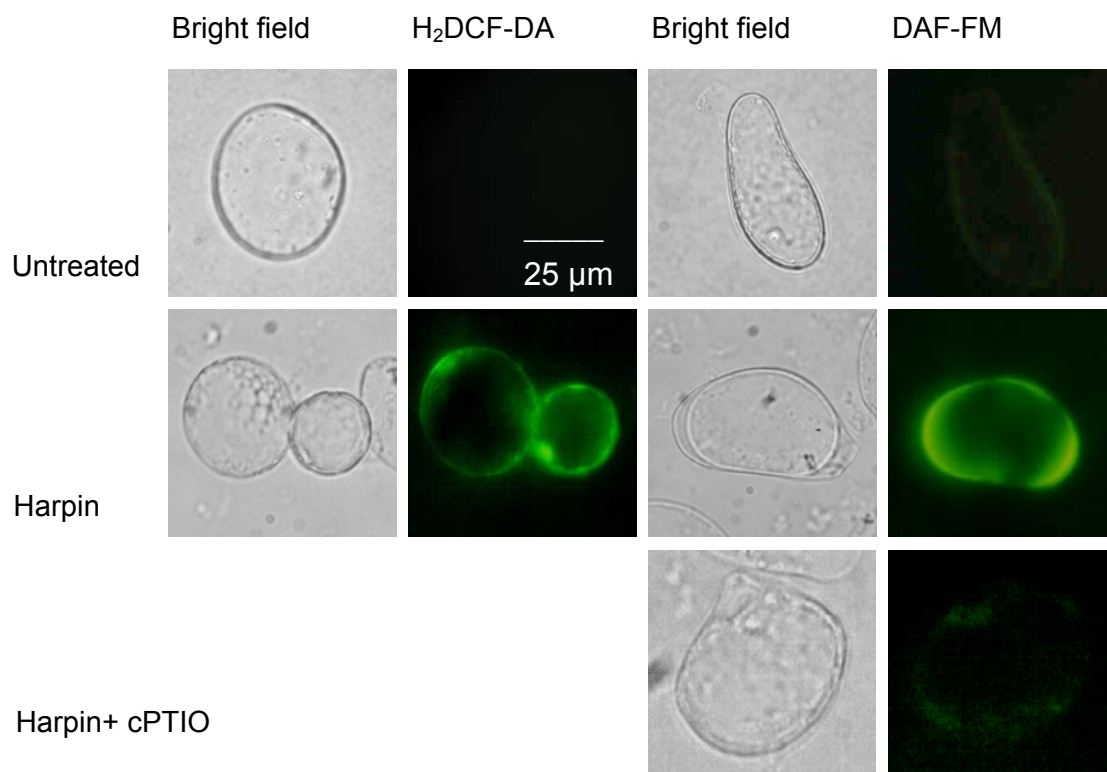


**Figure 8:** Fluorescence staining for NO and ROS detection in *Arabidopsis* suspension cells.

Cells were incubated with 50 µg/ml of harpin for 3 h. Treated and untreated cells either were stained with DAF-FM as NO-probe in the presence or absence of the NO scavenger cPTIO, or with H<sub>2</sub>DCF-DA to detect ROS. Stained *Arabidopsis* cells were observed under a fluorescent microscope. Photographs were taken under bright field and fluorescence light.



## 2. Mitochondria mediated apoptosis in *Arabidopsis* suspension cells

### 2.1. Mitochondrial formation of reactive oxygen species

Given the demonstrated roles of mitochondria in mammalian apoptosis, the effect of harpin from *Pseudomonas syringae* on mitochondrial functions in *Arabidopsis* suspension cells was investigated in detail. Because mitochondria are the major source of ROS in animal cells, mitochondrial-derived ROS may play an important role in the induction of apoptosis (Green and Reed, 1998). The question came up, whether mitochondria are involved in HR-associated ROS generation, as occurring in *Arabidopsis* after harpin exposure. A possible role of from mitochondria derived ROS has been suggested in controlling apoptotic cell death in oats (Yao et al., 2002). Harpin treated *Arabidopsis* suspension cells were double-stained with the ROS-indicating H<sub>2</sub>DCF-DA dye and MitoTracker Red 580 as a mitochondrial specific marker (Yao et al., 2002), and monitored using an Olympus BX C1 epifluorescence microscope and a black/white CCD-camera (Fig. 9). The images show that an oxidative burst was induced in mitochondria of the harpin treated cells. The intracellular localization of the DCF signal matched that of the MitoTracker signal, as data processing revealed strong yellow signals. Thus, these results suggest co-localization of mitochondria and ROS formation.

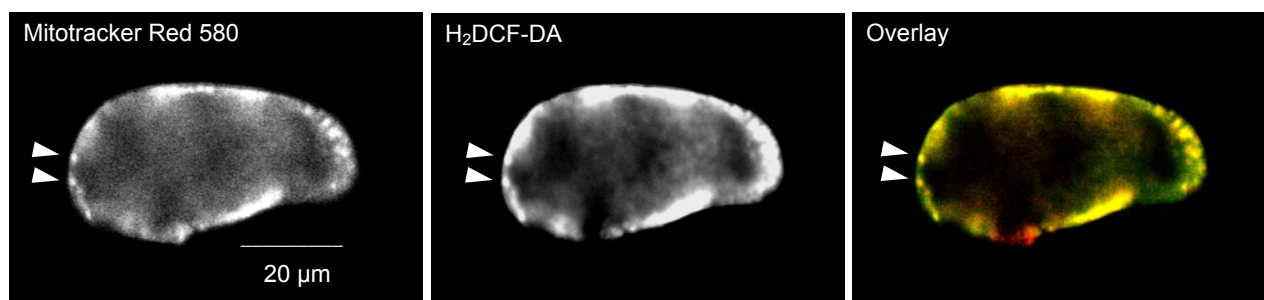


**Figure 9:** Cytological detection of mitochondrial ROS.

After treatment of 2 h with 50  $\mu\text{g}/\text{ml}$  of harpin, the exposed cells were labeled with MitoTracker Red 580 as a specific mitochondrial marker, and after further incubation for 1 h in the dark the cells were labeled with the ROS detecting dye H<sub>2</sub>DCF-DA. Note that this image is representative for a cell producing ROS. Similar responses can be detected within the first 4 h. Stained cell suspension was monitored and photographed using an Olympus BX C1 epifluorescence microscope and a black/white 12-bit CCD-camera (1376x1032 pixel). Mitochondria and the produced ROS show co-localization, which appears yellow.

### 2.2. Decrease of mitochondrial transmembrane potential $\Delta\Psi_m$

In mammalian cells, PCD is often associated with a collapse of the mitochondrial transmembrane potential ( $\Delta\Psi_m$ ). A decrease of  $\Delta\Psi_m$  is a typical feature of early apoptosis (Bossy-Wetzels et al., 1998; Heiskanen et al., 1999; Bal-Price and Brown, 2000; Goldstein et al., 2000). Here, it was sought to dissect the *Arabidopsis* cells early response to harpin induced stress in terms of mitochondrial changes. JC-1 is a dye widely used to probe mitochondrial membrane potential in living mammalian cells. High mitochondrial  $\Delta\Psi_m$  leads to J-aggregates of the dye, which fluoresce red (Botella et al., 1996). The depolarization is indicated by a decrease in ratio of red/green fluorescence intensities. This ratio is only dependent on the membrane potential, not on other factors like size, shape or

density of mitochondria. Using the JC-1 dye to probe the mitochondrial membrane potential in harpin treated *Arabidopsis* suspension cells a decline immediately after addition of the protein was observed. Already 1 h after treatment, the fluorescence signal was reduced by about 50% which corresponds to an even more pronounced decrease of  $\Delta\Psi_m$  (Fig. 10). The slight increase in  $\Delta\Psi_m$  in the control cells most likely reflects increasing respiration and energy demand during incubation. The early loss of potential is indicative of considerable cellular changes taking place soon after the application of harpin stress.

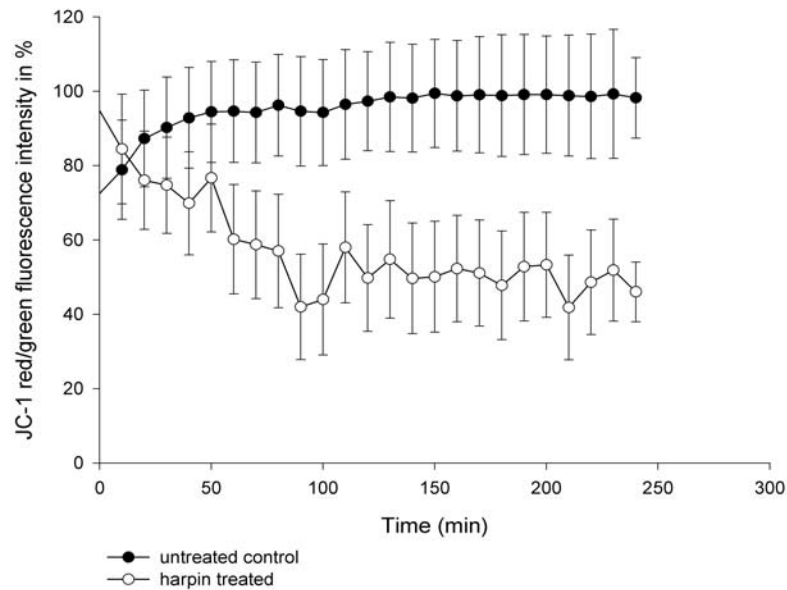


**Figure 10:** Implication of harpin on mitochondrial transmembrane potential  $\Delta\Psi_m$ .

The graph illustrates the depolarizing effect of harpin on mitochondrial membrane in *Arabidopsis* suspension cells in comparison with untreated control cells. JC-1 labeled cells were treated with 50  $\mu\text{g/ml}$  harpin or non-treated, followed by immediately measuring of red and green fluorescence intensity. The mitochondrial depolarization is indicated by a decrease in the red/green fluorescence intensity ratio like shown in the diagram over 240 min. Data are represented by 20 independent samples as means  $\pm$  SD.

### 2.3. Loss of intracellular ATP

A logical consequence of deteriorating  $\Delta\Psi_m$  would be a decreased phosphorylation capacity and a loss of intracellular ATP content. The rapid inhibition of ATP synthesis by harpin from *Erwinia amylovora* has already been reported for tobacco (*Nicotiana tabacum* cv. Xanthi) cell cultures (Xie and Chen, 2000). To examine how quickly a decrease of the mitochondrial transmembrane potential  $\Delta\Psi_m$  would lead to a decline in cellular energy metabolism, changes in intracellular ATP levels were measured. As a matter of fact, during the first 2.5 h of incubation the total ATP level decreased by approximately 50% (Fig. 11). In sum, harpin treatment of *Arabidopsis* cells affects mitochondrial  $\Delta\Psi_m$  and, as a consequence, ATP pool size.

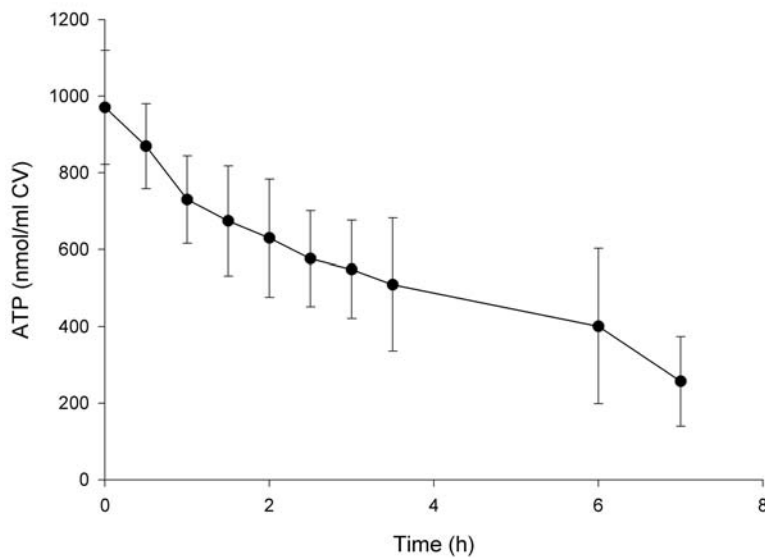


**Figure 11:** ATP levels in *Arabidopsis* suspension cells after exposure to 50 µg/ml harpin.

For determination of intracellular ATP cells were collected at indicated time points. Data for ATP concentration are the means  $\pm$  SD from three independent bioluminescence assays using a commercial ATP determination kit (Molecular Probes).

#### 2.4. Respiratory oxygen uptake

As a hallmark of harpin induced apoptosis, the early decrease in ATP synthesis already has been shown. Inhibition of ATP synthesis might be caused by uncoupling of electron transport from phosphorylation as a result of the depolarization of the inner mitochondrial transmembrane potential  $\Delta\Psi_m$ , as represented above. The decline in ATP synthesis further might be caused by blocking of mitochondrial electron transport, what would be associated with decreased respiratory  $O_2$  uptake. Respiratory oxygen consumption of isolated and then at different concentrations harpin treated mitochondria (Fig. 12a) was determined in a Clark-type oxygen electrode. Another experiment was the measurement of mitochondrial oxygen uptake after treating *Arabidopsis* cells with harpin (Fig. 12b). As shown, only a transient decline of about 25% in respiratory  $O_2$  uptake was observed up to 4 h after treatment, and the respiration was not blocked by a direct contact of mitochondria with harpin protein.

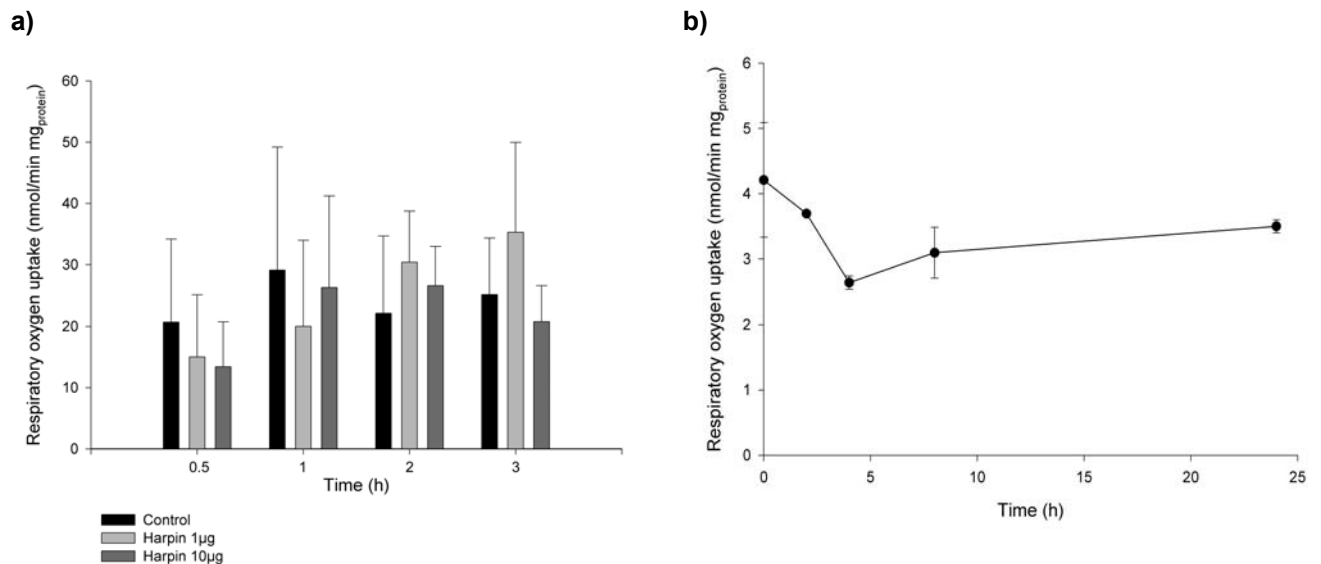


**Figure 12:** Respiratory O<sub>2</sub> uptake of isolated mitochondria after harpin treatment.

**a)** From *Arabidopsis* suspension cells isolated mitochondria were treated with harpin at different length of time and different concentrations. Respiratory O<sub>2</sub> uptake was estimated by Clark-electrode after addition of succinate as substrate and in the presence of ADP. Means  $\pm$ SD ( $n=3$ ) for oxygen consumption rates are presented.

**b)** Mitochondrial oxygen uptake after treating *Arabidopsis* cells with harpin at 50 µg/ml. At indicated time points cells were harvested, mitochondria were isolated, and O<sub>2</sub> uptake was measured at same conditions. Data are represented by 3 independent samples as means  $\pm$ SD.

## 2.5. Induction of alternative oxidase

A decline in cellular energy metabolism, measurably on decreasing intracellular ATP levels might also be caused by conversion of electron transport from cytochrome oxidase pathway to alternative respiration pathway via alternative oxidase (AOX). Inhibition of cytochrome c dependent respiration by antimycin or NO has been shown to be accompanied by induction of alternative oxidase (Huang et al., 2002; Vanlerberghe et al., 2002). AOX acts as part of the mitochondrial electron transport chain and can reduce mitochondrial generation of ROS. It catalyzes the oxidation of ubiquinol and the reduction of oxygen to water, bypassing the final steps of the cytochrome pathway. Therefore, AOX induction is regarded as a marker for mitochondrial oxidative stress and reduced cytochrome c dependent respiration.

The AOX1a probe constructed for Northern hybridization were based on primers as described previously and targets the coding region within the first exon of the AOX 1a gene (Huang et al., 2002). Cells were treated with harpin as described. Total RNA was extracted at the indicated time points and subjected to Northern blot hybridization (Fig. 13). The strong induction of the transcript encoding AOX1a with the highest level 4 h after treatment with harpin trails membrane depolarization and cytochrome c release from mitochondria.

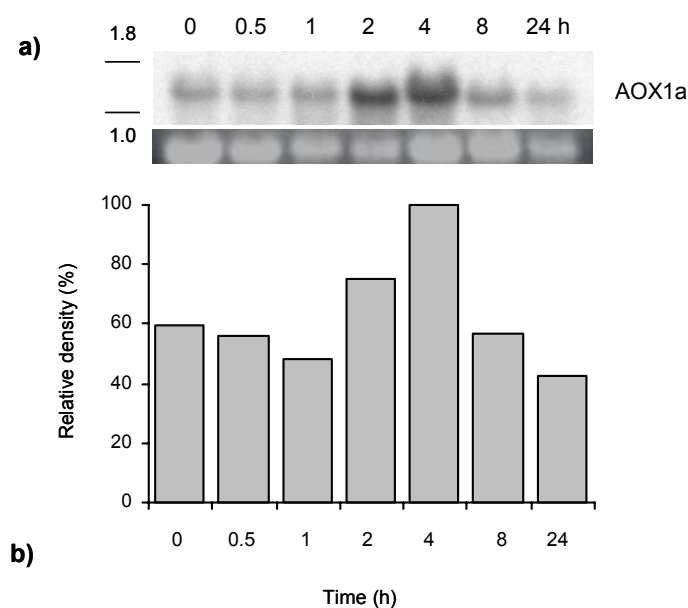


**Figure 13:** AOX1a gene expression in *Arabidopsis thaliana* suspension cells.

**a)** Cell suspension cultures were incubated with harpin (50  $\mu\text{g/ml}$ ) and collected at the times indicated for RNA preparation. Northern blot was probed with cDNA for AOX1a based on the primer pair as described in *methods*. Shown is the region between 1.8 and 1.0 kb. The upper panel represents the timecourse of AOX1a induction during a 24 h period. Ethidium bromide staining (lower panel) shows equal loading of the gel. The experiments were repeated three times.

**b)** AOX1a was quantified by densitometric scanning of the blot and plotted against time in hours after harpin treatment. The diagram shows the relative density at indicated time points, which refers to the maximum accumulation of AOX1a transcripts at 4 h.

## 2.6. Cytochrome c release from mitochondria

During the process of apoptosis in animals, elevated cytosolic  $\text{Ca}^{2+}$  level and oxidative stress both contribute to the opening of the mitochondrial permeability transition pore (PTP), which depolarizes the mitochondria and leads to mitochondrial swelling and subsequent release of cytochrome c from the intermembrane space (Goldstein et al., 2000). Cytochrome c normally functions as part of the respiratory chain, but when released into the cytosol (as a result of PTP opening) it becomes a critical component of the apoptosis execution machinery, where it activates caspases (cysteine aspartate proteases) and causes apoptotic cell death (Thornberry and Lazebnik, 1998).

There are few reports on release of cytochrome c from plant mitochondria. In tobacco treated with menadione as well as during agrobacterium induced apoptosis in maize, cytochrome c release has been associated with cell death (Sun et al., 1999; Hansen, 2000). Nevertheless, cytochrome c release by impact of ROS or by inhibition of electron transport has been postulated to activate plant PCD (Hoeberichts and Woltering, 2003). Here, treatment of *Arabidopsis* cells with harpin protein induced a rapid cytochrome c release from mitochondria into the cytosol as detected by immunoblotting using a commercial cytochrome c antibody. This release seems to be complete after 3 h (Fig. 14). A further and so far unknown protein of approximately 6-7 kD higher mass became apparent after 5 h of treatment whereas cytochrome c appears to decrease. In this context it should be noted that in yeast ubiquitin conjugation of cytochrome c has been observed (Pearce and Sherman, 1997).

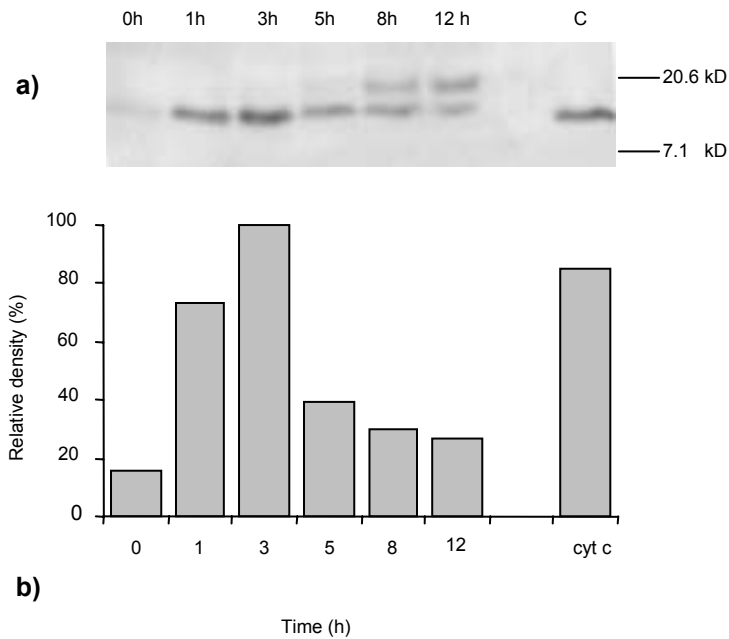


**Figure 14:** Cytochrome c release from mitochondria in response to harpin treatment.

**a)** Western blot analysis of cytochrome c in the cytosolic fraction of *Arabidopsis* suspension cells treated with 50  $\mu\text{g/ml}$  harpin. The 7H8.2C12 antibody identifies cytochrome c as a ~ 15 kD protein (lower band). An unidentified protein (upper band) of approximately 16-20 kD becomes prominent after 5 h. As positive control 0.01  $\mu\text{g}$  of mouse cytochrome c (Roche Diagnostics) were loaded on the gel (right lane).

**b)** The release of cytochrome c was quantified by densitometric scanning of the blot and plotted against time in hours after harpin treatment. The diagram shows the relative density at indicated time points which refers to the maximum amount of cytochrome c released.

## 2.7. Nuclear translocation of cytochrome c

Different cell death mechanisms control many physiological and pathological processes in mammals. Mitochondria play important roles in cell death through the release of pro-apoptotic factors such as cytochrome c, which activate caspase dependent and caspase independent cell death, respectively. A recent study has also demonstrated that cytochrome c, once released from mitochondria upon apoptosis induction, gradually accumulates in the cell nucleus. Parallel to the nuclear accumulation of cytochrome c, a release of acetylated histone H2A from the nucleus to the cytoplasm was observed. Cytochrome c was also found to induce chromatin condensation, the nuclear translocation of cytochrome c was independent of caspase activation (Nur et al., 2004).

Plant PCD shares many of the animal PCD features such as the involvement of mitochondria in apoptotic events. It was obvious to check, whether harpin induced cell death in *Arabidopsis* is likewise accompanied by a nuclear translocation of cytochrome c after its release into the cytosol.

Indeed, treatment of *Arabidopsis* cells with harpin induced an accumulation of cytochrome c in nuclear fractions as detected by immunoblotting under utilization of a signal enhancing chemiluminescence Western blotting kit (Fig. 15). In order to exclude a contamination of the nuclear fractions with cytochrome c containing mitochondria, the membrane was stripped and re-probed with a mitochondria specific anti- $\beta$ -ATPase monoclonal antibody (a gift from Thomas E. Elthon).

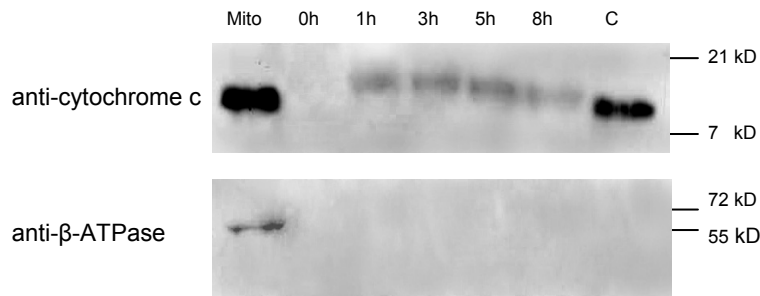


**Figure 15:** Harpin induces nuclear translocation of cytochrome c.

Immunoblotting study of cytochrome c distribution in nuclear fractions of harpin treated *Arabidopsis* suspension cells (upper panel). The purity of the nuclear fractions was verified by Western blotting using anti-β-ATPase antibody for detecting mitochondrial-specific protein (lower panel).

## 2.8. Analysis of the mitochondrial transcriptome

Harpin induces the expression of several plant defense genes including those encoding glutathione-S-transferase (GST), anthranilate synthase (ASA1) and phenylalanine ammonia-lyase (PAL) (Desikan et al., 1998). To identify genes encoding mitochondrial proteins that change in a harpin specific matter, expression profiling was performed on *Arabidopsis* suspension cells, exposed to treatment of 50 μg/ml harpin. Using commercial *Arabidopsis* microarrays consisting of ~21,500 oligomers, changes in mitochondrial transcript accumulation were monitored at four time points within 24 h after harpin treatment. At time 416 mitochondrial proteins are known (Heazlewood et al., 2004), 390 oligonucleotides of their encoding genes are localized on used arrays. Analysis of the array data revealed a total of 199 genes (see also supplement 1 at the attached CD-ROM) showed significant changes in transcript abundance in response to the bacterial elicitor (Fig. 16).

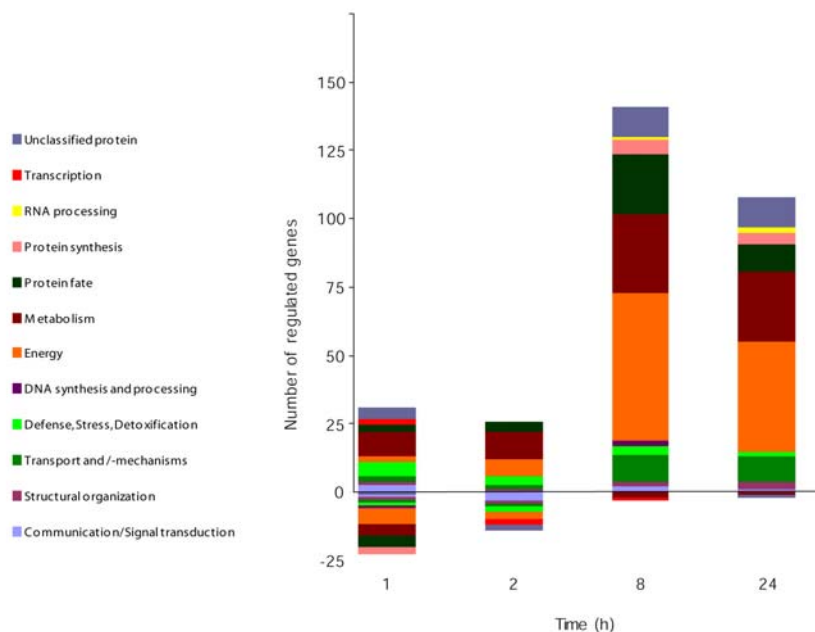


**Figure 16:** Changes in transcript accumulation of genes encoding mitochondrial proteins in *Arabidopsis*.

Shown are the gene expression dynamics for the first 24 h after harpin treatment. Differentially transcribed genes were grouped into twelve functional categories on basis of the TIGR and the MIPS *Arabidopsis thaliana* databases. Bars represent the number of significant regulated genes at each time point.

These up or down regulated genes were categorized according to the Arabidopsis Mitochondrial Protein Database (Heazlewood et al., 2004; Heazlewood and Millar, 2005). As shown, treatment with harpin protein caused a significant induction after 8 h. It mainly concerns genes which encoding mitochondrial enzymes involved in metabolism, energy, transport mechanisms, and protein fate. Very similar expression patterns were observed after 24 h. Comparing the mitochondrial and the global gene regulation dynamics during harpin treatment (Fig. 17), nearly contrary expression behaviour was observed: global, *Arabidopsis* cells show a rapid increase of transcript level after 1 h; already after 2 h the amount of repressed transcripts increases dramatically. In contrast, transcript level of genes encoding mitochondrial proteins reaches the maximum after 8 h, and shows nearly the same after 24 h, the number of down regulated genes seems steady to decrease but at a comparatively low level.

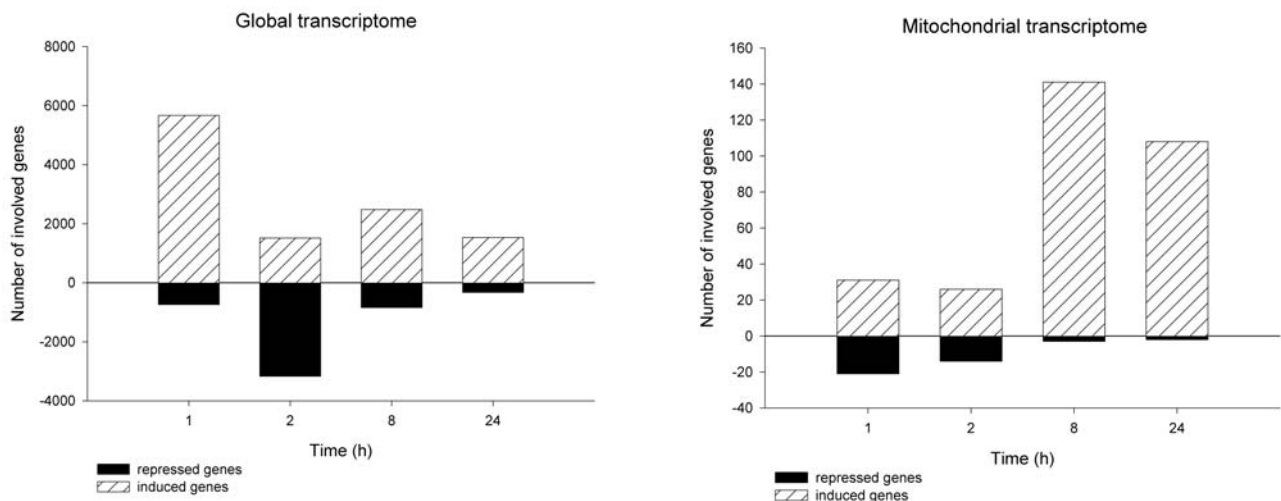


**Figure 17:** Comparison of mitochondrial and global gene expression dynamics during harpin treatment.

Bars represent the number of significant regulated genes, hatched for induced and black for repressed. Data derive from Agilent *Arabidopsis* 2 microarrays, consisting of ~21,500 oligonucleotides.

### 2.8.1. Increased transcript levels of citric acid cycle related genes

The rate of the tricarboxylic or citric acid cycle (TCA) is directly associated with the demand of cells for ATP. Cells are always anxious to keep their energy level constant. When electrons are transferred from NADH and FADH<sub>2</sub> to O<sub>2</sub> through the electron transport chain (ETC), the supply of NAD<sup>+</sup> and FAD signals a low energy charge.

Analyzing the transcript accumulation of genes encoding mitochondrial enzymes of the TCA (Fig. 18), a significant up-regulation for genes of all TCA cycle related enzyme complexes was observed. While 3 genes encoding fumarase (At5g50950), malate dehydrogenase (At5g58330), and aconitase (At2g05710) are clearly induced within 4 h the latest, the transcript levels of 22 other genes of the TCA cycle enzyme complexes are increased significant 8 h after harpin treatment, 12 of them still after 24 h.



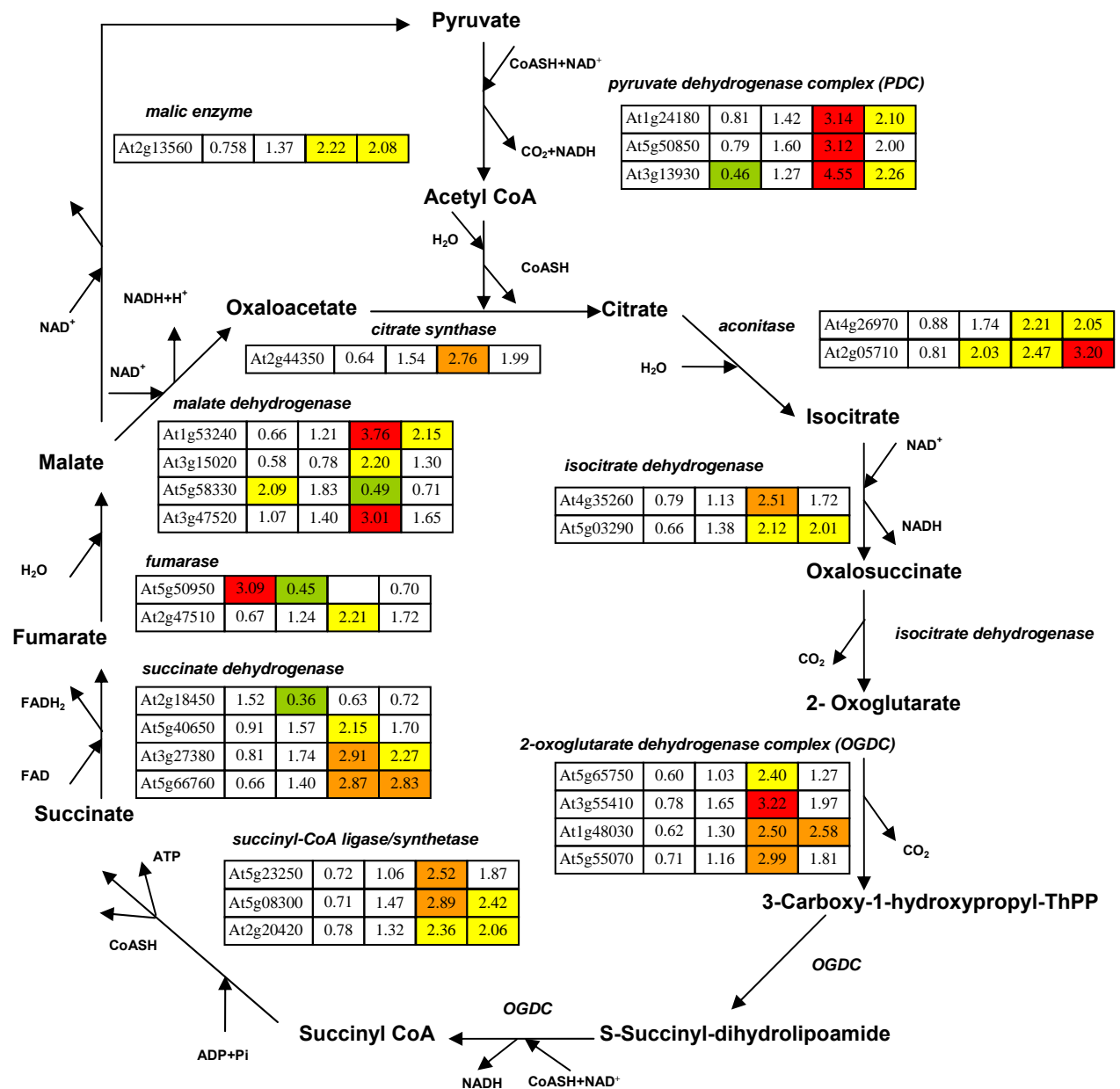


**Figure 18:** Transcript abundance of genes encoding proteins of the citric acid cycle.

Statistically significant changes at transcript levels are shown as yellow, orange, red (different strong induced) or green (repressed). Numbers in boxes indicate fold change relative to the appropriate control sample. Boxes from left to right contain AGI-number, and means of transcript regulation 1h, 4h, 8h and 24 h after harpin treatment.

### 2.8.2. Induction of genes of the electron transport chain

During the substrate-level phosphorylation, the catabolism (break down) of glucose by glycolysis and TCA cycle, some of the ATP is formed, needed by the plant. Substantially higher amounts of ATP are synthesized through the electron transport chain (ETC) and subsequent oxidative phosphorylation. Thereby NADH and FADH<sub>2</sub>, which derive from glycolysis and TCA cycle, are used as source of high-energy electrons. The electron transport chain passes the electrons through a series of protein complexes (complex I-IV), which are located in the inner mitochondrial membrane. It results in a transfer of electrons to O<sub>2</sub> and a conversion of ADP to ATP, this phosphorylation step is catalyzed by the ATPase complex (complex V).

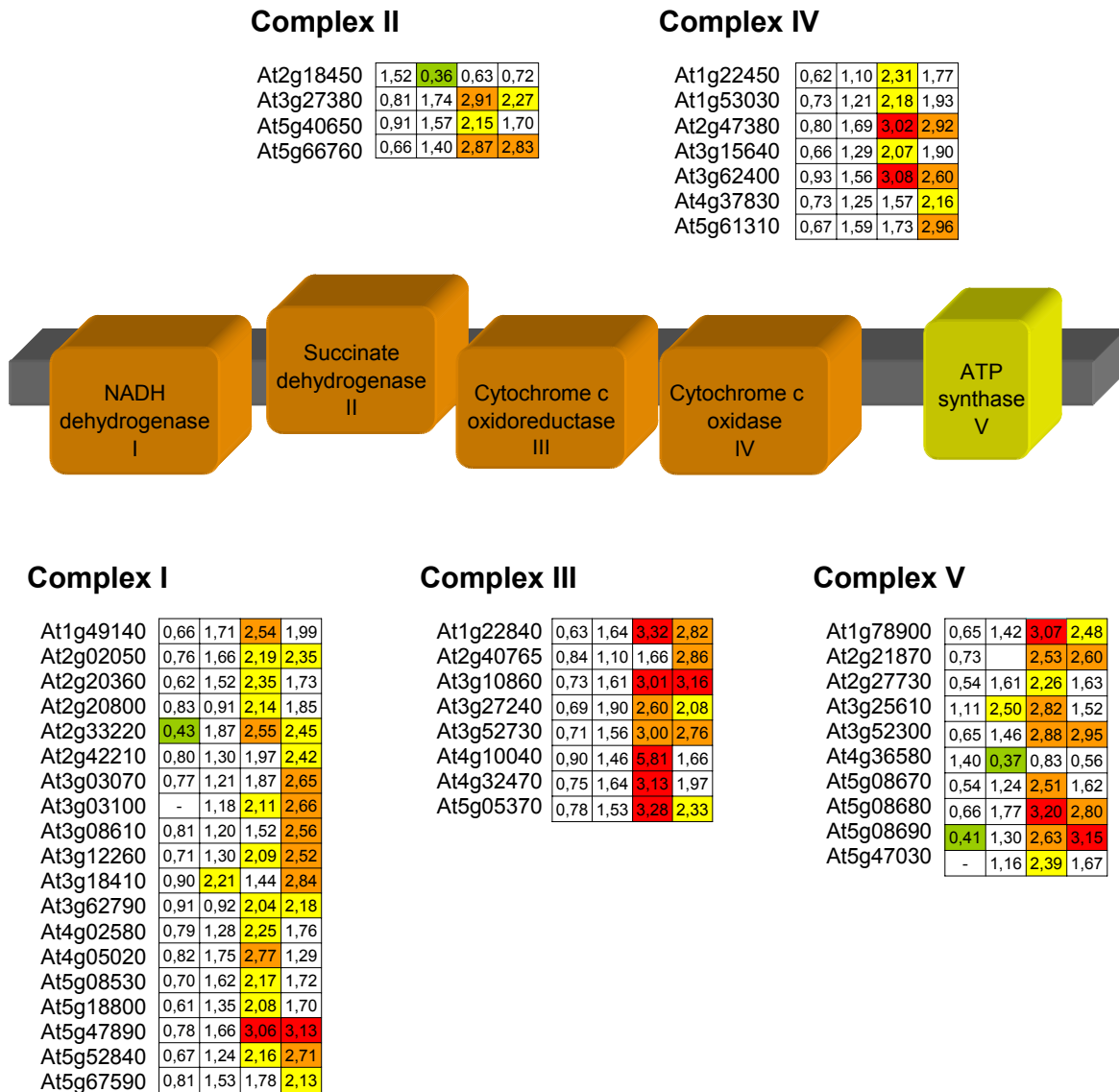


**Figure 19:** Induction of genes encoding proteins of the electron transport chain and oxidative phosphorylation.

Significant regulated genes encoding proteins of major mitochondrial complexes of electron transport chain (complex I-IV), and of oxidative phosphorylation (complex V), represented by AGI number. The genes with induction over 2.0 fold are marked by yellow, over 2.5 fold by orange and over 3.5 fold by red colored boxes. Repressed genes are green marked.

Figure 19 summarizes genes of the 5 complexes of the respiratory electron transport chain, observed as significant induced at transcript level 8 h or 24 h after harpin treatment in comparison with untreated controls.

### 2.8.3. Genomic analysis of mitochondrial carrier proteins and protein import apparatus

The mitochondrial inner membrane contains a family of proteins that transport a variety of metabolites across the membrane. In *Arabidopsis* about 50 putative members are known, but only a limited number of individual mitochondrial carriers have been functionally characterized (Fernie et al., 2004). Table 1 summarizes mitochondrial carrier identified as significant induced at transcript level under harpin stress. The porins or voltage-dependent anion-selective channel proteins (VDAC) are

mitochondrial membrane carriers which allow the channel transport of small molecules (<8 kDa) across the outer mitochondrial membrane (Millar et al., 2001). Three members of the porine family (At3g01280, At5g15090, and At5g67500) are up regulated 8 hours after treatment. Furthermore, transcripts from carriers of known function such as ADP/ATP translocator (At5g13490), phosphate translocator (At5g14040), and adenylate translocator (At3g08580) are induced at the same time, and the 2-oxoglutarate/malate carrier (At5g19760) after 24 h. The increased transcript accumulation of the gene encoding the ADP/ATP translocator is consistent with the observation of higher rates of TCA and oxidative phosphorylation respectively, which theoretical result in higher ATP amounts. Consequently there would be a need to export more ATP out of the mitochondria and into the cytoplasm. Likewise, more ADP must be transported back into mitochondria for conversion into ATP. The transcript of mitochondrial uncoupling protein (At3g54110) which is reported to lower the ROS formation and to influence the tricarboxylic acid cycle flux in potato mitochondria (Smith et al., 2004), is significant induced 8 h after harpin treatment.

**Table 1:** Transcriptional analysis of mitochondrial carrier proteins in *Arabidopsis thaliana*.

Genes with more than 2.0-fold activation are bold, repression is indicated by underlining. Unmarked numbers indicate weak signals that are less than two-fold greater than surrounding background. Gene names are supplemented by GeneBank accession numbers (AGI).

AGI	Description	1h	2h	8h	24h
<b>mitochondrial carrier</b>					
At1g32050	secretory carrier membrane protein	0.79	<b>2.18</b>	<b>3.48</b>	<b>2.99</b>
At5g13490	ADP/ATP carrier protein 2	0.78	<b>2.17</b>	<b>3.82</b>	<b>3.72</b>
At5g46800	carnitine/acyl carrier, putative	1.18	1.72	1.25	1.15
At5g01340	succinate/fumarate carrier	1.47	1.55	1.90	1.21
At5g14040	phosphate carrier	0.64	1.55	<b>3.89</b>	<b>2.85</b>
At3g08580	adenylate carrier	0.52	1.52	<b>3.60</b>	<b>3.73</b>
At4g01100	mitochondrial carrier protein family	0.57	1.49	<b>2.56</b>	<b>3.66</b>
At5g19760	2-oxoglutarate/malate carrier	0.61	1.43	1.80	2.20
At5g15640	mitochondrial carrier protein family	1.01	1.33	<b>2.62</b>	1.41
At3g54110	uncoupling protein (ucp/PUMP)	0.67	1.26	<b>2.16</b>	<b>2.03</b>
At1g79900	mitochondrial carrier protein family	0.86	0.93	0.93	0.98
At2g33820	mitochondrial carrier protein family	1.20	<u>0.49</u>	1.13	1.15
<b>mitochondrial membrane carrier</b>					
At3g01280	VDAC1	0.56	1.16	<b>2.90</b>	<b>2.44</b>
At5g15090	VDAC3	<u>0.49</u>	1.49	<b>3.59</b>	<b>2.09</b>
At5g67500	VDAC5	0.72	1.42	<b>2.32</b>	1.45

Mitochondria import nuclear-encoded cytosolically synthesized proteins via mitochondrial protein import apparatus, in *Arabidopsis* encoded by 31 genes. These genes are divided into subclasses according to their mitochondrial sub-compartment such as translocases of the outer membrane (TOM) and the inner membrane (TIM) as well as several chaperones (Lister et al., 2004). The transcript accumulation of genes encoding proteins of the mitochondrial protein import apparatus was analyzed using the MPIMP (Mitochondrial Protein Import Machinery of Plants) database (<http://millar3.biochem.uwa.edu.au/~lister/index.html>), presented in table 2. It is not surprising that transcripts show an increase of induction 8 h after elicitor treatment, this is the expression dynamic of nearly all genes encoding mitochondrial proteins. With 21 genes an induction of almost 68% of all known genes of the mitochondrial protein import apparatus was observed.

**Table 2:** Transcriptional analysis of the mitochondrial protein import apparatus.

Genes were identified and classified using the MPIMP (Mitochondrial Protein Import Machinery of Plants) database. Genes with more than 2.0-fold activation are bold, repression is indicated by underlining. Unmarked numbers indicate weak signals that are less than two-fold greater than surrounding background. Gene annotations are supplemented by GeneBank accession numbers (AGI).

Gene	AGI	Name	1 h	2 h	8 h	24 h
TIM9	At3g46560	small zinc finger-like protein TIM9	<u>0.49</u>	1.05	<b>2.61</b>	<b>2.86</b>
TIM10	At2g29530	expressed protein	0.66	1.08	<b>2.04</b>	<b>1.91</b>
TIM13	At1g61570	expressed protein	<u>0.41</u>	0.82	<b>2.37</b>	<b>2.11</b>
TIM14-3	At5g03030	DNAJ protein - like	0.56	1.55	<b>6.13</b>	1.44
TIM17-2	At2g37410	putative protein translocase	0.64	1.80	<b>3.48</b>	<b>2.84</b>
TIM23-2	At1g72750	inner mitochondrial membrane protein	0.87	1.47	<b>3.37</b>	0.82
TIM50	At1g55900	unknown protein	0.59	0.86	1.49	<b>2.39</b>
TOM5	At5g08040	putative protein	0.58	1.16	<b>2.68</b>	<b>2.44</b>
TOM6	At1g49410	expressed protein	0.54	1.09	<b>2.23</b>	<b>2.73</b>
TOM9-2	At5g43970	putative protein	<u>0.47</u>	0.92	<b>2.00</b>	<b>2.60</b>
TOM20-3	At3g27080	TOM20, putative	0.64	1.31	<b>2.07</b>	1.69
TOM20-4	At5g40930	protein import receptor TOM20, mitochondrial-like	0.52	1.54	<b>2.61</b>	1.90
MPP ALPHA	At3g16480	putative mitochondrial processing peptidase alpha subunit	0.52	1.59	1.69	<b>2.24</b>
MPP BETA	At3g02090	putative mitochondrial processing peptidase	0.53	1.64	<b>3.06</b>	<b>2.60</b>
TIM44-2	At2g36070	hypothetical protein	<u>0.49</u>	0.91	1.80	1.23
HSP70-4	At4g37910	heat shock protein 70 like protein	0.60	0.92	<b>3.81</b>	<b>2.02</b>
HSP70-5	At5g09590	heat shock protein 70 (Hsc70-5)	0.60	1.21	<b>8.94</b>	1.67
MGE	At5g17710	chloroplast GrpE protein	0.76	<b>2.10</b>	1.18	1.27
MDJ	At3g44110	DnaJ protein homolog atj3	0.89	1.58	<b>3.69</b>	<b>2.11</b>
HSP60	At3g23990	mitochondrial chaperonin hsp60	<u>0.48</u>	1.40	<b>4.78</b>	1.83
HSP10	At1g14980	10 kDa chaperonin (CPN10)	<u>0.49</u>	1.13	<b>3.68</b>	<b>2.53</b>

## 2.9. Analysis of the mitochondrial proteome

### 2.9.1. Regulation of mitochondrial proteins in response to harpin

Although an opulence of data is obtained when using transcript analysis to determine differential gene expression, it is clear that transcription, translation, post-translational modifications and the turnover of mRNA, proteins and metabolites are interconnected intense with one another. For this reason it makes sense to move toward integrated approaches wherein transcripts, proteins, and metabolites are measured (Fernie and Sweetlove, 2003). As next, analysis was focused on changes in abundance of mitochondrial proteins from *Arabidopsis* cells undergoing harpin stress. To identify significant regulations, proteins of isolated mitochondria from control cells, from 8 h harpin treated cells, and from 24 h harpin treated cells were separated by 2D-gel electrophoresis (Fig. 20). After gel staining, protein spots were quantified and normalized; spots that changed intensities at least 2-fold during time course in three replicate gels were identified using MALDI-TOF Mass Spectrometry for peptide fingerprint analysis<sup>\*)</sup>. As above mentioned, mitochondrial transcript analysis revealed a total of 199 genes encoding mitochondrial proteins, whose transcripts are significant up or down regulated in response to harpin.

<sup>\*)</sup> 2D-analysis and MALDI-TOF was done by TopLab company / Martinsried.

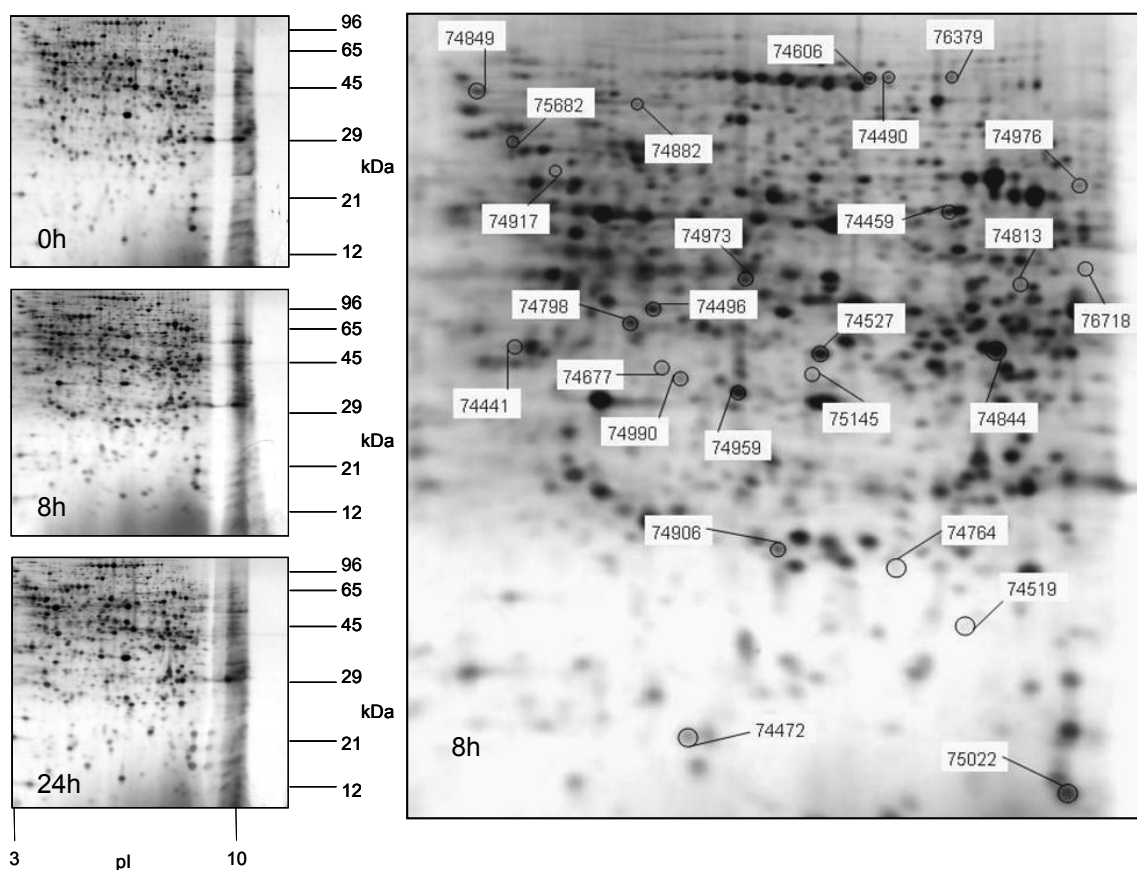


**Figure 20:** Two-dimensional separations of mitochondrial fractions from *Arabidopsis thaliana*.

Mitochondrial fractions of harpin treated *Arabidopsis* suspension cells were separated (pI 3-10) on 2-D Gels, proteins were visualized by Sypro Ruby staining. Circled spots (completed with spot ID's) are differentially regulated proteins at 8h or 24h or at 8h and 24h after harpin treatment, compared with protein spot intensities in untreated controls. Numbers on x axis are pI and numbers on y axis are apparent molecular masses. Each gel result was repeated in triplicate.

At protein level significant changes in regulation of 28 mitochondrial proteins were observed (Tab. 3), spot intensities of 13 proteins were at least 2-fold increased and of further 15 significant decreased in relative abundance. The overall strongest up regulation of a protein was determined for ATP dependent protease ClpC2 (At3g48870), increased by a factor of 6.79 (8h) and 3.26 (24h). The actin-depolymerizing factor ADF3 (At5g59880) was identified with a 3.75-fold increased abundance after 8h.

### 2.9.2. Proteins of the citric acid cycle

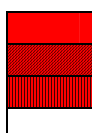
Noteworthy is the regulation of 9 citric acid cycle related proteins. Citrate synthase (At2g42790), NAD<sup>+</sup> isocitrate dehydrogenase (At3g09805), NAD dependent malate dehydrogenase (At1g53240), and the E1 beta subunit of pyruvate dehydrogenase (At5g50850) were identified as significant up regulated at protein level. Among proteins with decreased relative abundance 3 subunits of the 2-oxoglutarate dehydrogenase complex and 2 NAD dependent malate dehydrogenases were identified as exclusively up regulated at transcript level.

Further comparison of protein abundance changes with transcript abundance changes revealed an overlap for NAD-dependent malate dehydrogenase (At1g53240) and pyruvate dehydrogenase E1 beta subunit (At5g50850), showing same regulation patterns at both levels. The NAD<sup>+</sup> isocitrate dehydrogenase (At3g09805) transcript did not show significant change in abundance, but the protein, which was not detectable in controls, was up regulated in treated samples, suggesting a post-transcriptional control of protein abundance. The citrate synthase (At2g42790) likewise belongs to the group of proteins only are up regulated at protein level, but an isoform is regulated at transcript level too.

**Table 3:** Identification of 2-D separated proteins from *Arabidopsis* mitochondria.

Displayed are only significant regulated mitochondrial proteins identified from their peptide mass fingerprint by searching the NCBI database. Proteins with more than 2.0-fold up-regulation are bold; down-regulation is indicated by underlining. Unmarked numbers indicate weak signals that are less than two-fold greater than surrounding background. Protein annotations are supplemented by GeneBank accession numbers of the encoding genes (AGI). Additionally, the accordance of protein analysis with findings obtained from transcript analysis is marked in the last column.

Spot ID	Protein	AGI	MW (kDa)	pI	Sequence Coverage	Probability	Regulation 8h	Regulation 24h	Accordance
74441	pyruvate dehydrogenase E1 beta subunit	At5g50850	39.4	5.7	45%	2.3 e-19	1,79	<b>2,45</b>	
74459	2-oxoglutarate dehydrogenase, E3 subunit		50.3	6.0	28%	4.0 e-47	<u>0,48</u>	1,10	
74472	actin-depolymerizing factor 3 (ADF3)	At5g59880	14.2	5.0	77%	7.2 e-18	<b>3,75</b>	0,66	
74490	2-oxoglutarate dehydrogenase, E1 subunit	At3g55410	114.9	6.7	37%	3.1 e-75	<u>0,25</u>	1,27	
74496	glutamine synthetase	At5g35630	47.1	6.7	29%	5.0 e-22	<b>2,44</b>	0,76	
74519	NADPH:quinone oxidoreductase	At3g27890	21.5	6.8	63%	4.3 e-05	<u>0,34</u>	1,12	
74606	selenium-binding protein-like	At3g12780	78.9	8.3	14%	3.6 e-06	<u>0,42</u>	1,30	
74677	NAD-dependent malate dehydrogenase	At3g15020	36.0	8.5	52%	2.4 e-15	<u>0,48</u>	1,49	
74731	ATP-dependent Clp protease, ClpC1	At5g50920	103.7	6.4	32%	9.9 e-31	1,08	<u>0,40</u>	
74764	putative [Mn] superoxide dismutase	AT3g10920	25.5	8.5	56%	4.7 e-22	<u>0,23</u>	0,80	
74813	Alanine-glyoxylate aminotransferase 2	At4g39660	52.3	7.9	57%	1.2 e-40	<u>0,42</u>	0,64	
74844	glyceraldehyde-3-phosphate dehydrogenase	At3g04120	37.1	6.6	66%	1.0 e-50	<b>2,42</b>	0,73	
74849	heat shock protein, putative	At3g07770	91.2	5.3	45%	1.2 e-67	0,76	<b>2,95</b>	
74882	ATP-dependent Clp protease, ClpC2	AT3g48870	61.9	9.3	34%	1.4 e-34	<b>6,79</b>	<b>3,26</b>	
74906	glutathione S-transferase	AT1g02930	23.5	5.8	51%	1.4 e-20	<b>2,22</b>	<u>0,34</u>	
74917	methionyl-tRNA synthetase (AtpMetRS)	At3g55400	69.8	6.2	39%	6.5 e-39	<u>0,27</u>	1,15	
74959	NAD-dependent malate dehydrogenase	At1g53240	36.0	8.9	37%	1.4 e-24	1,74	<b>3,24</b>	
74973	stomatin-like protein	AT4g27585	45.1	6.3	74%	2.3 e-66	<u>0,46</u>	0,94	
74976	L-Galactono-1,4-lactone dehydrogenase	At3g47930	68.8	9.0	44%	1.2 e-50	<u>0,28</u>	<b>2,01</b>	
74990	NAD-dependent malate dehydrogenase	At1g53240	36.0	8.9	16%	7.5 e-11	<u>0,38</u>	1,25	
75022	nucleoside diphosphate kinase 3, NDPK3	At4g11010	25.8	9.3	29%	2.3 e-23	<u>0,48</u>	1,22	
75682	heat shock protein 70 like protein	AT4g37910	71.4	5.3	59%	2.6 e-77	<u>0,38</u>	1,41	
76379	2-oxoglutarate dehydrogenase, E1 subunit	At5g65750	117.6	7.1	37%	6.4 e-66	<u>0,39</u>	0,99	
74715-2	H <sup>+</sup> -transporting ATP synthase beta chain	At5g08680	60.0	6.1	25%	2.1 e-08	1,10	<u>0,40</u>	
74798-2	Putative acyl-acyl carrier protein desaturase	At1g43800	42.4	5.9	23%	7.8 e-05	<b>2,36</b>	0,94	
75145-1	NAD <sup>+</sup> isocitrate dehydrogenase, putative	At3g09805	40.9	6.7	37%	6.2 e-16	not in controls	not in controls	
76718-1	putative phospholipid cytidyltransferase	At2g38670	47.4	7.3	26%	2.1 e-11	<u>0,35</u>	<b>2,83</b>	
76718-2	citrate synthase, putative	At2g42790	56.3	7.2	22%	6.0 e-07	<u>0,40</u>	<b>2,80</b>	



Gene is significantly induced, and the protein accumulates significant over control level.  
Gene is significantly induced, and the protein recovers significantly from low 8h level.  
Gene is significantly induced, and the protein accumulation is statistically not significant.  
Gene induction is statistically not significant, and the protein accumulation is significantly regulated.

## 2.10. Activity of citric acid cycle related enzymes

The consequences of harpin treatment on enzyme activities in *Arabidopsis* mitochondria was investigated especially for citric acid cycle related enzymes (Fig. 21).

For the initial reaction of the TCA, the oxaloacetate dependent formation of citrate catalyzed by citrate synthase, no loss in activity was found. Aconitase, isomerizing citrate, showed an initial 60% decrease in activity during the first 2 h after addition of harpin, but it reaches the control level again after 12 h and no additional decrease occurred.

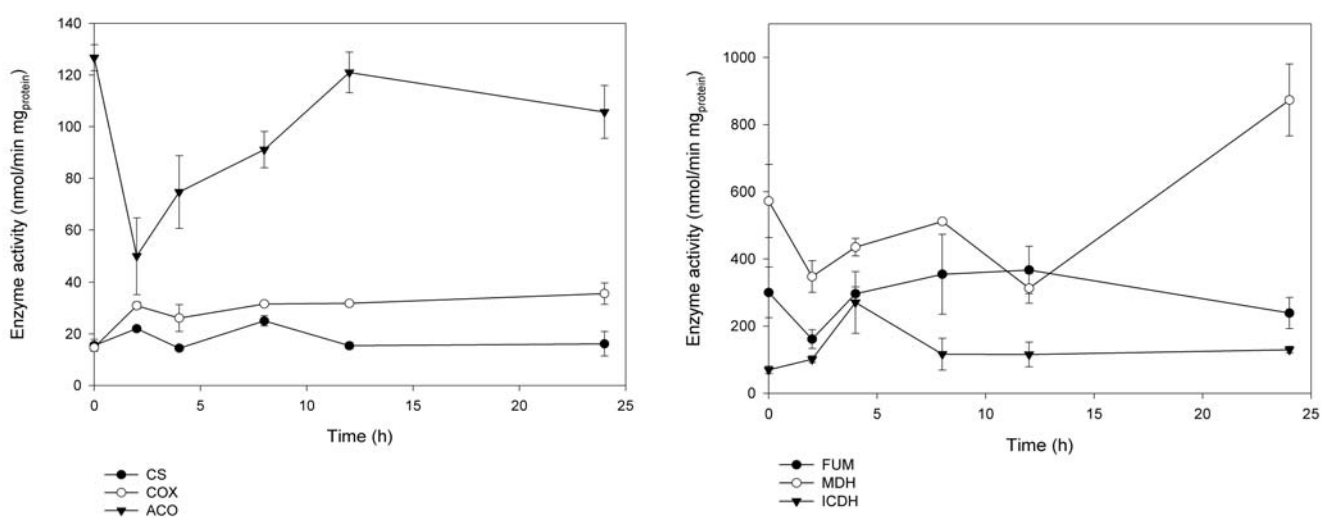


**Figure 21:** Enzyme activity in *Arabidopsis* mitochondria after harpin stress.

Specific activity is estimated in units per mg protein for the enzymes: citrate synthase (CS), cytochrome c oxidase (COX), aconitase (ACO), fumarase (FUM), malate dehydrogenase (MDH), and isocitrate dehydrogenase (ICDH). Data are means  $\pm$  SD from three independent experiments.

The oxidative decarboxylation of isocitrate, accomplished by isocitrate dehydrogenase is stimulated, within 4 h the activity quadruples but reaches the control level already 4 h later. For specific activity of fumarase, catalyzing the hydration of fumarate's double bond to form L-malate, an one-time decline after 2 h was monitored, otherwise it remains stable for 24 h. In a  $\text{NAD}^+$  dependent reaction malate dehydrogenase catalyzes the last reaction in the citric acid cycle. Following some fluctuations the activity of malate dehydrogenase increases of 50% after 24 h treatment. Summarizing, no or only a transient loss in activity of any of these enzymes was observed during 24 h after elicitor treatment.

## 2.11. Intermediates of the citric acid cycle

The results of the above experiments indicated an enhanced rate of the tricarboxylic acid cycle (TCA); further analysis was focused on intermediates of this process (Figure 22). For citrate we observed continuous increasing levels up to 300% after 24 hours. The due to the inactivation of

aconitase expected decline in isocitrate level was not confirmed. For 2-oxoglutarate level we observed an abrupt rise after 8 hours, and further a 60% decrease in oxaloacetate content, occurring within 2 hours. Like for enzyme activities, no significant decline in concentrations of citric acid cycle intermediates could be observed.

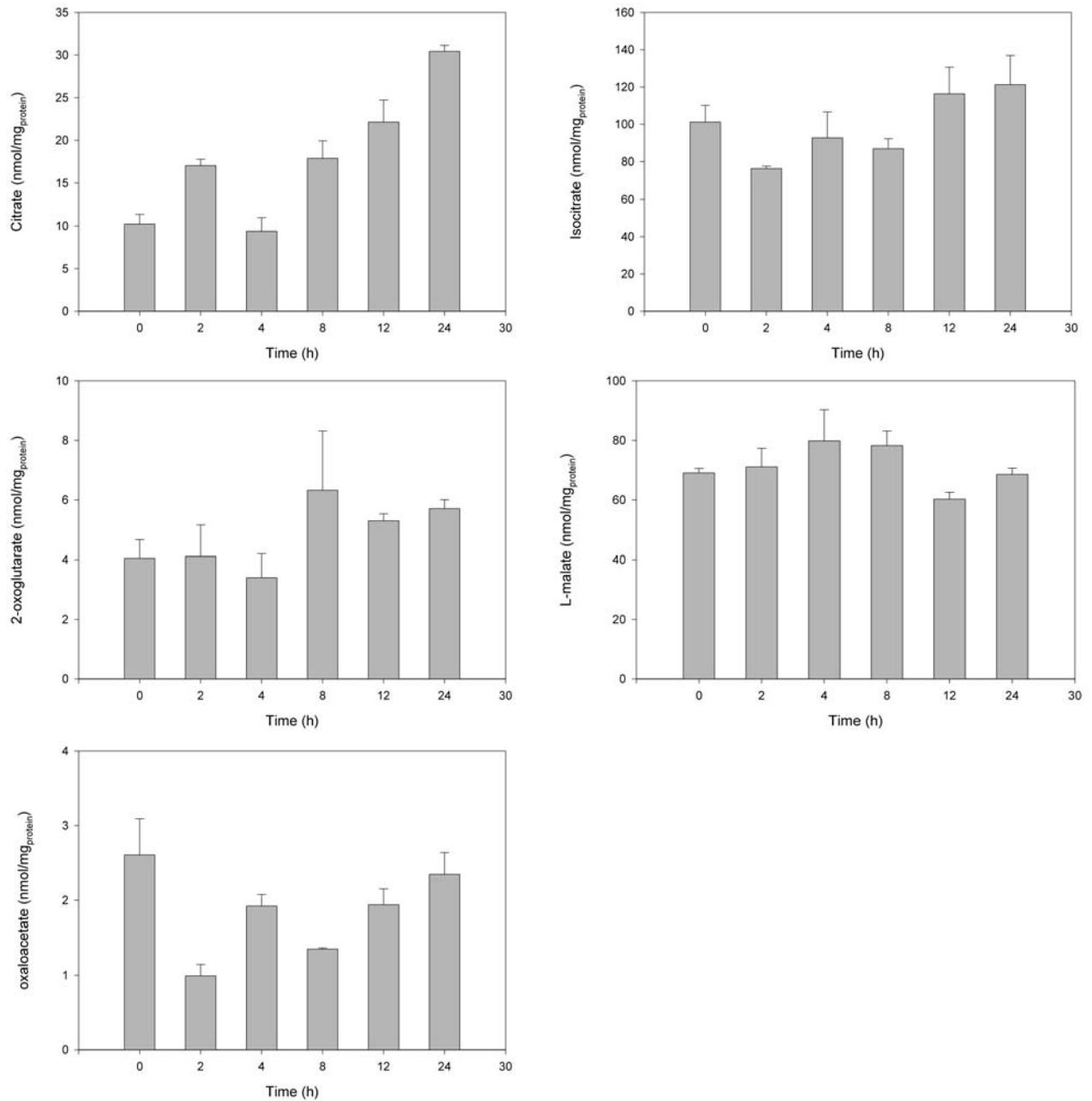


**Figure 22:** Levels of TCA metabolites in *Arabidopsis* cell extracts during harpin treatment.

All metabolite analyses were performed from the same samples of three independent experiments; concentrations are related to total protein content. Data are represented as means  $\pm$  SD.



### 3. The *Arabidopsis* transcriptome analysis of harpin induced apoptosis

#### 3.1. Two tiers of innate immune response: The transcriptome in response to harpin and LPS

(A common work of Maren Livaja and Dana Zeidler)

The aim of this work was to analyze transcriptional changes during the onset of basal of plant defense responses. There are several and particular comparing studies on *Arabidopsis* plant gene expression during pathogenic stresses such as *Pseudomonas syringae* pv. *tomato* carrying the Rpt2 gene (Scheideler et al., 2002), treatment with *Alternaria brassicicola* (Schenk et al., 2000) or infection by rhizobacteria *Pseudomonas thivervalensis* (Cartieaux et al., 2003). Further reported are transcriptome analyses of *Arabidopsis* plants stressed with from pathogens triggered defense related signaling molecules like salicylic acid (SA), methyl jasmonate (MJ), ethylene (Schenk et al., 2000; Zhong and Burns, 2003), and experiments with SAR inducing or SAR repressing treatments (Maleck et al., 2000). However, only few studies addressed basal defense or gene induction by PAMPs (Navarro et al., 2004). Here, high-density oligonucleotide microarrays (Agilent) were used to study the transcriptomes of *Arabidopsis thaliana* in response to the elicitor harpin and the PAMP LPS, respectively. Both effectors induce NO and ROS (Gerber et al., 2004; Krause and Durner, 2004), and for both effectors immunization effects were demonstrated (Grisham, 2000; Newman et al., 2002) (Tab. 4). Strikingly, while harpin treatment causes cell death in every plant species analyzed so far, LPS does not (Newman et al., 2002; Zeidler et al., 2004). Due to their homogeneity and repeatability, *Arabidopsis* cell suspension cultures were preferred for transcription profiling.

**Table 4:** Comparison of already known LPS and harpin caused events in plants.

Examples for effects in plants	LPS	Harpin	Citation
Increase of cytosolic Ca <sup>2+</sup> -levels	+	+	(Blume et al., 2000; Meyer et al., 2001; Gerber et al., 2004)
H <sub>2</sub> O <sub>2</sub> generation (oxidative burst)	+	+	(Desikan et al., 1998; Meyer et al., 2001; Gerber et al., 2004)
Media alkalinization	+	+	(Wei, 1992; Baker et al., 1993; Gerber et al., 2004)
NO generation	+	+	(Zeidler et al., 2004)
Cell death	-	+	(Xie and Chen, 2000; Krause and Durner, 2004)
Induction of resistance	+	+	(Newman et al., 2002; Dong et al., 2004)

#### 3.2. Global changes in transcriptional programs of LPS and harpin treated *Arabidopsis*

To identify genes that change in LPS and harpin stimulus specific matter, global expression profiling was performed on *Arabidopsis* suspension cells, exposed to treatments of 100 µg/ml LPS or 50 µg/ml of harpin, respectively. Using Agilent *Arabidopsis* cDNA microarrays consisting of about 15,000 oligomers, changes in transcript accumulation of treated cells and non-treated control cells were monitored at six time points within 24 h after elicitor treatment. Analysis of the array data revealed

1573 genes (see supplement 2 at the attached CD-ROM) whose expression showed significant changes in transcript abundance in response to LPS (309 genes), harpin (951 genes) or both (313 genes) of the treatments. Based on the TIGR and the MIPS *Arabidopsis thaliana* databases the elicitor specific changes in transcript abundance were categorized by function (Fig. 23). Harpin induced most transcripts very rapidly within 2 h, while the number of repressed genes remained on a comparatively low level. The great efforts of harpin-induced cells to withstand the pathogenic attack seemed to decline between 2 and 8 h after treatment, what is reflected in the simultaneous onset of cell death of harpin treated *tobacco* and *Arabidopsis* cells (Xie and Chen, 2000; Krause and Durner, 2004). In contrast, LPS induced transcript levels much slower and weaker. However, 24 h after treatment, a high number of LPS-induced genes were observed. The number of down regulated genes seemed to be nearly constant over one day. At the level of functional categories, a strong similarity between the 24-hour LPS pattern and the 30-minute pattern of harpin elicited cells is striking. At the level of individual genes, a very small overlap consisting of 25 genes after 30 minutes and 14 genes after 24 h was observed.

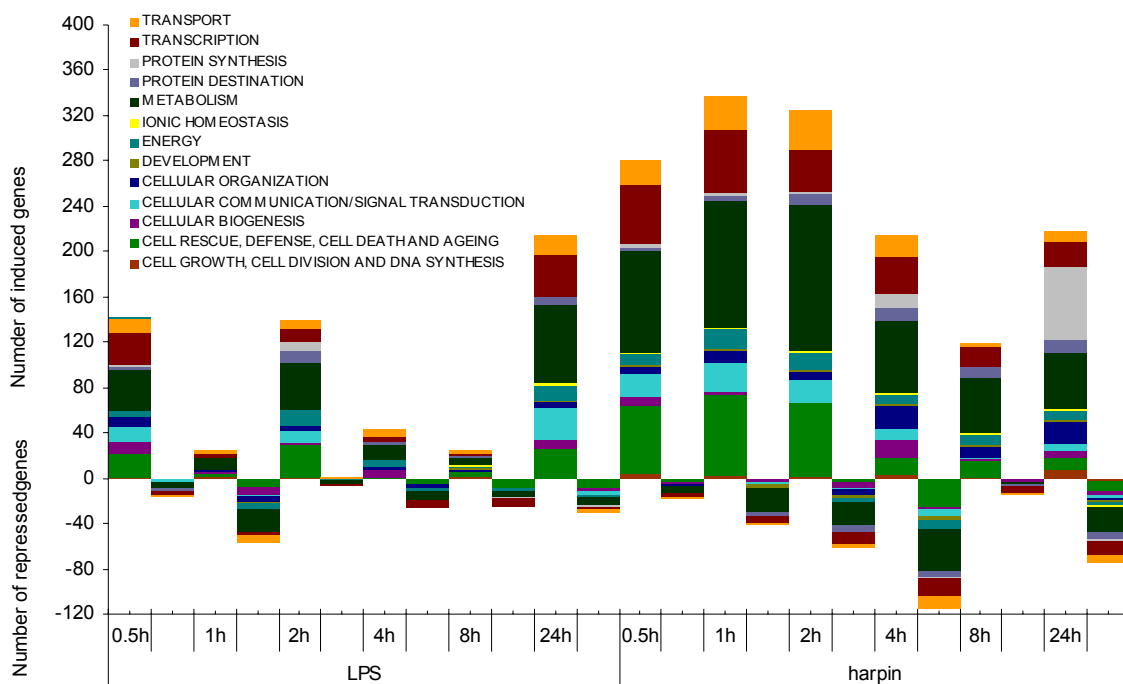


**Figure 23:** Gene expression in functional categories after LPS and harpin treatment.

Shown are the gene expression dynamics for the first 24 h after LPS and harpin treatment. Differentially transcribed genes were grouped into thirteen functional categories on basis of the TIGR and the MIPS *Arabidopsis thaliana* databases. Note that some genes can have more than one annotated function.

Interestingly, the biggest overlap (40) of genes was found between the early harpin response (30 minutes) and the late LPS response (24 h). Here, analysis is concentrated on genes encoding transcription factors, defense proteins, cell wall biogenesis related proteins and signal transduction components.

### 3.3. Majority of transcription factor genes are expressed in response to harpin

Based on the Arabidopsis Gene Regulatory Information Server (AGRIS) database of *Arabidopsis* transcription factors (Davuluri et al., 2003) the time dependent regulation of genes encoding transcription factors in *Arabidopsis* suspension cells after LPS and harpin exposure was analyzed. Genes involved in transcriptional regulation were classified by families based on sequence similarity. Currently there are 35 families listed consisting of 1.466 genes. The Agilent array used contained 1.138 transcription factor genes, of which 1.011 could be detected (Tab. 5).

**Table 5:** Summary of LPS and harpin induced transcription factor genes.

The numbers reflect classified, detected and regulated family members. The classification is based on Arabidopsis Gene Regulatory Information Server (AGRIS) database of *Arabidopsis* transcription factors (Davuluri et al., 2003).

Family name	Total	On array	Detected	%	LPS Regulated	Harpin Regulated	Σ Regulated	%
WRKY	74	55	49	89.1	4	13	14	28.6
AP2-EREBP	120	112	100	89.3	15	15	24	24.0
C2C2-Gata	28	18	13	72.2	2	2	2	15.4
G2-like	40	23	21	91.3	2	3	4	19.0
HB	66	60	56	93.3	7	5	10	17.9
MYB	137	124	108	87.1	9	14	18	16.7
bZIP	70	58	46	79.3	3	4	7	15.2
NAC	90	77	68	88.3	3	8	10	14.7
ABI3VP1	18	17	14	82.4	0	2	2	14.3
C2H2	98	85	77	90.6	5	10	11	14.3
C2C2-Dof	36	33	29	87.9	2	4	4	13.8
C3H	164	97	88	90.7	5	7	9	10.2
ARR-B	15	11	11	100.0	0	1	1	9.1
CCAAT-HAP5	13	12	11	91.7	2	1	1	9.1
C2C2-CO-like	30	26	24	92.3	1	1	2	8.3
GRAS	25	24	24	100.0	1	1	2	8.3
SBP	16	12	12	100.0	1	0	1	8.3
ARF	22	16	15	93.8	0	1	1	6.7
HSF	21	19	18	94.7	1	1	1	5.6
bHLH	146	73	66	90.4	1	2	3	4.5
Trihelix	29	24	22	91.7	0	1	1	4.5
MADS	100	79	63	79.7	0	2	2	3.2
Alfin	7	7	7	100.0	0	0	0	0.0
C2C2-YABBY	5	2	2	100.0	0	0	0	0.0
CCAAT-DR1	2	2	2	100.0	0	0	0	0.0
CCAAT-HAP2	10	10	9	90.0	0	0	0	0.0
CCAAT-HAP3	10	9	9	100.0	0	0	0	0.0
CPP	8	4	3	75.0	0	0	0	0.0
E2F-DP	8	5	5	100.0	0	0	0	0.0
EIL	6	6	5	83.3	0	0	0	0.0
GRF	9	1	1	100.0	0	0	0	0.0
MYB-related	9	8	8	100.0	0	0	0	0.0
Orphan	3	1	1	100.0	0	0	0	0.0
TCP	26	18	14	77.8	0	0	0	0.0
TUB	10	10	10	100.0	0	0	0	0.0

To identify transcription factor families, which might be involved in response of *Arabidopsis* to LPS and harpin gene expression for each family was analyzed. Overrepresented families were selected according to Hennig (Hennig et al., 2004) after following criteria: Families with less than two regulated genes were neglected. In case (i) 2 to 9 members were regulated and (ii) at least 30% of

the family was represented, the family was chosen. The same holds true if 10 or more regulated genes were counted and at least 5% of the family size was represented. Referring to these filter criteria the WRKY-family, AP2-EREBP-family, HB-family, MYB-family, NAC-family and the C2H2-family were identified as significant participated in transcriptional regulation. Again, in case of harpin, most transcription factor encoding genes responded quickly while LPS induced a much slower response (Fig. 24; see also supplement 3 at the attached CD-ROM).

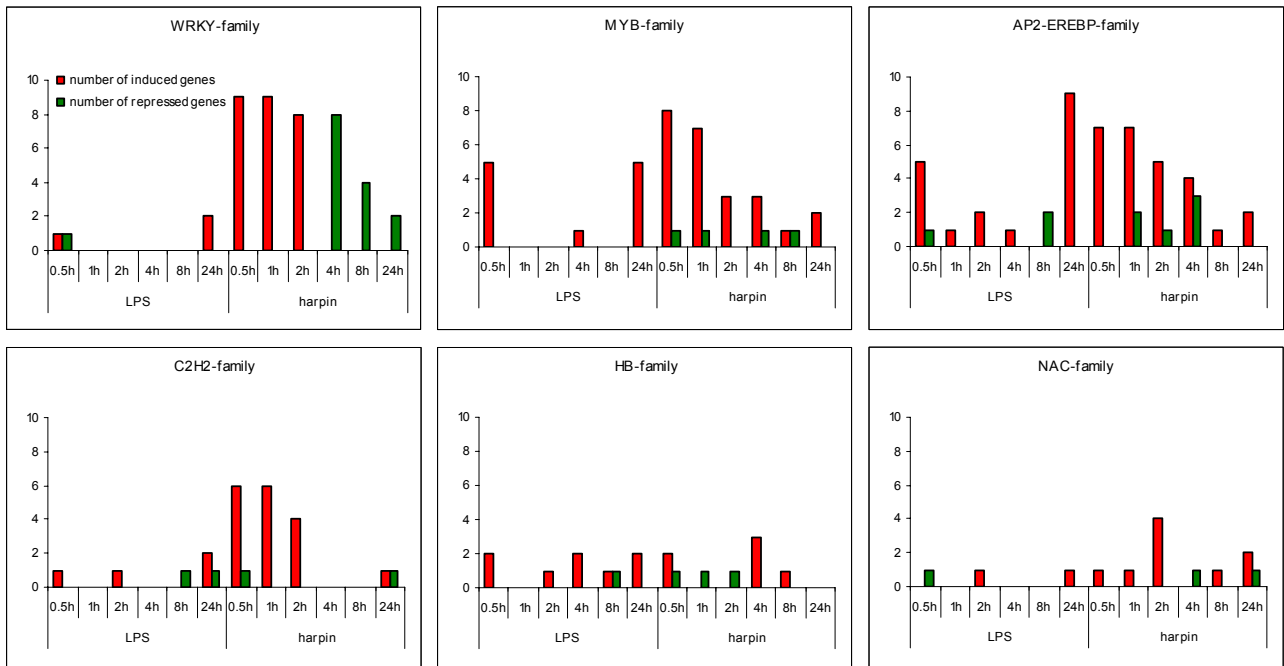


**Figure 24:** Expression patterns of six important transcription factor families regulated by LPS and harpin.

Genes with mRNA abundance induced or repressed above 2-fold are grouped into families on the basis of the Arabidopsis Gene Regulatory Information Server (AGRIS) database of *Arabidopsis* transcription factors: [<http://arabidopsis.med.ohio-state.edu>], (Davuluri et al., 2003).

In higher plants, the MYB protein family is extraordinarily diverse. They are known to be involved in a variety of cellular processes such as the regulation of biosynthetic pathways like phenylpropanoid or tryptophan biosynthesis, control of cell fate determination and regulation of the cell cycle (Zimmermann et al., 2004). AP2 (APETALA2) and EREBPs (ethylene-responsive element binding proteins) are prototypic members of a family of transcription factors unique to plants, and they play a variety of roles throughout the plant life cycle (Riechmann and Meyerowitz, 1998). MYB-type and AP2/EREBP-type transcription factors are reported as significantly induced by wounding stress (Cheong et al., 2002). The WRKY family of *Arabidopsis* contains 74 members, which are identified as W box (C/T)TGAC(T/C) binding proteins, a DNA sequence found in promoters of several defense-related genes (Ulker and Somssich, 2004). WRKY transcription factors are reported as differentially regulated in *Arabidopsis* treated with an avirulent *Pseudomonas syringae* strain and/or salicylic acid (SA). Different sets of AtWRKY genes were found as significantly induced or repressed by wounding stress (Cheong et al., 2002) in *Arabidopsis* plants as well as during flagellin treatment of *Arabidopsis* suspension cells (Navarro et al., 2004). A comparing data analysis revealed a remarkable induction

of 13 AtWRKY genes after harpin exposure, together with an almost complete absence of any AtWRKY gene regulation after LPS treatment (Fig. 24). A comparison with reported AtWRKY genes from pathogen, salicylic acid, wound and flagellin stress treatments in *Arabidopsis* is summarized in table 6. While some of the WRKY genes showed only regulation by harpin (AtWRKY10, AtWRKY17 and AtWRKY75) or harpin and *Pseudomonas syringae*, respectively (AtWRKY8 and AtWRKY31), two genes are induced by all stressors except LPS (AtWRKY22 and AtWRKY33). No surprise is the activation of the AtWRKY22 and AtWRKY29 genes by harpin. Both transcription factors are associated with the defense-induced mitogen-activated protein kinase (MAPK) signaling pathway which leads to resistance against bacteria and fungi (Asai et al., 2002). In sum, harpin but not LPS did induce a typical pattern of defense-related WRKYs.

**Table 6:** Comparison of AtWRKY genes differentially regulated during different stress treatments in *Arabidopsis*.

The classification is based on Arabidopsis Gene Regulatory Information Server (AGRIS) database of *Arabidopsis* transcription factors [<http://arabidopsis.med.ohio-state.edu>]; (Davuluri et al., 2003).

WRKY Type	ID	LPS	Harpin	Wounding <sup>1)</sup>	Flagellin (flg22) <sup>2)</sup>	Pathogen <sup>3)</sup>	Salicylic acid <sup>3)</sup>
AtWRKY8	At5g46350	-	+	-	-	+	-
AtWRKY9	At1g68150	+	+	-	-	-	-
AtWRKY10	At1g55600	-	+	-	-	-	-
AtWRKY17	At2g24570	-	+	-	-	-	-
AtWRKY22	At4g01250	-	+	+	+	+	+
AtWRKY25	At2g30250	-	+	-	-	+	+
AtWRKY29	At4g23550	-	+	-	+	+	-
AtWRKY31	At4g22070	-	+	-	-	+	-
AtWRKY33	At2g38470	-	+	+	+	+	+
AtWRKY40	At1g80840	-	+	+	-	+	+
AtWRKY48	At5g49520	+	-	-	-	+	-
AtWRKY53	At4g23810	-	+	+	+	-	+
AtWRKY55	At2g40740	-	+	-	-	-	+
AtWRKY75	At5g13080	-	+	-	-	-	-

<sup>1)</sup> (Cheong et al., 2002)

<sup>2)</sup> (Navarro et al., 2004)

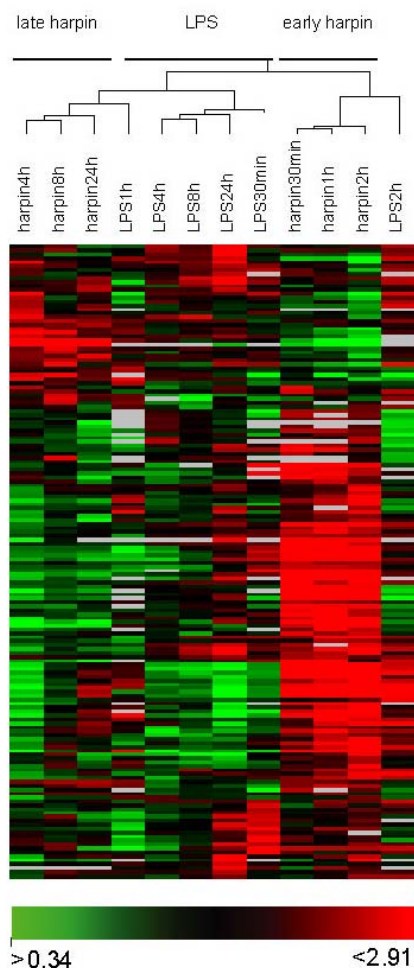
<sup>3)</sup> (Dong et al., 2003)

### 3.4. Genes involved in cell wall biogenesis and organization

Modification of cell wall architecture is an essential part of plant response to invading pathogens, a reason to focus on this area. Transcriptional analysis of genes which are involved in cell wall biogenesis and organization revealed mostly similar effects in gene expression after LPS- and harpin treatment. Primary cell walls from higher plant cells are composed predominantly of polysaccharides whose main parts are cellulose, hemicellulose and pectin, whereas the major component of secondary walls is lignin (Micheli, 2001). Here, 46 regulated genes (see supplement 4 at the attached CD-ROM) were found which are involved in cell wall biogenesis. About 20% were induced in both LPS and harpin treated *Arabidopsis* cells, respectively. Considering the function of encoded proteins the majority of them is responsible for cell wall modification, alteration and degradation. Six pectin esterase's whose action can result in loosening or disassembly of cell walls (Jiang et al., 2001) were found, and two pectate lyases which degrade the middle lamella of plant cell walls. Furthermore one

xyloglucan endotransglycosylase which catalyses the depolymerization or solubilization of the hemicellulose forming xyloglucan (Micheli, 2001) was detected. However, the very same gene has a reported role in restructuring primary walls at the time when secondary wall layers are deposited (Bourquin et al., 2002). The four pectin methylesterases induced by LPS and harpin catalyze the demethylesterification of homogalacturonic acid units of pectin and are known to be involved in stiffening and loosening of cell walls (Micheli, 2001; Al-Qsous et al., 2004). They are also reported to play a role in pathogen-plant interactions (Giovane et al., 2004). Harpin induced several putative cellulose synthases, which may be involved in cell wall assembly. After LPS treatment, a significant induction of two expansins was observed. In plants, expansins cause loosening and extension of cell walls (Rose and Bennett, 1999; Kalamaki et al., 2003), and might play a role in LPS-dependent progression of endosymbiosis (Mathis et al., 2005).

### 3.5. Different effects on cell rescue and defense



Cell rescue and defense related genes (see supplement 5 at the attached CD-ROM) represent more than 10% of the LPS and harpin regulated genes (165). Thereby 81 of them are up- or down-regulated by both stresses but at different time points or for different periods. A comparison of the expression changes across the defense genes for the two treatments is visualized by the clustergram (Fig. 25), wherein genes are ordered by related regulation patterns and expression amplitudes. LPS and harpin caused very different transcriptional answers. Harpin induced a very strong and transient response. After LPS treatment most of defense related genes showed a relative low level of transcripts, most of them are repressed or even not expressed, and the reduction of early induced genes is not as dramatic as in case of harpin elicited cells. The strongest answer to LPS regarding induction or repression of defense genes was measured 24 h post treatment. Because LPS as well as harpin are known to cause oxidative stress in *Arabidopsis* cells (Desikan et al., 1998; Gerber et al., 2004) we asked for the expression pattern of reactive oxygen species (ROS) associated genes (Tab. 7).

**Figure 25:** Clustering of *Arabidopsis* gene expression after treatment with LPS and harpin.

Transcript levels of 167 cellular rescue and defense related genes were analyzed 0.5, 1, 2, 4, 8 and 24 hours after elicitor treatment. Each horizontal line displays the expression data for one gene after normalisation at time points as indicated. The cluster tree at the left side displays the nodes of co-regulated gene expression over all 24 hours and both treatments. The relative abundance of any transcript in treated suspension cells was compared to untreated control cells. The colour scale at the bottom shows the normalised expression level.

Remarkable is the strong and primarily synchronous induction of superoxide forming respiratory burst oxidases and superoxide preventing alternative oxidases (Mittler et al., 2004) within 30 min after harpin treatment. After 4 h these genes are down-regulated, and the superoxide scavenging ferritin 1 precursor (op den Camp et al., 2003; Mittler et al., 2004) is activated. In case of LPS, genes of superoxide producing and scavenging enzymes (Mittler, 2002) are regulated at a very low level. However, after 8 h a superoxide dismutase (SOD) and a ferritin 1 precursor gene became very strong induced. In sum, only in harpin elicited cells a massive induction of ROS associated genes or genes involved in redox control were observed.

**Table 7:** Transcriptional analysis of genes associated with ROS generation and/or redox-balance.

The genes listed encode ROS-generating and/or protecting proteins such as ROS-scavenging enzymes or small heat shock proteins. At several time points after treatment, mRNA was isolated and hybridized to the cDNA array. Genes: more than 2-fold activation (bold); repression is indicated by underlining, and unmarked numbers indicate weak signals that were less than 2-fold greater than surrounding background.

Accession no.	ID	LPS						Harpin					
		0.5 h	1 h	2 h	4 h	8 h	24 h	0.5 h	1 h	2 h	4 h	8 h	24 h
<b>ROS related</b>													
<b>Avoiding superoxide</b>													
At1g32350	alternative oxidase, putative	1,00	0,66	0,78	0,86	0,71	0,56	<b>5,07</b>	<b>5,60</b>	<b>7,57</b>	<u>0,19</u>	0,70	-
At3g22370	alternative oxidase 1a	<u>0,46</u>	1,33	0,69	0,50	0,65	-	1,86	<b>2,82</b>	<b>3,36</b>	0,55	0,92	0,76
At3g27620	alternative oxidase 1c	0,55	1,04	-	0,50	0,65	0,50	1,96	<b>2,53</b>	<b>3,66</b>	0,54	0,88	0,82
<b>Producing superoxide</b>													
At5g51060	respiratory burst oxidase protein	-	-	-	-	0,87	1,05	1,82	<b>2,30</b>	<b>6,36</b>	<u>0,40</u>	0,65	-
At5g47910	respiratory burst oxidase protein	1,55	0,68	1,44	0,82	0,93	1,62	<b>4,58</b>	<b>4,39</b>	<b>5,12</b>	<u>0,44</u>	0,56	<u>0,44</u>
At1g23020	NADPH oxidase flavocytochrome	0,91	1,16	1,12	<b>2,23</b>	0,95	<u>0,36</u>	0,85	0,86	0,72	0,95	0,60	0,56
<b>Scavenging superoxide</b>													
At1g20620	catalase 3	<b>2,12</b>	-	1,27	1,70	-	1,35	0,86	-	-	-	-	-
At4g08390	stromal ascorbate peroxidase	1,03	0,74	1,32	0,68	1,74	1,94	0,60	0,94	-	1,05	1,24	<b>2,08</b>
At4g25100	superoxide dismutase	1,83	-	<b>2,17</b>	1,41	<b>2,04</b>	<b>3,72</b>	0,97	1,31	-	1,21	1,28	1,73
At4g11600	glutathione peroxidase	0,79	1,95	1,10	0,83	0,82	0,84	1,18	1,95	<b>2,91</b>	0,58	0,78	0,85
At5g01600	ferritin 1 precursor	-	-	-	-	<b>7,99</b>	<b>3,20</b>	0,58	0,51	-	<b>2,75</b>	<b>4,28</b>	<b>12,12</b>
<b>Redox control</b>													
At1g45145	thioredoxin, putative	-	-	1,10	-	0,75	-	1,06	1,58	-	1,03	<b>2,60</b>	<b>2,26</b>
At3g08710	thioredoxin-like protein	1,12	-	-	1,00	1,12	1,32	1,53	<b>2,30</b>	<b>2,00</b>	0,96	0,98	1,08
At1g62180	adenylylphosphosulfate reductase	1,10	0,68	0,78	0,53	0,52	0,87	1,13	1,64	<b>2,13</b>	0,70	1,03	0,94
At1g03850	glutaredoxin family	-	1,54	-	0,88	0,88	0,75	0,73	<u>0,39</u>	0,66	<b>2,49</b>	<b>2,58</b>	1,18
At1g28480	glutaredoxin, putative	1,10	-	-	0,92	-	1,14	<b>3,21</b>	<b>3,72</b>	<b>2,82</b>	0,54	0,77	0,69
<b>Small heat shock proteins</b>													
At5g12020	hsp 17.6	0,57	-	<b>5,31</b>	0,68	0,52	<u>0,29</u>	<b>4,37</b>	<b>5,56</b>	<b>5,81</b>	<u>0,44</u>	0,90	1,93
At1g59860	hsp 17.6A	0,55	1,28	<b>2,45</b>	-	<u>0,39</u>	<u>0,34</u>	<b>4,09</b>	<b>4,52</b>	<b>3,58</b>	<u>0,36</u>	0,83	1,14
At2g29500	hsp 17.6B	0,65	1,79	<b>2,29</b>	0,75	0,75	<u>0,41</u>	1,92	<b>2,55</b>	<b>3,49</b>	<u>0,45</u>	0,75	1,03
At1g53540	hsp 17.6C	0,57	1,88	<b>3,28</b>	0,64	0,66	<u>0,30</u>	<b>3,60</b>	<b>6,32</b>	<b>6,90</b>	<u>0,30</u>	0,68	<b>2,28</b>
At5g12030	hsp 17.7	-	-	<b>5,28</b>	0,58	-	<u>0,27</u>	<b>3,75</b>	<b>5,68</b>	<b>6,08</b>	<u>0,39</u>	0,84	<b>2,23</b>
At1g07400	hsp 17.8	0,55	1,19	<b>2,32</b>	0,50	<u>0,44</u>	<u>0,36</u>	<b>3,31</b>	<b>4,29</b>	<b>3,13</b>	<u>0,40</u>	0,83	1,08
At5g59720	hsp 18.1	0,78	-	<b>3,67</b>	1,30	0,80	<u>0,37</u>	1,25	<b>2,55</b>	<b>4,59</b>	<u>0,40</u>	0,84	1,80
At4g10250	hsp 22.0	-	-	-	-	-	-	<b>2,44</b>	<b>9,67</b>	<b>17,13</b>	<u>0,41</u>	0,99	1,74
At5g51440	hsp 23.5	0,68	1,10	1,90	<u>0,37</u>	0,63	<u>0,47</u>	<b>2,27</b>	<b>3,05</b>	<b>2,21</b>	0,65	1,31	1,56
At4g25200	hsp 23.6	<u>0,46</u>	-	<b>2,85</b>	<u>0,44</u>	-	<u>0,23</u>	<b>3,68</b>	<b>6,50</b>	<b>5,20</b>	<u>0,43</u>	0,79	1,28
At4g27670	hsp 25.3	-	-	-	-	0,94	-	<b>3,55</b>	<b>8,21</b>	<b>11,37</b>	<u>0,25</u>	0,59	1,18
At1g52560	small hsp	0,52	-	1,21	0,60	0,50	<u>0,29</u>	<b>3,69</b>	<b>5,58</b>	<b>7,19</b>	<u>0,35</u>	0,77	1,55

As next analysis was focused on inducible pathogenesis-related proteins (PR-genes), and proteins associated with activation of defense against pathogens (Kinkema et al., 2000; Schenk et al., 2000) such as phytoalexin production, oxidative stress protection, tissue repair and lignification. Most pathogen-related proteins have a damaging action on the cellular structures of a parasite: PR-1 and PR-5 interact with the plasma membrane, whereas  $\beta$ -1, 3-glucanases (PR-2) and chitinase (PR-3, PR-4, PR-8 and PR-11) attack  $\beta$ -1, 3-glucans and chitin, which are components of cell walls in most higher fungi. PR-5 proteins are thought to create transmembrane pores and have therefore been named permatins. Chitinases can also display lysosyme activity and hydrolyze bacterial peptidoglycan (Odjakova and Hadjiivanova, 2001). Surprisingly, both harpin as well as LPS induced only very few PR-proteins (basic PR-3-type chitinase and basic PR-4 hevein). In contrast, a remarkable induction was observed for small heat shock protein genes (sHSPs). Although the strength of induction differed after LPS and harpin treatment very similar expression patterns were found (Tab. 7). Both elicitors caused a strong, transient induction of all known sHSP genes with rapid down-regulation (Fig. 26). In addition to mitochondrial and cytosolic sHSPs the chloroplast-localized sHSP which is suggested to protect the photosystem II against oxidative stress and photoinhibition (Heckathorn et al., 1998) was strongly induced (Fig. 26).

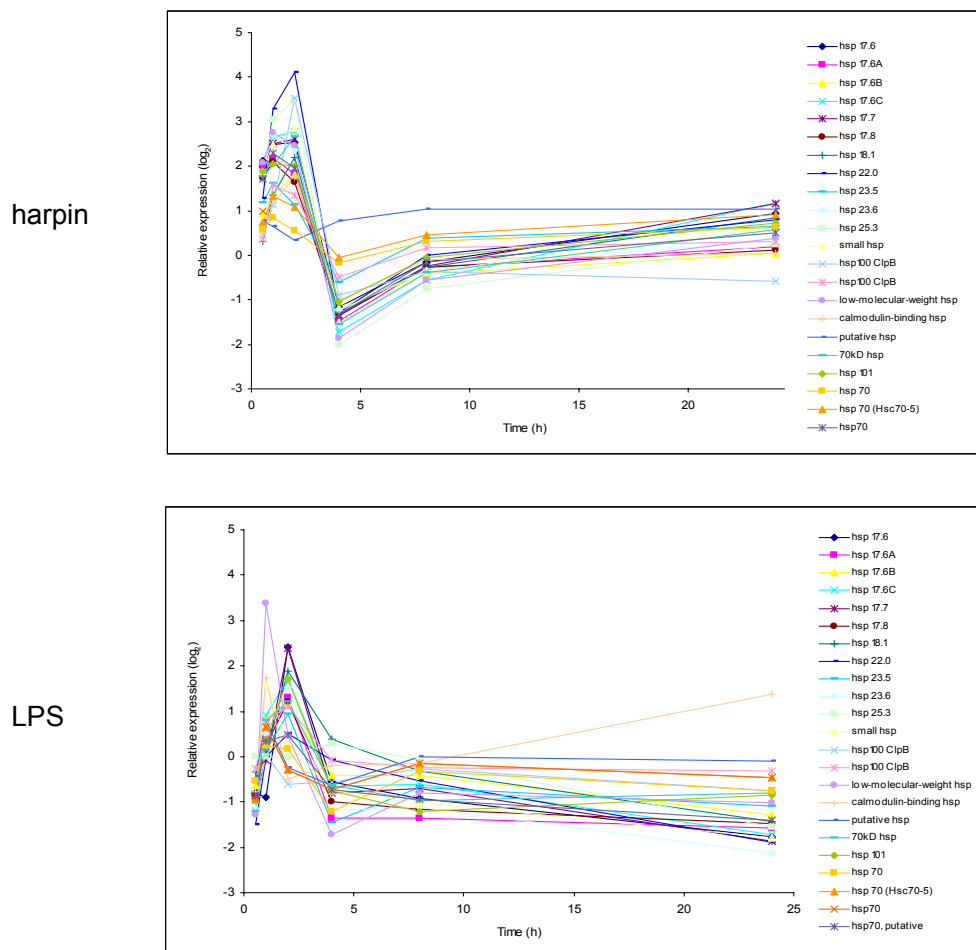


**Figure 26:** Heat shock protein gene expression in Arabidopsis after LPS and harpin treatment.

Shown are the profiles for the individual transcripts of all small HSPs and selected other HSPs for the first 24 h after elicitor treatment.



### 3.6. Cellular communication and signal transduction

Among the 101 LPS and harpin regulated genes assigned to signal transduction components, 54 protein kinases were found.

**Table 8:** Receptor-like kinases (subfamilies) induced by the treatment with LPS or harpin.

Accession no.	subfamily	LPS						Harpin					
		0.5 h	1 h	2 h	4 h	8 h	24 h	0.5 h	1 h	2 h	4 h	8 h	24 h
<b>CrRLK1-like RLKs</b>													
At5g54380	CRPK1L 1	<b>3,04</b>	-	0,50	-	1,05	0,83	0,76	0,51	-	<b>2,12</b>	0,79	0,94
At5g24010	CRPK1L 1	1,83	-	0,80	1,23	-	1,19	0,73	0,67	-	<b>2,28</b>	1,04	1,22
<b>DUF26-RLKs</b>													
At4g23190	DUF26	-	-	-	-	-	<b>2,63</b>	<b>3,33</b>	<b>3,34</b>	-	-	-	-
At4g05200	DUF26	1,21	-	-	1,38	1,65	1,76	1,07	1,63	<b>3,01</b>	<u>0,44</u>	0,78	<u>0,43</u>
<b>Lectin-RLKs</b>													
At5g60310	L-Lectin	-	-	-	-	0,91	<b>2,26</b>	-	-	-	-	1,21	-
At5g01540	L-Lectin	-	-	-	-	1,17	1,17	<b>3,43</b>	<b>2,95</b>	-	0,91	0,73	0,72
At5g60270	L-Lectin	1,17	-	-	-	0,49	<b>2,71</b>	<b>3,16</b>	<b>3,08</b>	<b>2,59</b>	0,77	0,74	0,62
At5g01550	L-Lectin	-	-	-	-	1,19	1,32	1,31	<b>2,45</b>	-	0,81	1,01	0,94
At5g60300	L-Lectin	1,22	-	0,72	1,74	0,93	1,66	0,85	-	-	<b>2,53</b>	1,38	1,54
At4g28350	L-Lectin	0,86	-	1,54	-	0,58	0,96	<b>3,18</b>	<b>2,56</b>	<b>2,34</b>	0,59	-	0,80
<b>LRR-RLKs</b>													
At5g25930	LRR	1,05	0,65	<b>2,27</b>	1,19	1,05	1,00	<b>4,98</b>	<b>6,71</b>	<b>4,53</b>	<u>0,41</u>	0,53	-
At5g16000	LRR II	<b>2,46</b>	-	-	-	1,74	1,46	-	-	-	<b>2,28</b>	-	0,85
At5g05160	LRR III	<b>2,73</b>	-	0,99	-	1,61	<b>3,13</b>	-	-	-	-	-	-
At4g22730	LRR IV	0,99	-	1,14	1,22	1,13	1,00	-	-	-	1,55	-	<b>2,66</b>
At2g25790	LRR IV	1,70	0,96	0,87	1,93	1,90	<b>3,78</b>	-	-	-	1,75	1,33	1,19
At1g66150	LRR IX	1,59	0,66	0,62	1,09	0,99	1,26	0,59	<u>0,35</u>	0,54	1,35	1,00	1,27
At4g22130	LRR V	1,59	-	-	-	1,34	1,16	0,96	0,62	-	<b>3,02</b>	0,67	1,12
At5g45840	LRR VI	<b>16,83</b>	-	-	-	-	1,21	-	-	-	<b>2,69</b>	0,93	1,39
At2g31880	LRR VII	1,25	0,79	-	1,13	1,17	1,51	<b>3,97</b>	<b>4,30</b>	<b>2,39</b>	0,71	0,76	0,78
At1g53430	LRR VIII-2	1,23	-	-	0,80	1,15	1,08	1,96	<b>2,30</b>	<b>2,79</b>	0,51	0,75	-
At3g09010	LRR VIII-2	0,59	-	-	-	0,96	1,04	<b>2,01</b>	1,28	-	0,74	1,09	0,75
At1g74360	LRR X	0,79	-	-	0,92	1,02	1,32	<b>6,91</b>	<b>5,90</b>	<b>4,52</b>	0,55	0,89	0,82
At3g24240	LRR XI	1,66	-	-	1,50	1,40	<b>2,53</b>	0,84	-	-	<b>2,36</b>	1,32	<b>2,96</b>
At4g26540	LRR XI	1,48	1,10	<b>2,00</b>	1,99	1,58	<b>3,87</b>	0,77	-	-	-	1,43	1,54
At4g08850	LRR XI	-	1,01	0,65	0,83	0,70	0,76	<b>2,26</b>	<b>3,43</b>	1,88	0,91	0,64	-
At5g65700	LRR XI	1,01	-	-	1,87	1,45	1,53	0,70	-	-	<b>2,60</b>	1,10	1,55
At1g09970	LRR XI	1,21	1,02	1,72	1,45	1,57	<b>2,63</b>	0,99	1,08	0,84	1,58	1,46	1,72
At5g46330	LRR XII	0,91	0,81	0,92	1,02	0,99	1,23	1,30	1,18	<u>0,45</u>	<b>2,05</b>	1,08	1,45
<b>PERK-RLKs</b>													
At1g68690	PERKL	1,13	-	-	-	1,10	0,83	1,60	1,63	<b>2,57</b>	0,71	0,70	0,67
<b>RLCKs</b>													
At4g17660	RLCK	-	-	-	-	0,97	<b>2,28</b>	-	-	-	-	-	-
At5g59010	RLCK II	1,30	-	0,80	1,27	1,02	1,12	-	-	-	<b>2,28</b>	1,53	1,38
At1g51620	RLCK IV	-	-	-	-	1,08	0,83	<b>2,08</b>	<b>2,20</b>	-	0,81	-	-
At5g10520	RLCK VI	-	-	1,57	1,82	1,42	<b>2,91</b>	1,46	1,40	-	1,38	-	0,94
At2g05940	RLCKVII	<b>2,25</b>	-	-	1,18	1,27	1,32	<b>3,61</b>	<b>3,82</b>	<b>3,74</b>	0,69	0,61	0,71
At5g56460	RLCKVII	1,21	-	1,23	0,70	1,02	1,19	0,79	0,83	-	<b>3,09</b>	-	<b>5,56</b>
At4g13190	RLCKVII	0,90	-	-	0,71	0,77	1,02	0,91	0,92	-	<b>2,95</b>	1,84	-
At3g59350	RLCKVIII	<b>2,20</b>	<u>0,30</u>	1,55	0,73	0,70	0,98	1,30	1,13	1,54	1,00	1,13	0,74
<b>SD-RLKs</b>													
At1g11330	SD-1	0,91	-	-	1,08	1,09	1,57	<b>2,40</b>	1,98	-	0,73	0,93	-
At1g61370	SD-1	-	-	-	-	1,04	0,95	1,87	<b>2,06</b>	-	0,82	1,01	0,87
At1g61360	SD-1	-	-	-	-	1,23	1,18	<b>6,06</b>	<b>11,57</b>	<b>6,42</b>	<u>0,38</u>	-	-
At5g35370	SD-2	1,01	0,64	1,71	0,98	0,94	<b>2,41</b>	1,47	1,43	1,05	0,97	0,85	0,92

Abbreviations for receptor-like kinase subfamilies are: CrRLK1, *Catharanthus roseus* RLK1; DUF26, domain of unknown function; LRR, leucine-rich repeat; PERK, proline extensin-like receptor kinase; RLCK, receptor-like cytoplasmic kinase; SD, S-locus glycoprotein-like domain.

Most of them are receptor-like kinases, whose induction was observed throughout the whole period of treatment. Almost 50% belong to leucine-rich repeat receptor-like kinases (LRR-RLK) which is the largest group of RLKs. Harpin caused an induction of 31 receptor-like kinases, whereas only 16 are up-regulated by LPS during 24 h (Tab. 8). Interestingly, LPS induced a LRR VI receptor-like kinase by nearly 17- fold after 30 minutes. A comparison of the expression data for harpin and LPS activated RLK genes with those published for *Arabidopsis* challenged with flg22, a peptide corresponding to the most conserved domain of flagellin, revealed that 6 of the 25 significantly by flg22 regulated RLK genes show nearly the same expression pattern one hour post treatment (Navarro et al., 2004).

The majority of the genes involved in cellular communication and signal transduction could be assigned to phytohormone or calcium/calmodulin related groups, respectively (Tab. 9). Harpin induced the gene encoding the abscisic acid responsive protein and LPS the gibberellic acid regulated GASA4 transcript, respectively (Aubert et al., 1998). Auxin, ethylene and calcium/calmodulin related signaling component transcripts were induced in response to both treatments. However, as mentioned above, responses to harpin were most prominent in the early phase after treatment, while transcriptional changes after LPS-treatment became apparent at the end of the 24 h period.

Regarding mitogen-activated protein kinases (MAPK) and their regulating upstream kinases a very strong and immediate induction of AtMPK11 by harpin was observed. Surprisingly, no activation of any stress and/or pathogen associated MAPKs such as AtMPK4 and AtMPK6 at the transcript level was monitored. LPS did not influence any of the currently annotated *Arabidopsis* MAPKs genes. While harpin and in some instances LPS induced genes encoding the upstream components MAPKKK Raf27, MPKKK5, MPKKK15, MPKKK16 und MPKKK19 (with the exception of the Raf-protein all belonging to the MEKK subfamily (Mizoguchi et al., 2000), the overall impact of these elicitors on genes of MAPK signaling networks was weak.

**Table 9:** Transcriptional analysis of genes involved in cellular communication and signaling.

*Arabidopsis thaliana* suspension cells were treated with LPS and harpin as described. In case of kinases, genes were identified and categorized by the PlantsP database of the University of California, San Diego [<http://plantsp.sdsc.edu>]. At several time points after treatment, *Arabidopsis* suspension cells were harvested and mRNA was purified and hybridized to the cDNA array. Genes: more than 2-fold activation (bold); repression is indicated by underlining, and unmarked numbers indicate weak signals that were less than 2-fold greater than surrounding background.

Accession no.	ID	LPS						Harpin					
		0.5 h	1 h	2 h	4 h	8 h	24 h	0.5 h	1 h	2 h	4 h	8 h	24 h
<b>Abscisic acid related</b>													
At5g13200	ABA-responsive protein - like	1,26	0,73	1,22	0,69	0,83	0,77	<b>2,38</b>	<b>4,13</b>	<b>3,33</b>	<u>0,49</u>	0,65	0,70
<b>Auxin related</b>													
At1g28130	auxin-regulated GH3 protein, putative	<u>0,35</u>	<b>2,79</b>	0,75	0,76	0,92	0,85	1,09	1,14	0,86	0,88	0,77	1,26
At4g37390	auxin-responsive GH3 - like protein	1,10	0,99	<b>3,70</b>	1,56	1,09	<b>2,51</b>	1,00	1,15	1,13	1,28	1,37	1,23
At3g44310	nitrilase 1	1,01	-	-	1,13	0,77	<b>2,08</b>	0,86	-	0,98	0,86	1,00	-
At4g13790	SAUR-AC - like protein	0,72	-	-	-	0,90	<b>2,26</b>	1,02	-	-	0,58	-	-
<b>Calcium and Calmodulin related</b>													
At4g17615	calcineurin B-like protein 1	0,69	1,99	1,70	0,64	1,19	<b>2,18</b>	<b>2,78</b>	<b>3,94</b>	<b>3,52</b>	0,52	0,80	1,00
At2g41090	calcium binding protein (CaBP-22)	<b>2,73</b>	-	<b>2,27</b>	<u>0,47</u>	1,19	1,71	<b>2,28</b>	1,03	-	-	-	-
At3g49370	CDPK - like	1,02	-	-	-	0,88	0,98	1,29	<b>2,11</b>	<b>3,46</b>	0,66	0,83	0,93
At4g20780	calcium-binding protein - like	1,03	1,04	1,44	0,63	0,82	1,16	<b>2,76</b>	1,75	1,76	0,81	0,75	0,76
At1g08650	CDPK, putative	<u>0,19</u>	-	-	0,53	0,61	<b>2,97</b>	1,75	<b>4,42</b>	<b>4,94</b>	<u>0,38</u>	-	0,77
At3g25600	calmodulin, putative	<b>2,39</b>	0,54	-	0,71	0,69	1,45	1,33	1,44	1,23	0,89	0,68	0,63
At3g51920	calmodulin, putative	1,18	1,04	1,09	-	0,84	0,94	<b>3,09</b>	<b>3,70</b>	<b>2,26</b>	0,65	0,68	0,52
At1g76650	calmodulin, putative	1,18	-	0,98	0,74	0,60	<b>2,48</b>	<b>9,44</b>	<b>7,32</b>	<b>18,53</b>	<u>0,23</u>	0,73	-
At5g26920	calmodulin-binding - like protein	1,96	0,67	1,05	-	0,90	1,62	<b>2,44</b>	<b>2,75</b>	-	0,50	-	0,78
At4g00500	calmodulin-binding hsp, putative	0,59	-	0,72	0,88	0,90	<b>2,61</b>	1,43	<b>2,23</b>	<b>3,41</b>	<u>0,49</u>	0,93	1,04
At4g31000	calmodulin-binding protein, putative	-	-	1,01	0,57	-	0,71	-	-	0,60	<b>2,09</b>	0,77	1,14
At2g41100	calmodulin-like protein	<b>3,01</b>	<u>0,34</u>	<b>2,40</b>	<u>0,48</u>	1,22	1,69	<b>2,33</b>	<b>2,25</b>	<b>2,17</b>	1,01	1,57	<u>0,45</u>
At5g37770	calmodulin-related protein 2	<b>2,16</b>	0,77	0,61	0,69	-	1,46	0,88	-	0,90	1,07	0,69	0,88
At4g14580	SNF1 like protein kinase	1,23	1,39	-	1,02	0,98	<b>2,15</b>	0,92	1,18	-	1,29	1,38	1,22
<b>Gibberellin related</b>													
At5g15230	GASA4	<b>5,70</b>	-	<b>3,82</b>	-	-	<b>3,65</b>	1,89	-	-	-	-	-
<b>Ethylene related</b>													
At4g11281	ACC synthase (AtACS-6)	1,33	1,53	-	0,61	0,67	<b>2,18</b>	<b>11,43</b>	<b>14,70</b>	<b>9,15</b>	0,51	0,75	1,00
At5g61590	ethylene responsive binding factor	0,78	-	<b>2,13</b>	-	<u>0,33</u>	0,57	0,70	<u>0,45</u>	-	1,95	<b>5,92</b>	<b>2,27</b>
At5g20550	ethylene-forming-enzyme-like	-	-	-	-	1,77	<b>2,17</b>	-	-	-	1,28	-	-
At5g20400	ethylene-forming-enzyme-like	1,19	1,86	1,05	0,77	1,04	<b>2,41</b>	1,00	1,11	0,93	1,15	1,15	0,91
At4g11650	osmotin precursor	0,95	1,25	1,28	1,13	1,24	<b>2,16</b>	1,04	1,10	1,42	0,78	1,51	1,29
<b>Other</b>													
At1g01560	MAP kinase (ATMPK11)	0,91	-	-	1,03	0,95	1,30	<b>3,49</b>	<b>3,65</b>	<b>6,05</b>	-	0,81	0,64
At5g66850	MAP kinase kinase kinase (MPKKK5)	-	-	-	-	-	-	1,16	<b>2,17</b>	-	0,76	-	-
At4g18950	MAP kinase kinase kinase Raf27	1,04	-	1,18	-	-	<u>0,45</u>	<b>4,14</b>	<b>4,60</b>	<b>5,76</b>	<u>0,35</u>	0,66	0,67
At5g67080	MAP kinase kinase kinase (MPKKK19)	-	-	-	-	0,50	<b>3,96</b>	1,77	<b>2,08</b>	-	0,62	0,74	0,87
At4g26890	MAP kinase kinase kinase (MPKKK16)	<b>4,51</b>	-	-	1,11	0,73	1,06	<u>0,44</u>	<u>0,31</u>	-	1,84	0,67	0,62
At5g55090	MAP kinase kinase kinase (MPKKK15)	<b>3,81</b>	-	-	-	0,51	1,36	1,24	1,88	<b>2,30</b>	0,66	-	0,68

### 3.7. Discussion of the chapter \*

The goal of this work was to compare the genetic programs in *Arabidopsis thaliana* behind the LPS-induced non-host response and the hypersensitive resistance response induced by the harpin elicitor from *Pseudomonas syringae*, respectively. Using Agilent *Arabidopsis* cDNA microarrays consisting of about 15,000 specific oligomers, changes in transcript accumulation of treated cells were monitored at six time points within 24 hours after elicitor treatment.

Using a large set of receptors, the plant innate immune system developed different strategies to become disease resistant. Cultivar-specific resistance conforms to the gene-for-gene-hypothesis, and is genetically determined by complementary pairs of pathogen-encoded avirulence (*AVR*) genes and plant resistance (*R*) genes (Dangl and Jones, 2001). In other cases receptors have broad range specificity and recognize many related molecular structures called PAMPs (pathogen-associated molecular patterns). The most important PAMPs are conserved cell-surface structures like flagellin, lipopeptides (LP), peptidoglycans (PG) and lipopolysaccharides (LPS) which are unique to bacteria. LPS are major parts of Gram-negative bacteria cell surfaces, composed of a hydrophobic lipid A, a covalently linked non-repetitive core oligosaccharide, divided into inner and outer core, and the O-antigen of oligosaccharide-repeating units (Meyer et al., 2001). LPS from various sources could trigger defense-related responses in several plant species without the synthesis of the resistance-related salicylic acid and without triggering of an oxidative burst (Newman et al., 2002). On the other hand, LPS from the phytopathogen *Xanthomonas campestris* pv. *campestris* could induce an oxidative burst reaction with accumulation of hydrogen peroxide ( $H_2O_2$ ) in tobacco cell cultures (Meyer et al., 2001), and LPS isolated from *Burkholderia cepacia* was found to trigger a rapid influx of  $Ca^{2+}$  into the cytoplasm of cells (Gerber et al., 2004). Furthermore, a recently published study proved that LPS induces a strong NO release accompanied by an up-regulation of a set of local and systemic defense genes (Zeidler et al., 2004).

Pathogenic bacteria possess several sets of pathogenic components like the gram-negative *Pseudomonas syringae*, which contain LPS and additional PAMPs, and produce harpins. Especially in case of avirulent strains, it is difficult to distinguish defense response after recognition of non-host and race-specific elicitors, respectively. However, in contrast to race-specific defense responses the basal resistance is poorly defined (Tao et al., 2003; Glazebrook, 2004).

Analysis of the array data revealed significant responses to harpin (about 1300 genes) and LPS (about 600 genes). Most genes have been previously associated with plant defense responses (see supplement 2 at the attached CD-ROM). However, responses to harpin were most prominent in the early phase after treatment, while transcriptional changes after LPS treatment became apparent at the end of the 24 h period (Fig. 23, p.34).

\* For a better readability the discussion of this chapter is separated from the general discussion.

Concentrating the analysis on genes encoding transcription factors, defense genes, cell wall biogenesis related genes and signal transduction components some interesting parallels, but also remarkably different expression patterns for the examined elicitors were monitored. Both, harpin and LPS induced an overlapping array of genes involved in cell wall biogenesis and/or strengthening, cellular communication and signaling. The pattern of induced genes associated with cell rescue and general stress responses such as small heat shock proteins was highly similar.

Harpin and LPS induce defense- or stress-associated genes, including glutathione S-transferases, cytochrome P450, and many genes encoding PR proteins. Interestingly, in case of LPS, PR gene transcript accumulation was independent of cell death, reminiscent of the action of flg22 peptide. Flagellin also acted as an elicitor in *Arabidopsis* plants, inducing an oxidative burst and leading to the induction of defense-related genes such as *PR1*, *PR5*, *PAL1*, and *GST1*, but just like LPS never induced a hypersensitive response type of necrosis as harpin does (Gomez-Gomez and Boller, 2002; Zeidler et al., 2004; Zipfel et al., 2004).

Small Heat shock proteins (sHSP) have been demonstrated to prevent cytochrome c release, and they disrupt the apoptosome by binding to cytochrome c. HSPs might protect cells from death (Hoerberichts and Woltering, 2003). Therefore, sHSP gene expression dynamics in harpin and LPS treated cells was analyzed. In *Arabidopsis*, there are 13 sHSPs, divided into 6 classes on the basis of their intracellular localization (Scharf et al., 2001). As presented (Tab.7, p.39; Fig. 26, p.40), harpin and LPS cause a strong, but transient induction of genes coding for the sHSP already in the first 30 min until 2 h after treatment. In addition to mitochondrial and cytosolic sHSPs, the chloroplast-localized sHSP which is suggested to protect the Photosystem II against oxidative stress and photoinhibition (Heckathorn et al., 1998) is induced strongly by harpin.

In contrast, a striking difference was observed regarding some of the most prominent, central components of plant defense such as transcription factors, receptor kinases, and oxidative burst-associated genes, whose expression became apparent only after treatment with harpin. Marked changes in transcript levels of transcription factor genes belong to the WRKY-, MYB-, AP2-EREBP- and C2H2-family were found after harpin treatment, whereas LPS changed transcript levels much slower and weaker (Fig. 24, p.36). Noteworthy is the almost complete absence of any AtWRKY gene regulation after LPS treatment at simultaneous really strong induction up to 13 AtWRKY genes after harpin exposure (Tab.6, p.37). But, this finding goes along with the likewise weak induction of AtWRKY genes by the PAMP flagellin flg22 (Navarro et al., 2004).

Survey of expression patterns further showed, that only in harpin elicited cells a massive induction of reactive oxygen species (ROS) related genes, or genes involved in redox control is present (Tab.7, p.39), although both elicitors are known to induce ROS formation (Meyer et al., 2001).

The overall impact of harpin and LPS on genes of mitogen-activated protein kinases (MAPK) signaling network was weak (Tab.9, p.43). On the other hand, transcriptional activation of plant MAPK signaling components by stress, pathogens or elicitors seems to be only one aspect of stress-induced MAPK activation which very often is controlled by post-translational mechanisms (Zhang and Klessig, 2001).

The defense machinery induced by harpin reflects the much more pronounced host response including cell death induction after treatment with this elicitor. Thus, while both harpin and LPS induce plant immunity, these differences reflect the HR-type response to harpin and the more subtle reactions to the PAMP LPS. It is an exciting goal for the future to investigate whether genes induced specifically by PAMPs are components of innate immunity and whether they contribute to the phenomenon of basal resistance.

#### 4. Studies with *Arabidopsis Mlo* knockout mutants

##### 4.1. Induction of transcript accumulation of *AtMlo* genes and *AtMlo* co-regulated calmodulin-encoding genes by harpin

While harpin is an inducer of cell death, there are also many endogenous factors that control apoptosis. Considering the regulatory function in cell death protection and plant defense of the wild-type MLO protein in barley it was asked for a possible role of MLO in harpin mediated cell death of *Arabidopsis*. The microarray analysis of *Arabidopsis thaliana* following harpin treatment revealed a significant increase in transcript accumulation of the *Mlo2*, *Mlo6*, and *Mlo12* genes (Tab. 10). Harpin causes a strong and transient induction in gene expression, detectable from 30 min onwards and up to 2 h after elicitation. Then, 4 h post harpin treatment, transcript levels declined below basal levels possibly indicating repression of gene expression.

**Table 10:** *AtMlo* gene induction after harpin treatment.

At several time points after treatment, *Arabidopsis* suspension cells were harvested and mRNA was purified and hybridized to the Agilent *Arabidopsis* 1.0 microarrays. Genes with more than 2-fold induction of transcript accumulation are shown in bold; putative repression is indicated by underlining, and unmarked numbers indicate statistically insignificant changes in transcript abundance in comparison with untreated controls.

Accession no.	ID	30min	1h	2h	4h	8h	24h
At1g11310	<i>Mlo2</i>	<b>2.32</b>	<b>3.64</b>	<b>3.40</b>	<u>0.38</u>	0.80	0.72
At1g61560	<i>Mlo6</i>	<b>6.21</b>	<b>8.03</b>	<b>4.91</b>	<u>0.33</u>	0.65	0.50
At2g39200	<i>Mlo12</i>	<b>5.40</b>	<b>5.25</b>	<b>2.83</b>	0.67	0.78	0.63

To ensure the reliability of the microarray results, transcript accumulation of the *Mlo2*, *Mlo6*, and *Mlo12* genes was verified by semi-quantitative RT-PCR using gene-specific forward and reverse primers (Fig. 27).

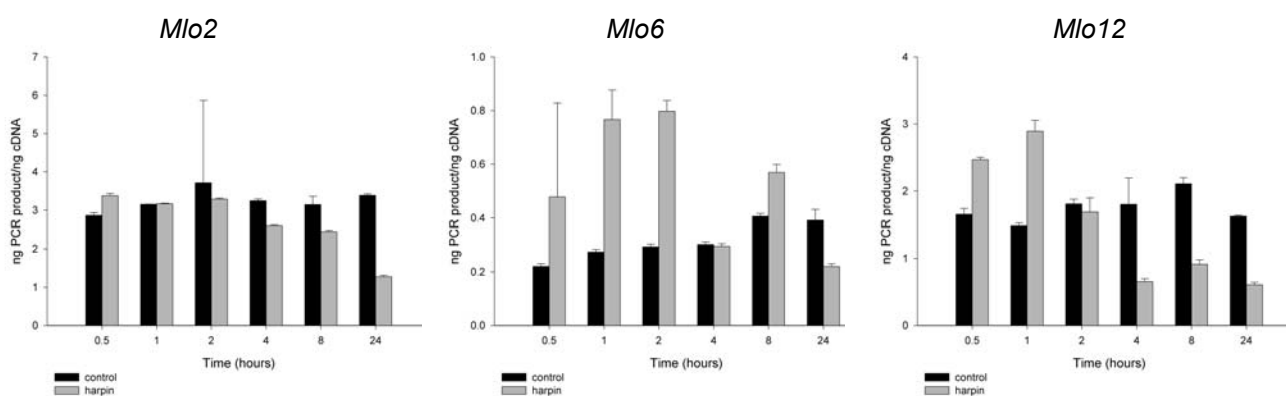


**Figure 27:** Harpin induces *AtMlo* gene induction in *Arabidopsis thaliana*.

*Arabidopsis thaliana* suspension cells were treated with harpin as described. The cells were harvested at the time points indicated for RNA isolation. RT-PCR products were quantified using the PicoGreen<sup>TM</sup> dsDNA quantitation kit and a Fluostar microplate reader. Analyses were performed from samples of three independent experiments; measurements were carried out three times for each sample. Data are represented as means  $\pm$  SD.

The strong and transient induction of *Mlo6* and *Mlo12* within 2 h post treatment is consistent with the expression data obtained from the arrays. For *Mlo2* which was weaker but nevertheless significantly induced in comparison with *Mlo6* and *Mlo12* on microarrays, no clear induction could be observed by RT-PCR. In plants,  $Ca^{2+}$  either directly activates a group of enzymes such as calcium-dependent protein kinases (CDPK) or acts indirectly through  $Ca^{2+}$ -modulator proteins such as calmodulin (Kim et al., 2002b). For barley it was reported that calmodulin interacts with the MLO protein to dampen defense reactions against the powdery mildew fungus (Kim et al., 2002a).

Harpin is known to stimulate calcium influx across the plasma membrane of cells. These increasing levels of cytosolic free  $Ca^{2+}$  are essential for initiation of defense mechanisms (Blume et al., 2000). Based on this background it was plausible to analyze the transcriptional activation of genes encoding calmodulins and calmodulin-related proteins, respectively (Tab. 11). During the whole period of 24 h a strong up-regulation of genes encoding various calmodulin isoforms was observed. This data is consistent with the previously reported sustained increases of cytosolic free  $Ca^{2+}$ -levels in harpin treated cells, monitored for a period of 24 h (Blume et al., 2000).

**Table 11:** Agilent Arabidopsis 2.0 microarray analysis of calmodulin and calmodulin-related transcripts.

At several time points after treatment (1, 2, 8 and 24 h) cells were harvested, mRNA was purified and hybridized to the cDNA array. Genes: more than 2-fold activation (bold); repression is indicated by underlining, and unmarked numbers indicate weak signals that were less than 2-fold greater than surrounding background. Gene annotations are supplemented by GeneBank accession numbers.

Accession no.	ID	1 h	2 h	8 h	24 h
At5g37780	calmodulin 1*	0,80	<b>2,01</b>	<b>2,36</b>	<b>2,53</b>
At2g41110	calmodulin 2*	0,83	<b>2,78</b>	<b>2,79</b>	<b>3,95</b>
At1g66410	calmodulin 4*	0,60	1,48	<b>3,28</b>	<b>2,24</b>
At3g43810	calmodulin 7*	0,97	<b>2,28</b>	<b>2,90</b>	<b>3,42</b>
At3g51920	calmodulin 9*	<b>2,11</b>	<b>3,49</b>	<b>3,47</b>	<b>2,87</b>
At2g41100	calmodulin 12*	<b>5,84</b>	<b>5,29</b>	<b>3,05</b>	1,81
At4g12860	calmodulin, putative	0,65	<b>2,50</b>	0,97	<b>4,20</b>
At3g07490	calmodulin, putative	1,64	<b>2,01</b>	1,04	1,66
At1g24620	calmodulin, putative	<b>2,50</b>	0,58	-	<u>0,48</u>
At1g76650	calmodulin, putative	<b>2,17</b>	<b>4,02</b>	1,20	0,95
At3g25600	calmodulin, putative	0,91	1,81	<b>2,32</b>	1,68
At5g56360	calmodulin-binding protein	<u>0,47</u>	1,06	<b>2,17</b>	<b>2,32</b>
At2g38800	calmodulin-binding protein	0,79	1,32	1,64	<b>2,16</b>
At5g40190	calmodulin-binding protein	0,72	<b>2,96</b>	1,37	1,26
At4g28600	calmodulin-binding protein	0,82	1,62	<b>2,72</b>	0,98
At5g49480	calmodulin-like	0,99	1,87	<b>3,79</b>	1,64
At3g10190	calmodulin-like	0,64	<b>2,86</b>	1,67	<b>2,95</b>
At5g44460	calmodulin-like	<b>2,18</b>	1,18	0,93	1,07
At5g17470	calmodulin-like	1,12	<b>2,48</b>	0,57	1,25
At3g50770	calmodulin-like	<b>3,58</b>	0,54	-	0,69
At2g41410	calmodulin-like	0,70	<b>2,47</b>	<b>2,69</b>	<b>2,72</b>
At3g03410	calmodulin-like	0,96	<b>2,70</b>	-	<b>2,17</b>
At1g66400	calmodulin-related protein	1,36	<b>2,49</b>	<b>2,27</b>	<b>2,82</b>
At5g37770	calmodulin-related protein 2 (TCH2)	1,61	1,84	<b>2,75</b>	<b>2,45</b>

\* identified and accessed according to (Luan et al., 2002)



#### 4.2. Infections with the fungus *Alternaria alternata*

As mentioned above, a disease resistance-enhancing character of harpin against diverse viral, bacterial, and fungal pathogens has been observed for a range of plant species. To test whether MLO proteins contribute to harpin-mediated resistance or tolerance against pathogens, pathogen assays were performed using homozygous *Arabidopsis* insertion mutants. These *mlo2*, *mlo6*, *mlo12*, *mlo2-6*, *mlo2-12*, *mlo6-12*, and *mlo2-6-12* knockout mutants were obtained from Ralph Panstruga, MPI für Züchtungsforschung, Köln. Pathogen experiments were carried out with the fungus *Alternaria alternata*. *Arabidopsis* wild type and *AtMlo* mutant plants were sprayed with water (control) or pre-treated with harpin, followed by inoculation with *Alternaria* spore suspension after 5 days. Disease phenotypes were macroscopically scored 5 days post inoculation (Fig. 28).

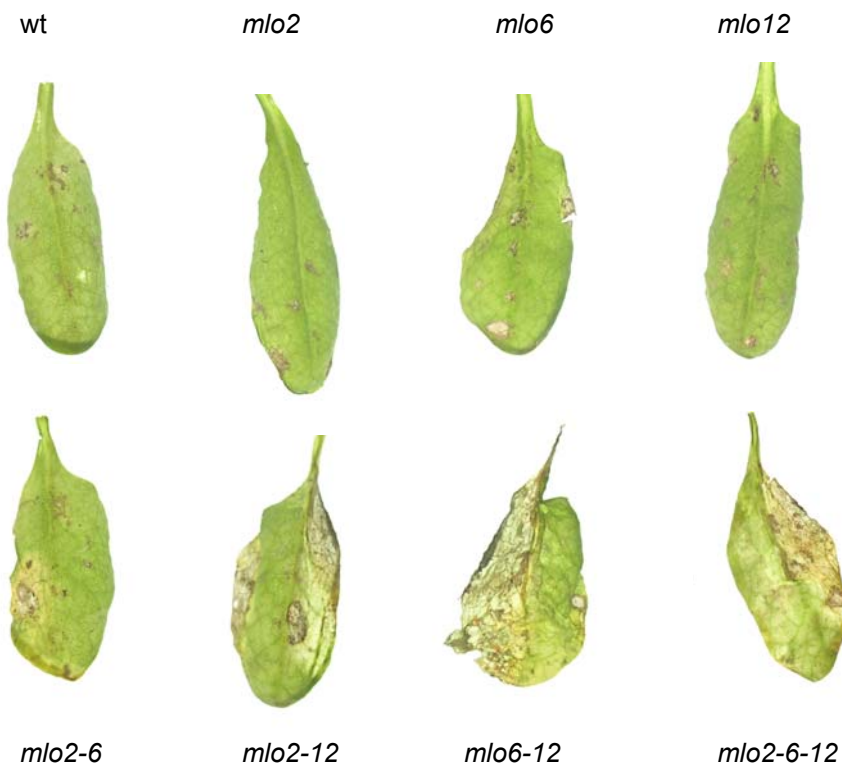


**Figure 28:** *Arabidopsis* leaf inoculation with *Alternaria alternata*.

Macroscopically visible symptoms on *Arabidopsis* wild type and *AtMlo* mutant plants caused by the fungus *Alternaria alternata* five days after spraying with fungal spore suspension.

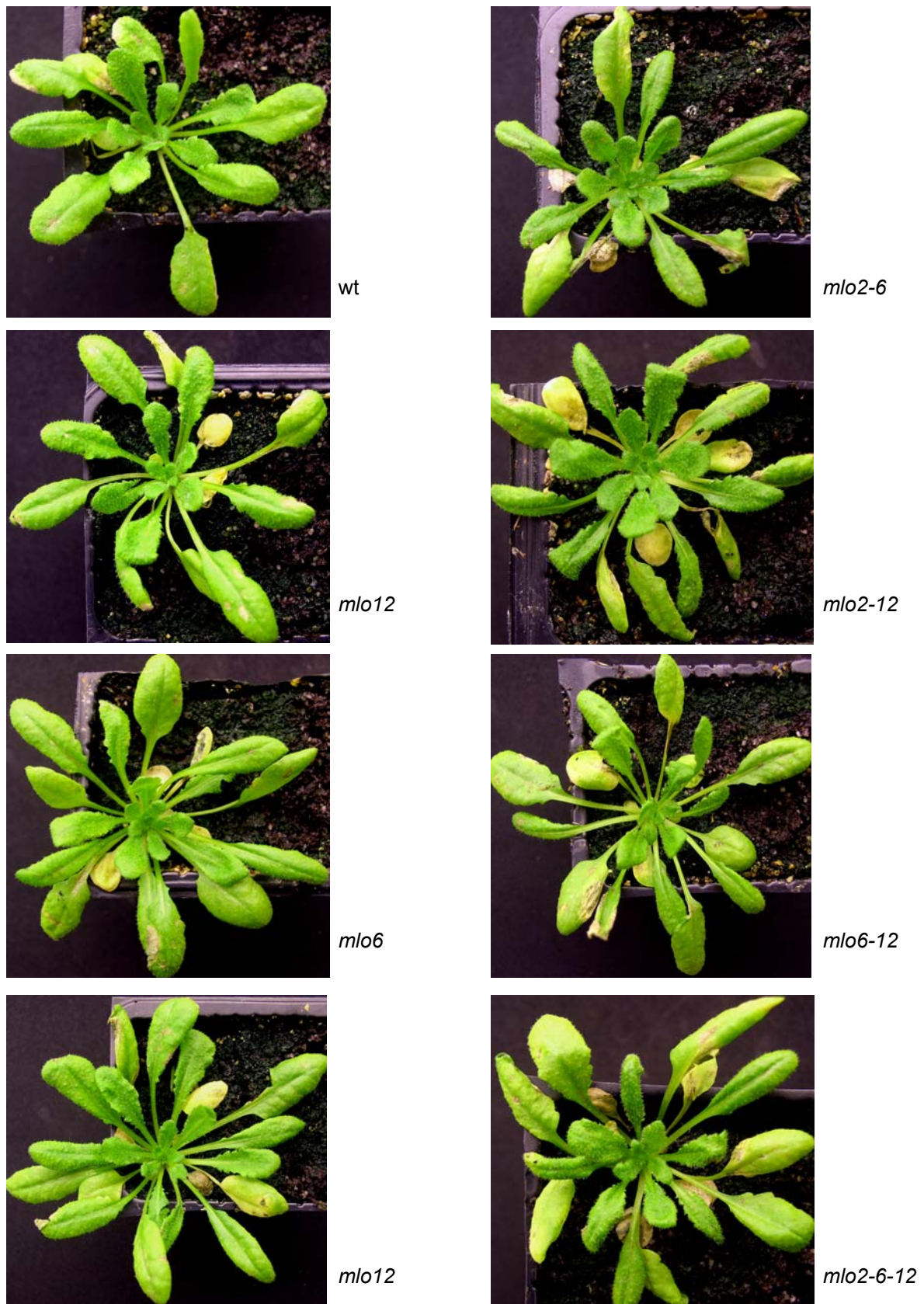


**Figure 29:** Macroscopic symptoms on plants infected with *Alternaria alternata*.

Wild-type *Arabidopsis* and homozygous *Arabidopsis* insertion mutants *mlo2*, *mlo6*, *mlo12*, *mlo2-6*, *mlo2-12*, *mlo6-12*, and *mlo2-6-12* were inoculated by spraying spore suspension onto the rosette leaves. Inoculated plants were maintained in climate chambers under saturating humidity. Chambers were provided with a 14 hours light (20°C) / 10 hours dark (18°C) cycle. Pictures show representative plants 5 days after treatment.

Symptoms became first visible at 48 h after infection manifested as black punctual spots on the leaf surface. In the course of progressive infestation with *Alternaria alternata* individual leaves appeared complete chlorotic, apparent as total yellowing, see Fig. 29. Since the visual rating of leaf damage only reflects the extent of host cell death but not the proliferation of fungal hyphae, the amount of fungal mycelium was approximated by quantitative PCR using fungal DNA extracted from inoculated leaf samples as template in combination with *Alternaria*-specific primers (Fig. 30).

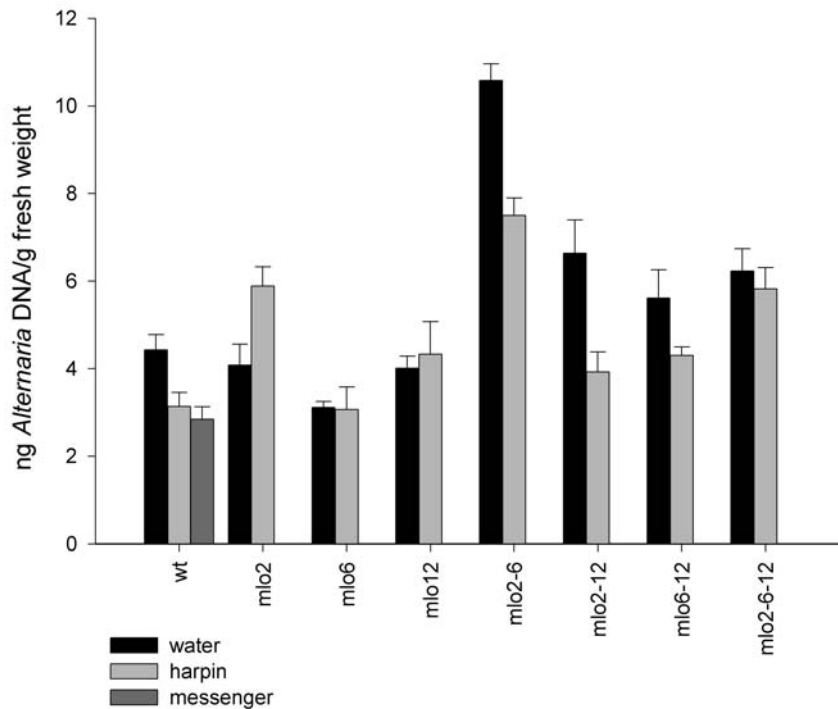


**Figure 30:** Quantification of fungal DNA in pathogen-challenged *Arabidopsis* wild-type and *AtMlo* mutant plants.

Wild-type and *AtMlo* knockout mutants were pre-treated for 5 days with 12  $\mu\text{g}/\text{ml}$  of harpin, or sprayed with water respectively. Bar graphs indicate the detected amount of *Alternaria* DNA related to a constant amount of plant material 5 days after inoculation. Values represent mean  $\pm$  SD from 5 independent experiments.

Based on the PCR data, water-sprayed (i.e. non-treated) *AtMlo* single knockout mutants *mlo2*, and *mlo12* showed slightly less fungal proliferation as *Arabidopsis* wild-type plants (-6.8% and -9.1%, respectively), whereas the *mlo6* mutant showed a significant reduced fungal biomass (-29.5%). All double and triple knockout mutants became more susceptible (or in other words: less resistant) to *Alternaria*. In comparison with the wild-type control an increase of detectable *Alternaria* DNA of 26.8% (*mlo6-12*) up to 139% (*mlo2-6*) was observed.

The application of harpin prior to a challenge infection with *Alternaria alternata* resulted in a significant reduction of detectable *Alternaria* DNA in wild-type *Arabidopsis* (-29.1% compared to water-treated sample), as well as in *mlo2-6* (-29.1%), and *mlo6-12* (-28.2%) knockout mutants. With -40.8% the highest degree of relative protection by harpin was monitored on *mlo2-12* mutant plants. In contrast, in the single knockout mutant *mlo2* harpin pre-treatment caused significant enhanced *Alternaria* DNA amounts than they showed without pre-treatment. This also correlated with higher amounts of *Alternaria* DNA.

### 4.3. Salicylic acid accumulation in *Mlo* knockout mutants

Salicylic acid (SA, 2-hydroxybenzoic acid) has shaped up as a key signaling molecule responsible for activating the hypersensitive response (HR) and the systemic acquired resistance (SAR) in plants. In both tobacco and *Arabidopsis*, exogenous SA induces the expression of pathogenesis related *PR* (*PR-1*, *PR-2*, and *PR-5*) genes and enhanced disease resistance. Several studies revealed a good correlation between increases in the endogenous levels of SA and its conjugates in infected plants and both the expression of *PR* genes and the development of disease resistance. Moreover, when SA accumulation is prevented in *Nicotiana tabacum* and *Arabidopsis* plants (e.g. by constitutive expression of the *nahG* transgene encoding the SA-degrading enzyme salicylate hydroxylase), *PR* gene expression and resistance to several pathogens is compromised.

In the present work it shall be examined whether harpin causes a rapid increase of salicylic acid content in *Arabidopsis* wild-type plants and if and how salicylic acid accumulation is induced in *AtMlo* knockout mutants.

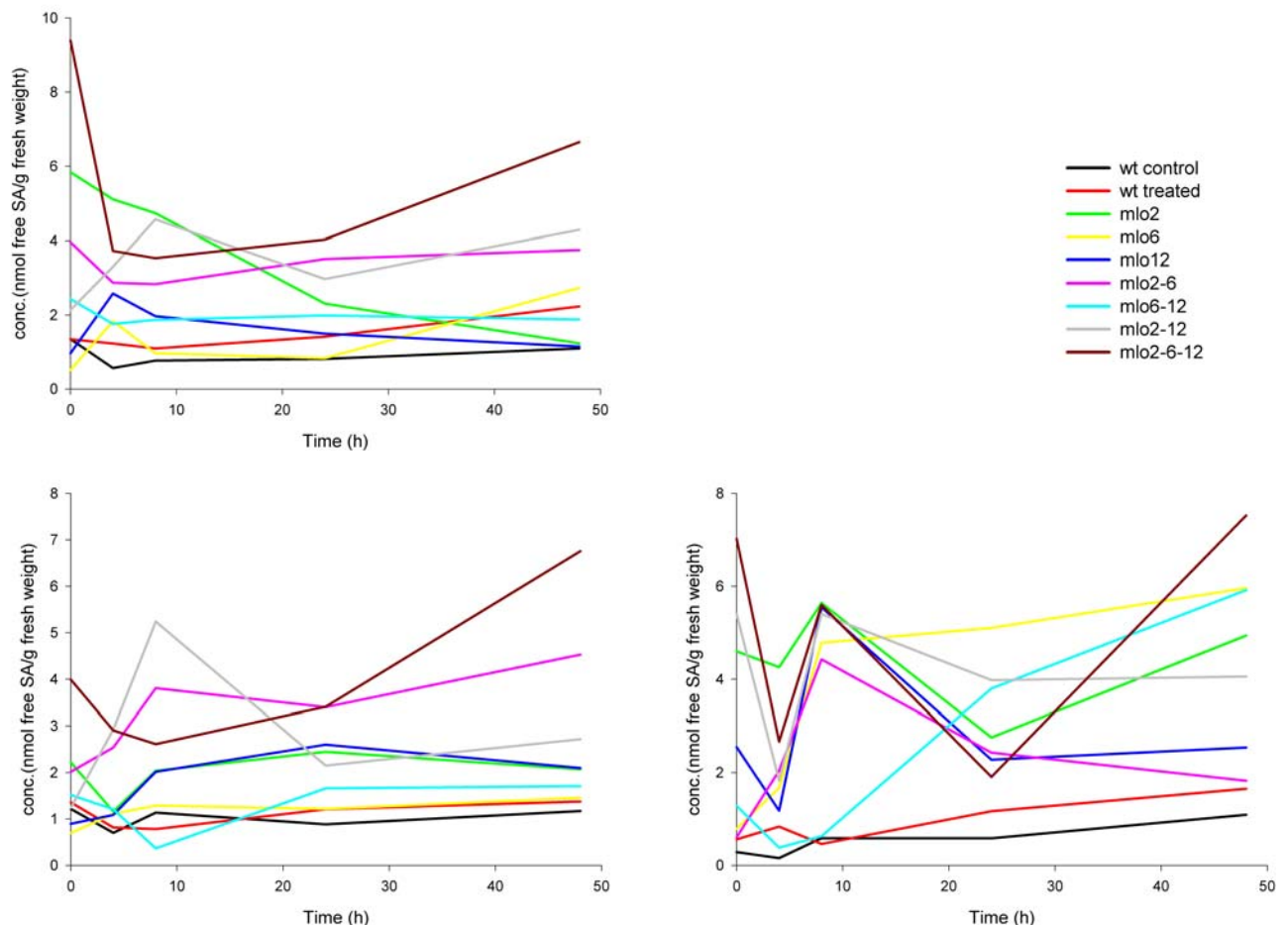


**Figure 31:** Accumulation of free salicylic acid in *Arabidopsis* plants after harpin treatment.

Six week old *Arabidopsis* wild-type and *AtMlo* knockout plants were treated with 12  $\mu\text{g/ml}$  of harpin. At indicated time points leaf samples were frozen in liquid nitrogen and stored at  $-80^\circ\text{C}$  until measurement of SA. The results of three independent experiments are presented in separated diagrams to ensure the clearness.



Figure 31 shows that within 48 h after harpin treatment no increase in free salicylic acid levels was detectable for *Arabidopsis* wild-type plants. In contrast, *AtMlo* knockout mutants accumulated constitutively elevated amounts of free SA that did not further increase upon harpin treatment. This effect was particularly evident for *mlo2*, *mlo2-6*, *mlo2-12*, and *mlo2-6-12* (i.e. all mutants bearing a *mlo2* knockout).

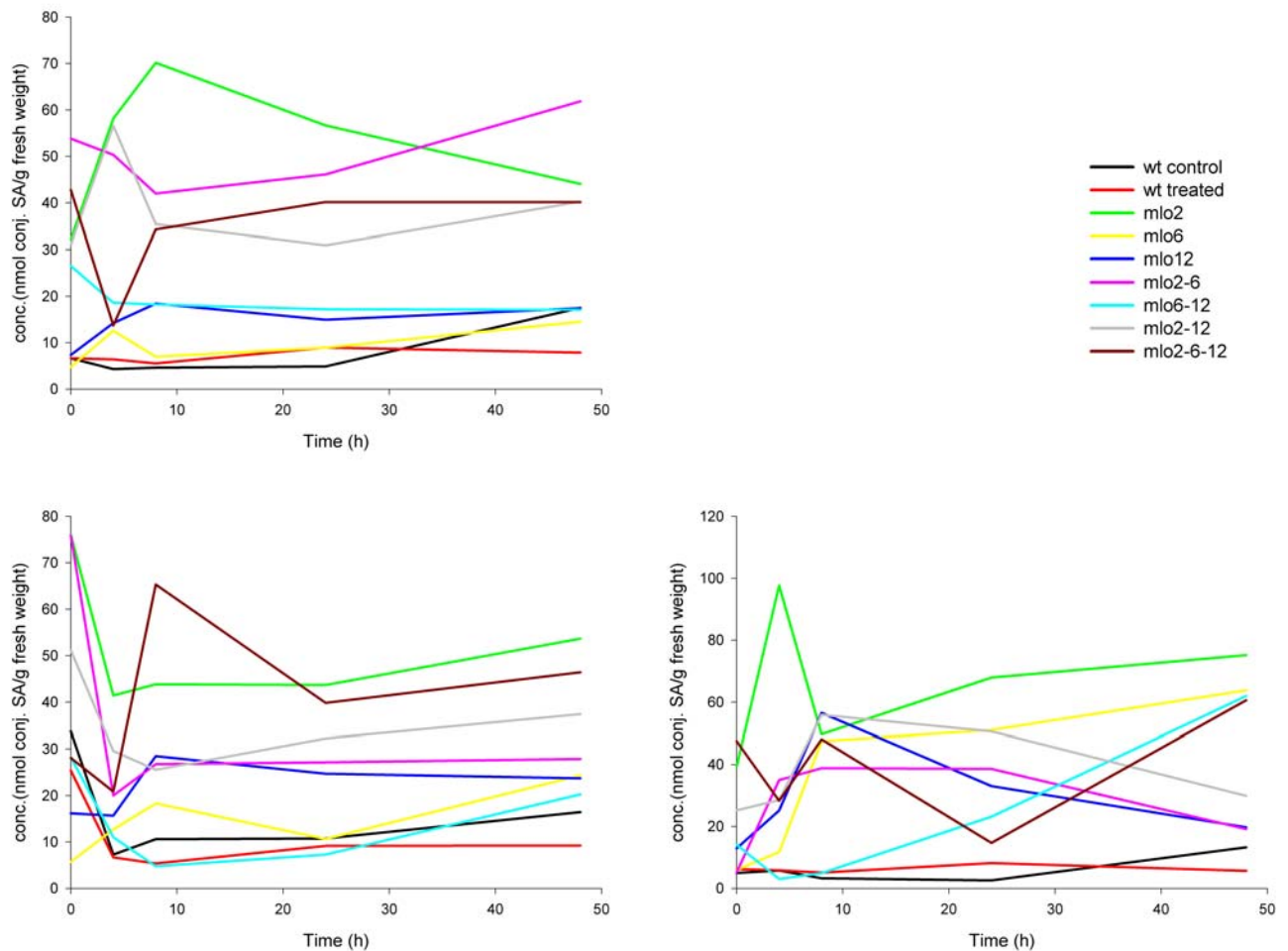


**Figure 32:** Accumulation of conjugated SA in *Arabidopsis* plants after harpin treatment.

Six week old wild-type *Arabidopsis* and *AtMlo* knockouts were treated with 12  $\mu\text{g/ml}$  of harpin. At indicated time points leaf samples were frozen in liquid nitrogen and stored at  $-80^{\circ}\text{C}$  until measurement of SA. The results of three independent experiments are presented in separated diagrams to ensure the clearness.

Likewise, enhanced constitutive accumulation of conjugated salicylic acid was found in all *Arabidopsis* insertion mutants carrying a *Mlo2* knockout (Fig. 32). To substantiate these findings, free and conjugated salicylic acid contents were determined in untreated plants in an independent set of experiments comprising three independent replicates (Fig. 33). This verified the constitutive SA accumulation in six week-old plants. The *mlo2* knockout mutants exhibit additional phenotypes that are under strict developmental control. Six week old untreated *mlo2* mutants start to exhibit massive spontaneous callose accumulation and sporadic mesophyll cell death. Therefore, it was investigated

in further experiments whether the constitutively elevated SA levels are likewise under developmental control. Exemplary, time course analysis of constitutive SA accumulation in the *mlo2-6-12* mutant was carried out using 4, 5, 6 and 7 week old plants (Fig. 34).

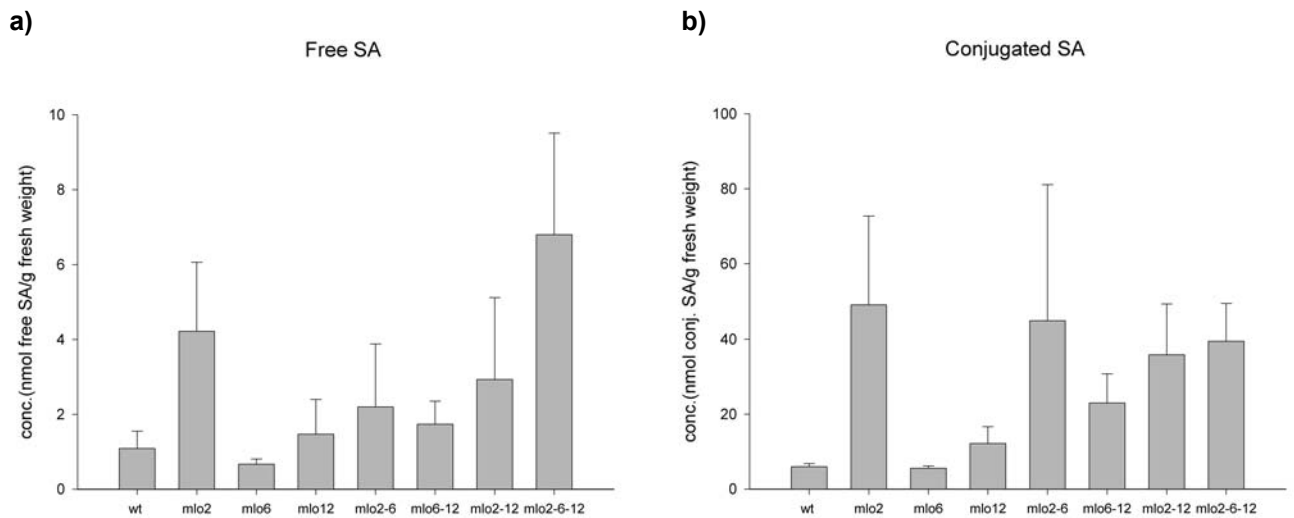


**Figure 33:** Salicylic acid accumulation in untreated *Atmlo* mutants.

Content of free (a) and conjugated (b) salicylic acid in 6 weeks old *Arabidopsis* wild-type plants and *AtMlo* knockout mutants. Values represent mean  $\pm$  SD from 3 independent experiments.

This experiment revealed that changes in SA accumulation are closely associated with the development status of the plants. Whereas 4 and 5 week old *mlo2-6-12* mutants showed nearly the same contents of salicylic acid as found in wild-type *Arabidopsis*, the amount of free SA in 6 and 7 week old *mlo2-6-12* mutants reached the 4-fold, and the amount of conjugated SA actually the 10-fold value of the younger mutant plants and of the wild-type plants, respectively.

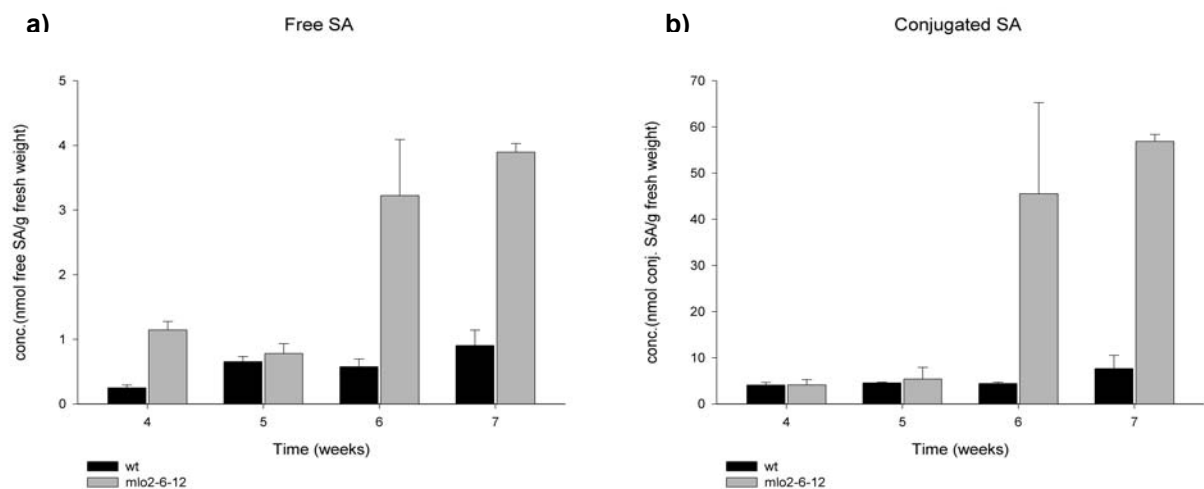


**Figure 34:** Time course analysis of constitutive SA accumulation in untreated *mlo2-6-12* mutants.

Content of free (a) and conjugated (b) salicylic acid in untreated *Arabidopsis* wild-type plants and *mlo2-6-12* knockout mutants of various ages. Values represent mean  $\pm$  SD from 3 independent experiments.

#### 4.4. Discussion of the chapter ✱

Recent findings, however, indicate a role for AtMLO2, AtMLO6, and AtMLO12 that is equivalent to barley MLO function. Loss-of-function mutations in *AtMlo2* confer enhanced powdery mildew resistance which becomes fully effective in the *Atmlo2-6-12* triple mutant. Moreover, the *Atmlo2* mutant exhibits similar pleiotropic effect as barley *mlo* genotypes (R. Panstruga and co-workers, personal communication).

Significant increases in transcript abundance of the *Mlo2*, *Mlo6*, and *Mlo12* gene were observed in *Arabidopsis* suspension cells after harpin treatment (Tab.10, p.47). This transient up-regulation was confirmed by semi-quantitative RT-PCR (Fig. 27, p.47). These findings are reminiscent of an increase in barley *Mlo* transcript accumulation upon elicitor treatment (Piffanelli et al. 2002) and further underline the common biological role of barley *Mlo* and the *Arabidopsis AtMlo2*, *6*, and *12* genes.

For barley it was reported that calmodulin interacts with MLO to dampen defense reactions against the powdery mildew fungus. A loss of CaM binding reduced the ability of MLO to negatively regulate defense against *Blumeria graminis* f.sp.*hordei* by ~50% (Kim et al., 2002a). Cytosolic free calcium serves as an important messenger in plants and is implicated in regulating many diverse processes, either by a direct activation of calcium-dependent protein kinases (CDPK) or indirectly through  $Ca^{2+}$ -modulator proteins such as calmodulin (Kim et al., 2002b). The ubiquitous calmodulin (CaM) is one of the major  $Ca^{2+}$  sensors, and is thought to be a primary transducer of intracellular calcium signals. However, many of the proteins that CaM binds are unable to bind calcium themselves, and as such use CaM as a calcium sensor, and signal transducer. Harpin stimulates calcium influx across the plasma membrane of cells. These increasing levels of cytosolic free  $Ca^{2+}$  are essential for initiation of defense mechanisms (Blume et al., 2000). This motivated the analysis of the transcriptional activation of genes encoding calmodulins, and calmodulin related proteins, respectively. During the observed time frame of 24 h, a strong up-regulation of genes encoding calmodulins was observed in harpin-treated *Arabidopsis* cells (Tab.11, p.48). This data correlate with the reported sustained increases of cytosolic free  $Ca^{2+}$ -levels in harpin-treated cells, monitored for 24 h (Blume et al., 2000).

##### 4.4.1. Pathogen experiments

As mentioned above, a disease resistance enhancing character of harpin against diverse viral, bacterial, and fungal pathogens has been monitored for different plant species. To test whether *Arabidopsis* MLO proteins contribute to harpin-mediated resistance or tolerance against pathogens homozygous *Arabidopsis* insertion mutants were made employed for pathogen assays. Inoculations were carried out with the pertotrophic fungus *Alternaria alternata*, whereas *Arabidopsis* wild-type and *AtMlo* mutant plants were sprayed with water or pre-treated with harpin for 5 days, followed by inoculation with the spore suspension for another 5 days.

✱ For a better readability the discussion of this chapter is separated from the general discussion.

As revealed by quantitative PCR to determine the amount of fungal DNA (Fig. 30, p.51), non-treated *Atmlo6* single knockout mutants showed a significant reduced *Alternaria* biomass (by nearly 30%) in comparison with wild-type plants. In contrast, *Atmlo2* and *Atmlo12* mutants did not exhibit altered accumulation of fungal DNA. This finding suggests that the *Atmlo6* mutant is possibly able to partially prevent the cell wall penetration of epidermal host cells by fungal appressoria or the subsequent formation of haustoria, intracellular feeding structures that are developed by most ascomycetes. Alternatively, fungal development is impaired in *Atmlo6* mutants at the post-penetration stage. Interestingly, as mentioned above, the *Atmlo2* knockout mutant was identified by its enhanced resistance to a further ascomycete, the virulent powdery mildew pathogen *Golovinomyces orontii*. In contrast, single T-DNA insertions in the *AtMlo6* and *AtMlo12* genes did not affect the outcome of this interaction (Schulze-Lefert, 2004). Infection phenotypes to the bacterial pathogen *Pseudomonas syringae*, and the oomycete *Peronospora parasitica* appeared unaltered in all tested *Atmlo* knockout mutants (Panstruga, 2005).

In the *Alternaria* inoculation experiments, the double and the triple knockout mutants became more susceptible, or less resistant to the fungus. Collectively, these findings suggest an antagonistic role of *AtMlo* genes in the context of the Arabidopsis-*Alternaria* pathosystem.

The application of harpin from *Pseudomonas syringae* prior to a challenge infection with *Alternaria alternata* resulted in a significant reduction of detectable *Alternaria* DNA in wild-type *Arabidopsis* as well as in knockout mutants with exception of the *Atmlo2* knockout mutant, where harpin pre-treatment caused an increase in the amount of fungal DNA compared to the control without any pre-treatment. Thus, the knockout of the *AtMlo2* gene and the subsequent lack of the MLO2 protein appear to prevent the harpin-mediated increased resistance against *Alternaria* as shown for wild-type *Arabidopsis*. Surprisingly, this effect was neither seen in the double mutants containing the *mlo2* mutation nor in the triple mutant.

#### 4.4.2. Salicylic acid accumulation

In dicotyledonous plants such as *Arabidopsis*, activation of the salicylic acid (SA)-dependent defense pathway has been shown to induce an array of defense genes, resulting in systemic acquired resistance (SAR), which occurs in distant plant organs upon a local encounter with a pathogenic microbe. It is reported that activation of the SA-pathway increases the resistance of *Arabidopsis* to *Erysiphe cichoracearum*, whereas disabling of signaling through the SA pathway enhances susceptibility to *Golovinomyces orontii* and to *Peronospora parasitica*. In addition, further studies indicate that activation of the SA pathway limits powdery mildew growth on *Arabidopsis* (Durner et al., 1997; Shah et al., 1999; Schulze-Lefert and Vogel, 2000).

In the present work it was examined whether harpin as inducer of SAR causes a rapid increase of salicylic acid content in *Arabidopsis* wild-type plants and, if and how salicylic acid is induced in *AtMlo* knockout mutants. Due to strong variation in the results of the three independent experiments no clear statement can be made regarding changes in SA accumulation after harpin treatment in *Arabidopsis* wild-type and *mlo* mutants (Fig. 31,32, pp.52-53). Maybe, the time points selected for



this set of experiments were not appropriate to resolve potential differences. However, the results clearly show that the knockout of the *Mlo2* gene apparently leads to constitutive higher amounts of accumulating salicylic acid, independent from any treatment (Fig. 33, p.54). Moreover, the time course analysis of SA content in the triple knockout mutant *mlo2-6-12* revealed that changes in SA accumulation are closely associated with the developmental status of the plants (Fig. 34, p.54). Such developmental changes in SA levels were already reported for wild-type rice seedlings, grown up to 35 days. Further it was shown that inoculation of rice plants with *Pseudomonas syringae* D20, which results in a hypersensitive response and induction of *PR* genes, did not cause significant changes in SA content. Inoculations with *Magnaporthe grisea*, the causal agent of rice blast, like inoculation with *P. syringae*, did not alter SA levels in rice (Silverman et al., 1995). The correlation in the increase of SA in the *Arabidopsis* *Atmlo2* mutant and the spontaneous deposition of callose (R. Panstruga, personal communication) might serve as first indication that the developmental increase in SA is directly linked to the abnormal callose deposition. Further studies are required to resolve whether SA accumulation is the cause or consequence of these cellular perturbations.

## 5. Uptake and fate of harpin

One of the most exciting questions is where goes harpin, once applied to the plant surface. Does it enter a plant cell or is its intruding into the cell prevented by the constitution of the cuticula?

Using a green fluorescent dye the FPLC-purified harpin was labeled for cytological detection. *Arabidopsis* suspension cells and protoplasts from leaves were treated with harpin for two hours in the dark and then observed and photographed under fluorescent light and bright field. Images (Fig. 35) prove that harpin goes into cells and does not only adherence at the cell wall, but the accurate target region of the protein has to be investigated on the whole organism, an *Arabidopsis* plant.



**Figure 35:** Cytological detection of fluorescence labeled harpin protein.

*Arabidopsis* suspension cells (left images) and protoplasts from *Arabidopsis* leaves (right images) were treated for 2 h with green fluorescent harpin. Cells were observed under fluorescent microscope, photographs were taken under fluorescence light (left) and bright field (right).

Thin sections from harpin treated and untreated *Arabidopsis thaliana* plants were cut and incubated with rabbit anti-harpin serum and a secondary anti-rabbit immunoglobulin labeled with FITC (Fluorescein isothiocyanate). Untreated controls (incubated with primary and secondary antibody) showed no, or in rare cases an unspecific labelling (Fig. 37). A strong specific fluorescence labeling was visible in the epidermal layer of harpin treated leaves (Fig. 36, 37). Thereby the fluorescence is not distributed diffuse in the intercellular space, but rather localized at the cell confining wall. These findings suggest that harpin has an affinity to cell membranes. However, this assumption has to be verified by electron microscopy immunogoldlabeling at ultrastructural level.

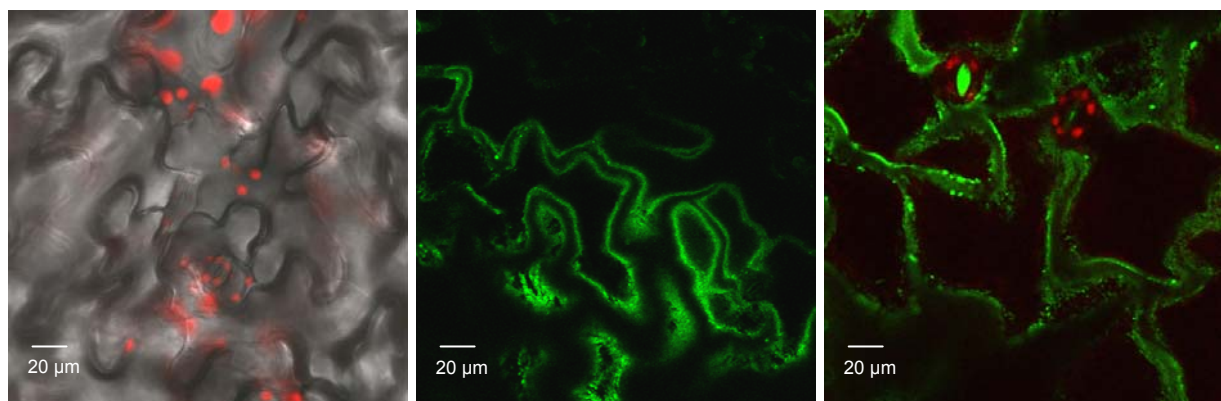


**Figure 36:** Fluorescence microscopy immunolabeling of harpin in *Arabidopsis* leaves.

Epidermal layer of *Arabidopsis* leaves from untreated plants with translucent red autofluorescence of chloroplasts in the mesophyll layer (left image). Epidermis from harpin treated plants (middle image) contains embedded stomata with red fluorescent chloroplasts (right image). Photographs were taken by confocal laser-scanning microscopy.

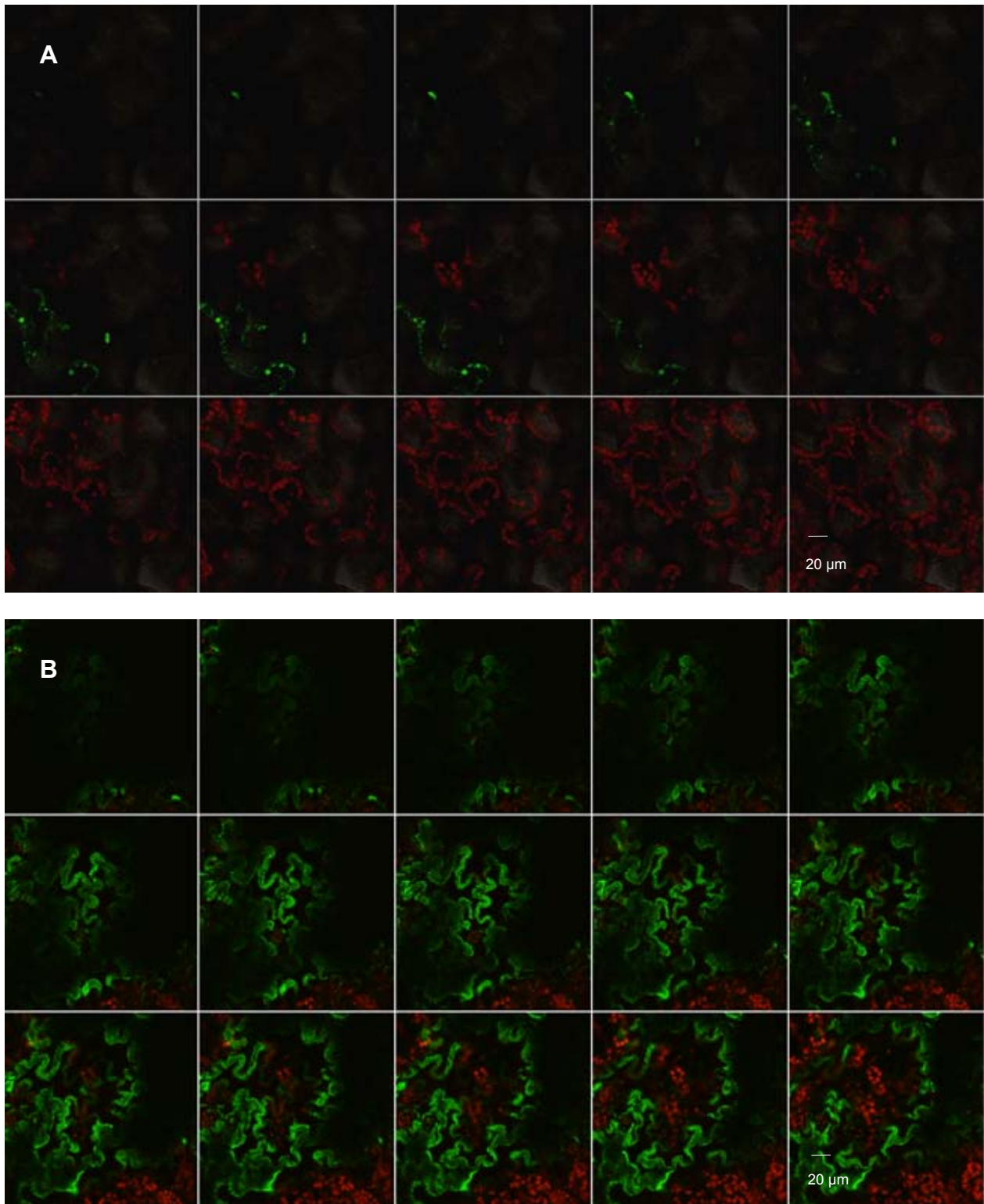


**Figure 37:** Immunodetection of harpin in *Arabidopsis* leaves.

Semi-thin sections of untreated (A) and 12 hours harpin treated (B) *Arabidopsis* leaves are presented. After FITC immunofluorescence labeling, harpin appears highly fluorescent in epidermal layers, whereas the red fluorescence derives from chloroplasts in the subjacent mesophyll layers. For control leaves photographs were taken in 1.5µm- and for treated leaves in 1µm- successive steps into the leaf by confocal laser-scanning microscopy.

### III. Discussion \*

In this study, biochemical and molecular features of *Arabidopsis thaliana* cells undergoing cell death induced by the type III elicitor harpin were investigated. Taken together with results from recently published reports, these findings will be integrated in a model describing PCD in plant cells. Functions conserved throughout the animal and plant kingdom will also be compared.

#### 1. Harpin induces ROS and NO

One of the hallmarks of plant defense responses is the induction of a strong oxidative burst after contact with a pathogen-derived elicitor. There is convincing evidence that reactive oxygen species (ROS) play important roles in the initiation of defense responses and cell death (Dangl and Jones, 2001).

As shown, harpin can induce cell death (Fig. 4, p.12) as well as ROS (Fig. 7, p.15). Interestingly, several recent studies have reported that generation of  $O_2^-$  and  $H_2O_2$  after harpin treatment of tobacco was not required for apoptotic cell death induced by harpin or other elicitors (Sasabe et al., 2000; Xie and Chen, 2000). Moreover, harpin and  $H_2O_2$ , although both initiating cell death in *Arabidopsis* spp., have been shown to activate different sets of defense genes (Desikan et al., 1998). These results suggest the existence of branched signal transduction pathways that following harpin recognition.

Previously, it has been suggested that NO and ROS play a major regulatory and/or executive role in plant defense responses and cell death events associated with microbial pathogen attack (McDowell and Dangl, 2000; Van Camp et al., 1998). ROS may possess direct antimicrobial activity and function in cell wall reinforcing processes. Plant responses to ROS are dose-dependent, high doses trigger HR-related PCD, whereas low doses induce antioxidant enzymes. It was postulated that ROS act as a trigger for PCD locally and as diffusible signal for the induction of cell defenses in neighbouring cells (Vranova et al., 2002). NO acts synergistically with ROS to increase host cell death of soybean suspension cells and inhibitors of NO compromise HR in *Arabidopsis thaliana* and tobacco (Delledonne et al., 2001).

Due to the close interaction of ROS with defense associated NO induced by microbial attack, it was asked for a possible role of NO in defense responses elicited by harpin. Here, a NO sensitive fluorescein derivative (DAF) in conjunction with fluorescence microscopy was used to directly measure the NO burst in harpin treated *Arabidopsis* cells (Fig. 8, p.16). This technique has been applied previously to document NO production within living cells (Foissner et al., 2000; Garcia-Mata and Lamattina, 2002; Neill et al., 2002; Pedroso et al., 2000). NO production after harpin treatment was much slower compared with an elicitor-induced NO burst in tobacco or mechanical stress of various gymnosperms (Foissner et al., 2000; Pedroso et al., 2000). Induction of NO paralleled ROS production, which started within a few minutes after addition of harpin (Fig. 7, p.15).

\* For a better readability the discussion of chapter 3 and 4 is separated from the general discussion.

In the recent study of Xie and Chen (Xie and Chen, 2000) harpin from *Erwinia amylovora* induced an inhibition of the ATP pool in tobacco cell cultures. Notably, diphenylene iodonium, an inhibitor of the oxidative burst (although a rather non-specific agent) (Moller, 2001), did not block cell death. Given the recently demonstrated roles of mitochondria in apoptosis, it has been suggested that the rapid inhibition of mitochondrial functions may play a role in harpin-induced hypersensitive cell death. This work provides the evidence that harpin severely affects mitochondria in *Arabidopsis* spp.

Although plant mitochondria are known to produce high amounts of ROS (Moller, 2001), they frequently have been overlooked as a source of ROS in the context of defense responses. In animals, a variety of key events in apoptosis focus on ROS-mediated events in mitochondria, including the release of caspase activators such as cytochrome c, changes in electron transport, loss of mitochondrial transmembrane potential, altered cellular oxidation reduction, and participation of pro- and anti-apoptotic Bcl-2 family proteins (Green and Reed, 1998).

Here, it was shown that harpin treatment of *Arabidopsis* cells leads to ROS production in mitochondria (Fig. 9, p.17). Thereby it has to be noted that the obtained MitoTracker Red signals require intact membrane potential, ruling out the possibility that destroyed or non-functional mitochondria contribute to the ROS stain. One possible source of mitochondrial ROS which include superoxide ( $O_2^{\cdot-}$ ), hydrogen peroxide ( $H_2O_2$ ), and the hydroxyl free radical ( $\cdot OH$ ) in plants might be the ubiquinone pool (Moller, 2001). This assumption would coincide with previous studies on isolated animal mitochondria, which detected ROS forming sites in the mitochondrial electron transport chain (ETC), namely the ubiquinone site in complex III (Turrens and Boveris, 1980; Turrens et al., 1985). But, the same study proposed an at that time unknown site in complex I as ROS forming site, which recently was identified as the primary physiologically and pathologically relevant site of ROS generation: the flavin mononucleotide (FMN) group of complex I (Liu et al., 2002).

Co-localization of mitochondria and ROS formation does not necessarily implicate a key role for mitochondrial ROS during early stages of apoptotic response to harpin. On the other hand, similar results have been found with victorin-treated oat, which also suggested a possible involvement of mitochondria, especially mitochondrial-derived ROS generation, as an important regulator in controlling apoptotic cell death (Yao et al., 2002). However, it is unclear at present whether mitochondrion-mediated  $H_2O_2$  plays a role in cell death mediated by harpin or other elicitors. NO and antimycin A (mitochondrial complex III inhibitors) certainly induce ROS eruption in mitochondria as well as cell death (data not shown; Yao et al., 2002), but a convincing causality is still lacking.

In contrast to the mitochondria localized  $H_2O_2$ , NO could not be observed within this organelles after harpin treatment. Previously, we reported on NO production or accumulation in chloroplasts and, most likely, in peroxisomes, but not in mitochondria (Foissner et al., 2000). However, (negative) data on intracellular localization of NO or  $H_2O_2$  based on the use of dyes should be interpreted with caution. DAF-derivatives are single-wavelength probes, and no adjustments can be made for differential accumulation of the probe within the cell (i.e. no loading of specific organelles). Very recently, Planchet and associates identified the mitochondrial electron transport chain as a major source for reduction of nitrite to NO in addition to nitrate reductases in *Nicotiana tabacum* using inhibitors and purified mitochondria. Interestingly, at equal respiratory activity they found that

mitochondria from suspension cells had much higher capacity to produce NO than leaf mitochondria (Planchet et al., 2005).

## 2. Decrease of mitochondrial transmembrane potential $\Delta\Psi_m$ and loss of ATP

Associated with (but not necessarily caused by) ROS production are dramatic changes in mitochondrial condition and metabolism. Mitochondria are organelles with two well-defined compartments: the matrix, surrounded by the inner membrane (IM), and the intermembrane space (IMS) surrounded by the outer membrane (OM). The IM is folded into numerous cristae, which contains the protein complexes from the electron transport chain (ETC), and the ATP synthase. To function properly, the IM is almost impermeable in physiological, thereby allowing the respiratory chain to create an electrochemical gradient ( $\Delta\Psi_m$ ). The mitochondrial transmembrane potential  $\Delta\Psi_m$  results from the respiration-driven, ETC-mediated pumping of protons out of the IM and is indispensable for driving the ATP synthase which phosphorylates ADP to ATP. ATP generated on the matrix side of the IM is then exported in exchange for ADP by ADP/ATP carrier (Siedow and Umbach, 1995; Vercesi et al., 1995; Vedel et al., 1999).

An early cellular response to elicitors such as ultraviolet (UV) light is the disruption of the mitochondrial transmembrane potential  $\Delta\Psi_m$  in mammalian cells (Bal-Price and Brown, 2000; Goldstein et al., 2000). In plants (epidermal peels of oat leaves), a rapid decrease of the  $\Delta\Psi_m$  was induced by the fungal toxin victorin (Yao et al., 2002).

Results of this study show a dramatic loss of the mitochondrial transmembrane potential in *Arabidopsis* cells after contact with harpin (Fig. 10, p.18). A logical consequence of deteriorating  $\Delta\Psi_m$  would be a decreased phosphorylation capacity and of ATP pool size, as reported for *tobacco* cells treated with salicylic acid (SA) or harpin from *Erwinia amylovora* (Xie and Chen, 1999; Xie and Chen, 2000). A significant decrease of ATP in harpin-treated cells was demonstrated (Fig.11, p.19). Interestingly, previous studies suggest that responses to harpin depend on a functional ATPase and on a certain basal level of ATP (He et al., 1993). It should be noted, however, that measurements of the ATP pool size do not give any indication of the direction of the fluxes. Furthermore, because the mitochondrial membrane potential has decreased to a stable level after 1 hour and the ATP concentrations continuously decreases for 7 hours, additionally factors appear to affect the ATP pool.

## 3. Cytochrome c release from mitochondria

A prominent apoptosis-activating factor in animals is mitochondrial cytochrome c, which acts in the cytoplasm by recruiting caspases, which in turn are central players of apoptotic events (Green and Reed, 1998). Cytochrome c release into the cytosol occurs in several ways, all dependent on calcium fluxes in presence of low ATP levels. One route is via the permeability transition pore (PTP), a complex of voltage-dependent anion channel (VDAC) with other proteins (Goldstein et al., 2000). Cytochrome c release also might be important in plant cell death.

Here, for the first time it was shown, that plant mitochondria release cytochrome c into the cytosol upon contact with a pathogen elicitor (Fig. 14, p.22). The harpin induced cell death in *Arabidopsis* spp. was accompanied by a nuclear translocation of cytochrome c after its release into the cytosol (Fig.15, p.23), a result which complies with observations in animal apoptosis where the nuclear translocation of cytochrome c was independent of caspase activation (Nur et al., 2004).

I would like to point out that cytochrome c release event could be the key component of the plant cell death program. Previous reports have documented that cytochrome c release precedes heat- and menadione-induced (a redox active quinone that generates intracellular superoxide) death in plant cells (Balk et al., 1999; Sun et al., 1999). Further, H<sub>2</sub>O<sub>2</sub> or SA-induced death in tobacco was characterized by a cytochrome c release (Vanlerberghe et al., 2002). In addition, it has been shown that maize cells induced to die by the addition of D-mannose release cytochrome c to the cytosol. A plausible explanation for mannose action is that it lowers the ATP level and raises ROS levels to a point where the high calcium level found in the culture medium trigger the permeability transition pore and cytochrome c release (Stein and Hansen, 1999). Evidence for the role of PT pores in plants has been published very recently. Ultrastructural analysis using a cytochemical assay detected H<sub>2</sub>O<sub>2</sub> eruption at pore-like sites on the mitochondrial membrane in oat cells treated with victorin or after treatment with antimycin A (Yao et al., 2002).

Without true caspases in the *Arabidopsis* genome, the mechanism of cytochrome c activation of plant cell death is unclear. Therefore, it has been proposed that cytochrome c release per se generates lethal levels of mitochondrial ROS (Yao et al., 2002), because the moving cytochrome c leaves a non-functional and ROS-generating electron transport chain behind (Jones, 2000). In this context it should be noted that in animals, cytochrome c release occurs independently of membrane depolarization (Bossy-Wetzel et al., 1998).

#### **4. Alternative respiration through AOX pathway**

Plants are able to handle ROS-generation in mitochondria much better than animals do. In addition to cytochrome c oxidase, plant mitochondria possess a second terminal oxidase, alternative oxidase (AOX), localized in the inner mitochondrial membrane. AOX catalyzes the oxidation of ubiquinone and the reduction of oxygen to water, bypassing the final steps of the cytochrome c pathway. Unlike the cytochrome c pathway, which is coupled to oxidative phosphorylation via proton translocation, electron transport from ubiquinone to AOX is non-phosphorylating and releases energy as heat, thereby preventing overreduction of the ubiquinone pool and ROS generation under conditions where ATP synthesis is not critical.

Antisense tobacco cells lacking mitochondrial AOX undergo an irreversible cell death response, marked by a nuclear DNA fragmentation, when incubated with specific inducers, that is H<sub>2</sub>O<sub>2</sub> and salicylic acid (SA), known for their involvement in the hypersensitive response (HR), or cantharidin, a Ser/Thr protein phosphatase inhibitor (Robson and Vanlerberghe, 2002). AOX frequently is induced during plant-pathogen interactions and plant defence, and seems to play a role in containment of lesions and control of initial plant defense reactions (Chivasa and Carr, 1998; Lennon et al., 1997).

Internal triggers of AOX induction might be SA and NO (Huang et al., 2002; Vanlerberghe and McIntosh, 1997).

In contrast to Boccara (Boccara et al., 2001), who found no significant induction of this enzyme after treatment of *Nicotiana sylvestris* with harpin from *Erwinia amylovora*, here, Northern analysis indicates a dramatic, transient increase of AOX in *Arabidopsis* suspension cells (Fig. 13, p.21).

This result is supported by that of Simons and associates, who reported an enhanced expression of AOX during infection of *Arabidopsis* spp. with harpin-secreting *Pseudomonas syringae* pv. *tomato* (Simons et al., 1999).

Despite the rapid induction of protecting or scavenging systems such as AOX (Fig. 13, p.21) and sHSPs (Tab. 7, p.39; Fig. 26, p.40), a cytochrome c release after harpin treatment was shown (Fig. 14, p.22). That is not necessarily inconsistent with a protective role of these components. Recent studies have shown that treatment of transgenic *Nicotiana tabacum* lacking AOX with H<sub>2</sub>O<sub>2</sub> or SA is characterized by a massive decrease of cytochrome c respiration (Vanlerberghe et al., 2002).

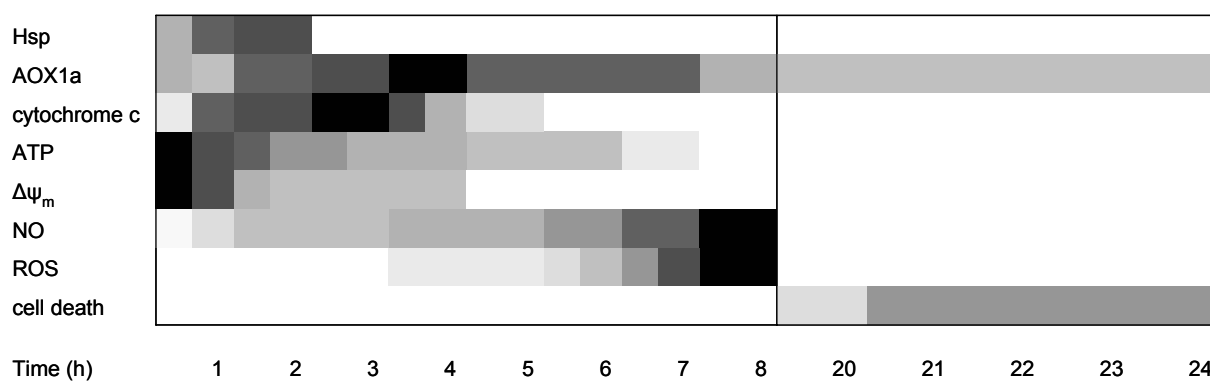


**Figure 38:** Relative timing of mitochondria-associated parameters after harpin treatment.

Figure illustrates the relative timing of the analyzed mitochondrial events in *Arabidopsis* spp. after treating with harpin. Data are plotted in a timeframe of 24 hours in a greyscale picture, with the maximum response/value in black, and the minimum response/value in light-grey. Note that the axis breaks after 8 hours.

Figure 38 summarizes the relative timing of the analyzed mitochondrial parameters after treating *Arabidopsis* with harpin. It was shown that harpin induces accumulation of mitochondrial ROS, membrane depolarization, cytochrome c release and induction of redox-protecting components, all defense responses often associated with apoptosis in animals and plants.

## 5. Induction of genes encoding mitochondrial proteins

Due to the inactivating effect on mitochondrial functions, the genetic program of mitochondria behind the harpin induced apoptosis was surveyed.

A comprehensive expression analysis of genes revealed a total of 199 transcripts that changed significantly in abundance during 24 hours of harpin treatment (Fig. 16, p.23; see also supplement 1 at the attached CD-ROM). Of note is the up-regulation of transcripts essential for mitochondrial



metabolism, transport mechanisms such as mitochondrial protein import apparatus (Tab. 2, p.28), and for energy budget affecting processes like TCA cycle (Fig. 18, p.25) and ETC (Fig. 19, p.26). A temporally oppositional behaviour in mitochondrial and global gene regulation was observed (Fig.17, p.24).

The harpin induced decrease of the mitochondrial transmembrane potential  $\Delta\Psi_m$  (Fig. 10, p.18) results in a decline of the cellular energy metabolism, displayed by a rapid loss of intracellular ATP content (Fig.11, p.19). As the level of ATP falls there is a concomitant increase of ADP and AMP which serve as activators of the pyruvate dehydrogenase complex (PDC), citrate synthase (CS), and isocitrate dehydrogenase (ICDH). This accelerates the tricarboxylic acid cycle (TCA) to produce more ATP. Under these circumstances a transcriptional activation of genes encoding mitochondrial proteins of TCA cycle and ETC as well as of mitochondrial carriers is necessary as a requisite for later synthesis of proteins essential for ATP production and ATP transfer. Furthermore, the expression of components of the mitochondrial import apparatus was up regulated significantly may be as a result of the possibly harpin caused mitochondrial damage and protein turnover that require replacement through mitochondrial biogenesis.

Moreover, a decline in ATP synthesis might be caused by blocking of mitochondrial electron transport, what would be associated with decreased respiratory  $O_2$  uptake. It has already been shown that salicylic acid (SA) and its analogs inhibited both ATP synthesis and respiratory oxygen uptake (Xie and Chen, 1999; (Xie and Chen, 2000).

Here, only a transient decline in respiratory  $O_2$  uptake was observed, and the respiration was not blocked by a direct contact of mitochondria with harpin protein (Fig.12a, b, p.20). These findings go along with the fact that the TCA cycle and most notably the electron transport chain seems to be activated during harpin stress, at least at transcript level (Fig. 18,19, pp.25-26).

The increase in transcript abundance of a high number of genes encoding protein subunits of the TCA cycle and the ETC suggests that harpin stress does not restrict the respiratory capacity of mitochondria within the first 24 hours after treatment. Taken together, the microarray analysis of the mitochondria from *Arabidopsis* spp. shows an adaptation by the mitochondrial metabolic activities in response to harpin. Thus, the transcriptional profiling successfully identified novel aspects of the harpin induced alterations in the expression of the genes related to mitochondrial function and biogenesis.

## **6. Harpin activates mitochondrial enzymes**

Based on observed up-regulation of genes belong to all TCA cycle enzyme complexes and of nearly 50% of ETC-enzyme encoding genes, this study was extended to proteome analysis of mitochondrial fractions. Thus, the activating effect of harpin on mitochondrial enzymes in *Arabidopsis* could be confirmed at protein level using IEF/2-D gel electrophoresis, comparison of protein spot abundances and mass spectrometry.

Significant changes in regulation of 28 mitochondrial proteins were observed (Fig. 20, p.29; Tab. 3, p.30), spots of 13 proteins increased significantly during harpin stress, and 15 were down-regulated at the same time. Noteworthy is the significant regulation of 9 TCA related enzymes. The influence of harpin on all citric acid cycle related enzyme complexes at transcript level was partially recovered at proteomic level.

The glutathione S-transferase (At1g02930) GST1 as well as glyceraldehyde-3-phosphate dehydrogenase (At3g04120) GAPDH were found as up regulated at protein level as reported after H<sub>2</sub>O<sub>2</sub> and menadione treatment (Sweetlove et al., 2002). Some GSTs have been shown to act within mammalian mitochondria. But, they are also reported as early markers for biotic and abiotic stresses in *Arabidopsis* such as oxidative stress, where significant inductions at transcript level were observed (Reuber et al., 1998; Kliebenstein et al., 1999; Grant et al., 2000; Rate and Greenberg, 2001). Recently, the evidence for a role in detoxifying lipid peroxidation products was cited for a mitochondrial GST after oxidative stress. The glycolytic GAPDH was proposed to be associated with mitochondria to play a role in DNA repair or signaling after oxidative damage (Sweetlove et al., 2002). Given the usually high abundance of these proteins in other cell fractions than mitochondria, it is possible that they adhered to the mitochondria during isolation procedure, but, no such association was seen with the control mitochondria.

Like caused by H<sub>2</sub>O<sub>2</sub> and menadione treatment (Sweetlove et al., 2002), the actin-depolymerizing factor ADF3 (At5g59880) was identified as significant increased in protein abundance during harpin stress. The ADF/cofilin proteins are stimulus-responsive actin-severing proteins, members of which are regulated by reversible phosphorylation. In maize this protein is known to accumulate in growing root hair tips (Jiang et al., 1997), to bind phosphatidylinositol-4,5-bisphosphate (PIP<sub>2</sub>), which forms a tip-to-base gradient in growing hairs (Braun et al., 1999) and to localize to the initiation site during swelling formation (Braun et al., 1999). Further, for maize ADF was shown that it is phosphorylated by calmodulin-like domain protein kinase(s) CDPK(s), a class of protein kinases unique to plants and protozoa (Allwood et al., 2001).

The overall strongest up regulation of a protein was determined for the ATP dependent protease ClpC2 (At3g48870). The ClpC protein is a molecular chaperone of the Hsp100 family, in *Arabidopsis* represented by ClpC1 and ClpC2, recently reported to play a vital role in chloroplast function and leaf development, and to be likely involved in biogenesis of the photosystem (Sjogren et al., 2004). In contrast to the ClpC2 protein which was not observed as significant regulated at transcript level, the ClpC1 protein (At5g50920) was identified as down regulated at protein level but up regulated at transcript level. Consistent with observations in rotenone (an inhibitor of complex I of mitochondrial electron transport chain) treated *Arabidopsis*, the microarray analysis indicates an upregulation of mitochondrial ATP dependent proteases from Lon and Clp families (Lister et al., 2004) which are proposed to play an important role in the tolerance to oxidative stress induced by environmental conditions (Janska, 2005).

A number of proteins were significantly decreased in abundance following harpin stress. Among them, the stomatin-like protein (At4g27585) was identified, which belongs to a superfamily of plant

proteins, named PID (proliferation, ion, and death), and may be involved in signaling and programmed cell death via modulation of ion channel activity (Nadimpalli et al., 2000).

The mitochondrial manganese superoxide dismutase (Van Camp et al., 1990) MnSOD (At3g10920) whose overexpression enhances primarily the oxygenradical-scavenging capacity of the stromal system (Slooten et al., 1995) was down regulated at observed time points. In addition, a nucleoside diphosphate kinase 3, which is localized in the mitochondrial intermembrane space and function to equilibrate nucleoside triphosphate pools (Sweetlove et al., 2001).

Some enzymes which are related to the TCA cycle such as the E1 beta subunit of pyruvate dehydrogenase, citrate synthase,  $\text{NAD}^+$  isocitrate dehydrogenase, NAD dependent malate dehydrogenases, and subunits of the 2-oxoglutarate dehydrogenase complex have been shown to be responsive to harpin stress. The sensitivity of TCA cycle enzymes of pyruvate dehydrogenase complex (PDC), and 2-oxoglutarate dehydrogenase complex (OGDC) has already been documented for oxidative damage of plant mitochondria by  $\text{H}_2\text{O}_2$  or lipid peroxidation products (Millar and Leaver, 2000; Swidzinski et al., 2004). However, here a down regulation of the proteins belong to the OGDC was observed after harpin treatment. In contrast, pyruvate dehydrogenase as the key enzyme in oxygen-dependent metabolic pathways by shifting intermediates of glucose metabolism into TCA cycle was identified as significant up regulated as well as citrate synthase, and malate dehydrogenase. The isocitrate dehydrogenase was not detectable in control mitochondria, but up regulated at both time points, 8 and 24 hours after treatment, suggesting a post-transcriptional control of protein abundance. The electron transport chain and ATP synthase, here represented by the complex I NADH-ubiquinone oxidoreductase (At3g27890) and the ATP synthase  $\beta$  subunit (At5g08680) were also affected by harpin stress. Both were decreased during harpin treatment, as reported for oxidative stress on *Arabidopsis* mitochondria induced by  $\text{H}_2\text{O}_2$ , menadione, and antimycin A (Sweetlove et al., 2002).

These changes in protein abundance will significantly impair the capacity of oxidative phosphorylation and consequently the formation of ATP.

The apparent activation of mitochondrial energy budget affecting processes was confirmed by studying the activities of appropriate enzymes and determination of intermediates of the citric acid cycle. It was shown, that during the time frame of 24 hours no or only a transient loss in TCA enzyme activity (Fig. 21, p.31) as well as in TCA metabolite content (Fig. 22, p.32) was detectable. For citrate content as example, we observed an increase up to 300%. A possible explanation is the above mentioned rapid reduction of aconitase activity, which catalyzes the formation of isocitrate from citrate. In plants, the resulting citrate enrichment has been already reported from  $\text{H}_2\text{O}_2$  (hydrogen peroxide) and MFA (monofluoroacetate) treatments (Vanlerberghe and McIntosh, 1996), which inhibit the aconitase enzyme. Moreover, citrate has been implicated as a signal metabolite in regulating AOX1 gene expression (Vanlerberghe and McIntosh, 1996; Djajanegara et al., 2002) such as recently reported for exogenous supplied malate and 2-oxoglutarate (Gray et al., 2004). Further, a repression of mitochondrial and cytosolic aconitase resulted in an enhanced rate of photosynthesis and increased fruit yield of tomato (Carrari et al., 2003). The increase in 2-oxoglutarate content after

8 hours coincides with a down regulation of three 2-oxoglutarate dehydrogenases at protein level. The 60% decrease in oxaloacetate content, occurring within 2 hours, seems nearly to be compensated after 24 hours. Because the concentration of malate as a pre-stage of oxaloacetate is constant over time, fluctuations of malate dehydrogenase activity can explain this behaviour: it converts malate to oxaloacetate, and likewise shows a loss in activity after 2 hours and a dramatic increase of enzyme activity after 24 hours.

Thus, it can be demonstrated that the harpin caused stress response does not only share similarities with oxidative stress induced responses. The results also implicate a harpin specific pattern of mitochondrial metabolic alterations. Summarizing these findings and combining them with already published reports, a model can be prepared describing mitochondrial events during harpin induced apoptosis in plant cells (Fig. 39).

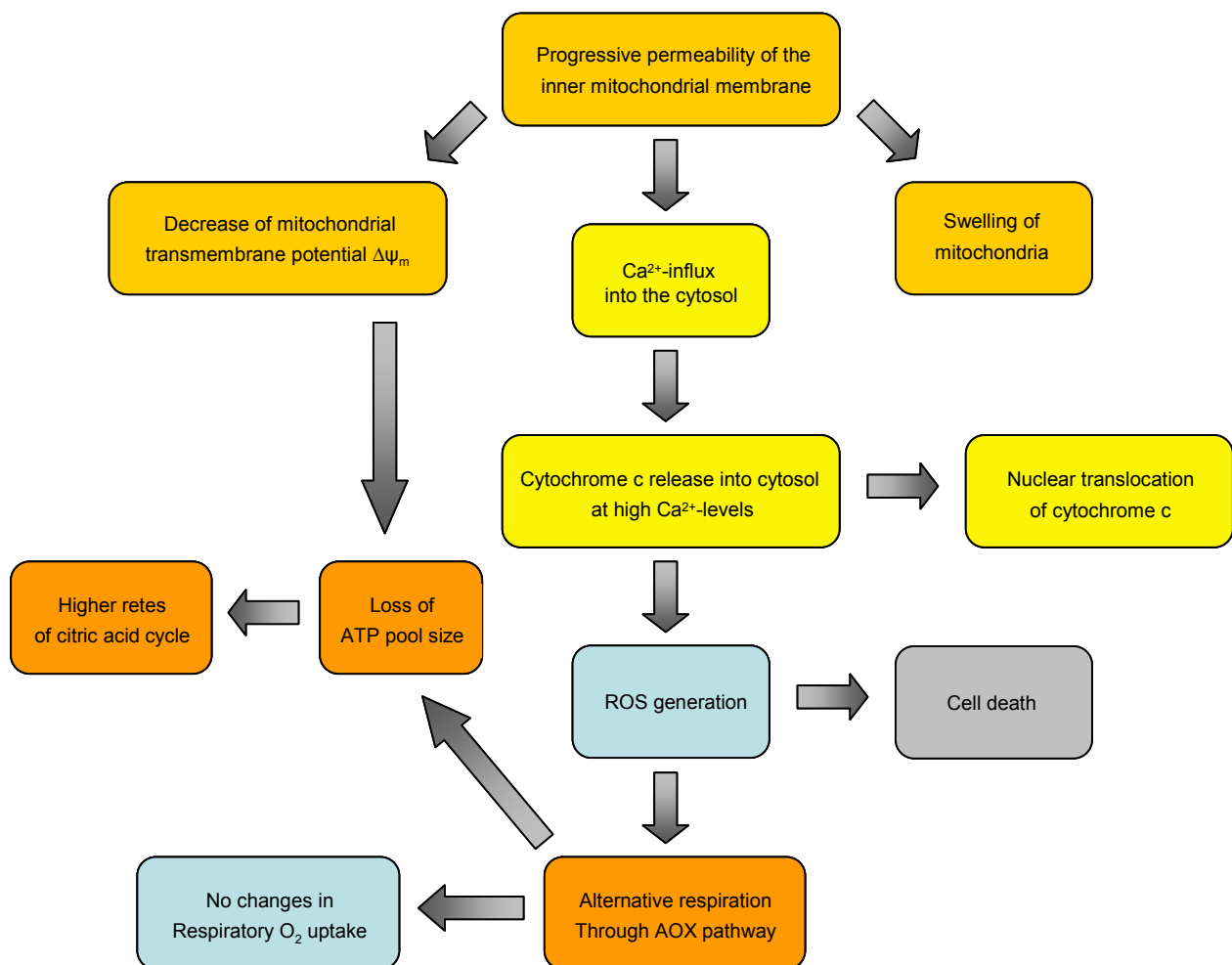


**Figure 39:** Overview of mitochondrial events in harpin induced PCD.

## IV. Methods

### 1. Harpin

#### 1.1. Preparation of harpin protein

A full length *Pseudomonas syringae* 61 hrpZ ORF, subcloned into pBluescript vector (a gift from Alan Collmer), was transformed into competent cells. The heat shock transformation into *E.coli* DH5alpha cells was done according to the standard protocols (Sambrook et al., 1989). About 350 ng of plasmid were added in 40 µl suspension of competent cells, which were thawed on ice. The tubes were stored on ice for 1 h, placed in a preheated 42°C water bath for exactly 150 sec, and cooled on ice again for 5 min. After addition of 900 µl SOC medium the tubes were transferred to a shaking incubator (Eppendorf, Hamburg) set at 37°C. Cultures were incubated for 1 h to allow the bacteria to recover and to express the antibiotic resistance marker encoded by the plasmid. A volume of 100 µl of transformed competent cells was transferred onto agar DYT medium containing ampicillin (100 µg/ml) as well as X-gal (100 µg/ml) for blue-white screening. Petri dishes were incubated for 20 h at 37°C; then white bacterial colonies were picked up. The recombinant *E.coli* were grown in LB medium containing ampicillin (100 µg/ml) at 37°C by shaking at 250 rpm overnight and then inoculated into fresh LB medium at 1/200 volume. The expression of harpin protein was induced by 1 mM IPTG. Following purification steps for the harpin protein are slightly modified from those published in (Andi et al., 2001). After 16 h of incubation at 37°C and 250 rpm the cells were harvested by centrifugation at 14 000xg at 4°C for 30 min. The pellet was re-suspended in 10 mM KH<sub>2</sub>PO<sub>4</sub>, pH 6.5, and sonicated on ice. After centrifugation at 14 000xg at 4°C for 30 min the supernatant was denatured at 95°C for 15 min, once again centrifuged at 23 000xg at 4°C for 45 min and filtrated through 0.45/0.2 µm filters. The protein containing solution was further concentrated with Centricon YM-10 cellulose filter tubes by centrifugation at 2000xg and 4°C for 45 min. After adding harpin storage buffer total protein concentration was estimated according (Bradford, 1976). Harpin protein was stored at -20°C.

#### 1.2. Purification by FPLC

Harpin was further purified via FPLC on an ÄKTA purifier (Amersham Biosciences, Uppsala, Sweden) equipped with a fraction collector Frac-900 and controlled by the Unicorn software. Size fractionation of the harpin containing sample was performed on a prepacked HiPrep 26/60 Sephacryl S-200 HR gel filtration column (Amersham Biosciences, Uppsala, Sweden). Prior to gel filtration, the system was primed at different flow rates and stroke volumes, first with water for at least 10 min, and then with buffer (50mM Tris-HCl, 50 mM NaCl, pH 8.0) for at least 10 min, in order to equilibrate the entire system and to remove residual air. After equilibration of the column with at least five column volumes (CV) of the buffer, sample was loaded onto the column using a Superloop at 1 ml/min. The column was eluted with 2 CV of the same buffer, a flow rate of 1.3 ml/min, and fractions of 7.5 ml were collected. Both sample loading and elution steps were on-line monitored spectrophotometrically at 280 nm. Fractions of interest were analysed by SDS-PAGE using a 12.5% SDS-gel (Bio-Rad,

München) according to instructions of the manufacturers and visualized by Coomassie staining. The TRIS-HCl buffer was exchanged on PD-10 desalting columns and replaced by PBS. Protein content was determined according (Bradford, 1976).

### 1.3. Fluorescence labeling

The FPLC purified harpin was fluorescence labeled using the Alexa Fluor® 488 protein labeling kit. To 500 µl PBS buffered protein (2 mg/ml) 50 µl of 1 M sodium bicarbonate were added. The reactive dye was warmed up to room temperature, and the protein solution transferred to this vial. In the meantime the column gadget was assembled and the resin packed into the column. After incubation for 1 h in the dark at room temperature, the labeled protein was applied onto the column. Within 30 min after addition of elution buffer the labeled harpin was separated from unincorporated dye. The labeling degree was checked by measuring the absorbance of the conjugate solution at 280 nm ( $abs_{280}$ ) and 494 nm ( $abs_{494}$ ) in a cuvette (1cm) using an Ultraspec spectrophotometer (Amersham Biosciences, Freiburg). Concentration of the protein in the sample was calculated as follows:

$$C_{\text{protein}} = [abs_{280} - (0.11 \times abs_{494})] / \epsilon$$

where 0.11 is a correction factor to account for absorption of the dye at 280 nm, and  $5690 \text{ cm}^{-1}\text{M}^{-1}$  is the molar extinction coefficient  $\epsilon$  of harpin.

### 1.4. Antibody extraction

Harpin antibody production was performed commercially by PINEDA Antibody Service (Berlin, Germany). For immunohistochemistry and immunoblotting, antiserum against harpin was raised in rabbits immunized with the FPLC purified harpin (see chap. IV, 1.2.). Two rabbits were preimmunized in intradermal manner and later by subcutaneously injection of harpin. For pre-immunization on the first day, Freund's complete adjuvant, and for following boosts Freund's incomplete adjuvant were used. Booster injections were performed 20, 30, 40, 61, and 75 days after the first immunization. The serum was tested by Western blot analyses 61 and 90 days after boosting.

## 2. Plant material

### 2.1. Maintenance of *Arabidopsis* cell culture and treatment with harpin

*Arabidopsis thaliana* cell cultures were maintained in the dark on an orbital shaker (120 rpm) at 27°C, and sub-cultured every 7 days by dilution in fresh growth medium. AS medium used for this cell culture was modified after (Murashige and Skoog, 1962), supplemented with 2% (w/v) sucrose as

carbon source. Six days after sub-culturing *Arabidopsis* suspension cells were treated with 50 µg/ml fresh prepared harpin, control cells with an equal volume of suitable storage buffer. At indicated time point after treatment, cells were harvested by sucking off the medium and stored at -80°C.

## **2.2. Growth conditions of *Arabidopsis* plants and treatment with harpin**

Seeds from *Arabidopsis thaliana* were sown on sieved potting compost, containing seventh part silica sand (Dorsilit, Hirschau). After vernalizing two days at 4°C plants were grown in climate chambers (Vötsch, Balingen) for 4-6 weeks. Plant growth chambers were provided with a 14 hours light (20°C) / 10 hours dark (18°C) cycle, relative humidity was adjusted to 69%. Harpin was applied by spraying 2 ml protein containing buffer (0.012 g/l final concentration) on dishes covered with 5 plants. The commercial available plant activator messenger<sup>®</sup> (Eden Biosciences, Bothell, USA) containing harpin protein from *E. amylovora*, was solved in ddH<sub>2</sub>O and sprayed at the same concentration onto the plants. Plant material was harvested, frozen in liquid nitrogen and stored at -80°C until further use.

## **2.3. Fractionation of *Arabidopsis* suspension cells**

### **2.3.1. Cytosolic extracts**

*Arabidopsis* suspension cells were collected by centrifugation at 1500xg at 4°C for 5 min, and the pellet was re-suspended in ice-cold cytosol extraction buffer. Cells were homogenized with mortar and pestle and then filtrated throughout two layers of Miracloth. Flowthrough was centrifuged at 15 000xg at 4°C for 15 min. The supernatant was concentrated with Centricon YM-3 cellulose filter tubes according suppliers instructions; total protein content was determined according (Bradford, 1976).

### **2.3.2. Nuclei preparation**

Isolation of nuclei from *Arabidopsis* suspension cells was carried out at 4°C in ice water cooled vessels. A total of 200 ml control or harpin treated cells was filtered through one layer of Miracloth, and the cells were disrupted in a potter (B.Braun, Melsungen) under addition of nuclei homogenization buffer. After two-stage filtering through 1000 µm and 71 µm nylon mesh the homogenate was centrifuged at 1500xg for 15 min using a swinging bucket rotor. The resulting pellet was gently decanted, re-suspended with a small brush in nuclei wash buffer, and again centrifuged for 5 min at 1500xg. Wash and centrifugation steps were repeated twice, for storage the nuclei fraction was re-suspended in nuclei wash buffer containing 40% glycerol, frozen in liquid nitrogen and kept at -80°C.

### **2.3.3. Mitochondrial isolation**

Mitochondria were isolated and purified by differential centrifugation on Percoll gradients essentially as described by (Millar et al., 2001). All procedures were carried out at 4°C in detergent-free vessels. A total of 800 ml control or harpin treated cell suspension (8x 100 ml) was filtered through one layer

of Miracloth, after adding 100 ml of mitochondria extraction buffer cells were disrupted in a blender (Waring). Extract was filtered by wringing through two layers of Miracloth, centrifuged at 1500xg for 10 min, and the supernatant anew at 18 000xg for 15 min. The pellet was diluted in 50 ml wash medium, washed by repeating the two centrifugation steps, and re-suspended in 1 ml mitochondria wash buffer. Washed organelles were pipetted onto a Percoll gradient, consisting of 40%, 23% and 18% steps, and centrifuged at 40 000xg for 30 min with the break off. The whitish/light-brown band at the 23 to 40% Percoll interface was collected, diluted by adding wash medium, and centrifuged at 18 000xg for 10 min twice. The re-suspended pellet was further purified using a 28% self forming Percoll gradient, and the above mentioned wash and centrifugation steps (Millar et al., 2001). The final brown pellet was re-suspended in a small volume of wash medium, and stored at -80°C.

#### 2.3.4. Mitochondrial purity measurements

To estimate the purity of the mitochondria containing fractions the specific activities of marker enzymes: mitochondrial cytochrome c oxidase (Neuburger, 1985) and peroxisomal catalase (Cohen et al., 1996) were determined. Enzyme activities were measured in the initial crude extract and in purified mitochondrial fraction. Reagents and Buffers for the catalase assay were stored at 0°C in an ice-water bath, except for the 0.6 N H<sub>2</sub>SO<sub>4</sub> which was held at room temperature. The reaction kinetics were conducted at 0°C with 6 mM H<sub>2</sub>O<sub>2</sub>, the final reaction volume was 1 ml. Cell extract and mitochondria sample respectively (50 µl) was added to tubes containing 800 µl phosphate buffer, pH 7.0. Sodium azide (50 µl, 0.5 mM final concentration) was used to distinguish catalase activity from other factors that might induce loss of H<sub>2</sub>O<sub>2</sub>; matched controls received an equal volume of water. The reaction was started by the addition of 100 µl of 60 mM H<sub>2</sub>O<sub>2</sub>, followed by gentle mixing. At fixed time intervals, duplicate 100 µl aliquots were removed and quenched by addition to a mixture of 4.0 ml of 0.6 N H<sub>2</sub>SO<sub>4</sub> plus 1 ml of 10 mM FeSO<sub>4</sub> at room temperature. After all samples were collected, the color was developed by addition of 400 µl of 2.5 M KSCN. Subsequently, the samples were covered with aluminium foil to protect them from light. An Ultraspec spectrophotometer (Amersham Biosciences, Freiburg) was used to measure the red color of ferrithiocyanate. Colorimetry was conducted at room temperature in a 1ml cuvette at a wavelength of 460 nm, samples were analyzed kinetically at two time points and results are expressed, as follows:

$$\text{Enzyme activity} = [\ln (\text{abs}_1/\text{abs}_2)/t] / C_{\text{protein}}$$

where ln is the natural logarithm, abs<sub>1</sub> and abs<sub>2</sub> are the observed mean absorbances at the selected time points, t is the time differential between the two time points in min, and C<sub>protein</sub> is the protein concentration of individual sample in mg/ml.

The colorimetric assay for cytochrome c oxidase is based on observation of the decrease in absorbance at 550 nm of ferrocytochrome c caused by its oxidation to ferricytochrome c by



cytochrome c oxidase. The ferrocytochrome c substrate solution was made by dissolving 2.7 mg cytochrome c in 1 ml water, followed by addition of DTT to a final concentration of 0.5 mM in order to reduce the protein. After incubation for 5-15 min at room temperature the  $abs_{550}/abs_{565}$  ratio of an aliquot diluted 20-fold with assay buffer was determined using an Ultraspec spectrophotometer (Amersham Biosciences, Freiburg). To ensure that the substrate has been sufficiently reduced the  $abs_{550}/abs_{565}$  ratio should be between 10 and 20. The reaction kinetics were conducted at 25°C, the final reaction volume was 1.1 ml. Cell extract and mitochondria sample respectively (50  $\mu$ l) was added to cuvettes containing 950  $\mu$ l assay buffer and 50  $\mu$ l enzyme dilution buffer. After mixing by inversion the reaction was started by the addition of 50  $\mu$ l of ferrocytochrome c substrate, the initial reaction rate was measured at 550 nm during the first 45 sec of the reaction. The enzyme activity of samples was calculated as follows:

$$\text{Enzyme activity} = [V_{\text{react}}(abs_1 - abs_2)/t] / V_{\text{sample}} \times \Delta\epsilon \times d$$

where  $V_{\text{react}}$  is the reaction volume in ml,  $V_{\text{sample}}$  is the volume of sample in ml,  $abs_1$  and  $abs_2$  are the observed absorbances at the selected time points,  $t$  is the time differential between the two time points in min,  $\Delta\epsilon$  is the difference in extinction coefficients between reduced and oxidized cytochrome c (21.84  $\text{cm}^2 \mu\text{mol}^{-1}$  at 550 nm), and  $d$  is the deposit thickness of utilized cuvettes (1 cm).

Total activity in mitochondria was expressed as percentage of that in the initial crude cell extract. The purity was accepted, if a 10-fold enrichment of mitochondria in comparison to peroxisome (Lee Sweetlove, personal communication) was observed. Total protein concentrations of cell extracts and mitochondrial fractions were estimated according (Bradford, 1976). For proteome analysis mitochondrial fractions were lyophilized and stored at -80°C.

## 2.4. Preparation of protoplasts

Protoplasts were prepared from leaves of 5 week old *Arabidopsis* plants. Leaves were rinsed three times with distilled water, blotted dry on filter paper, and chopped with a razor blade (approximate final size 10  $\text{mm}^2$ ). Tissue of about 40 leaves was transferred into 10 ml protoplasting solution and vacuum infiltrated three times for 3 min. Leaf tissue was further incubated with this cell wall digesting solution at room temperature with gentle agitation (40 rpm). When the majority of protoplasts were released, digested material was filtrated through a 71  $\mu\text{m}$  screen to separate the protoplasts from leaf tissue. Protoplasts were pelleted by centrifugation at 100 $\times$ g for 2 min using a swinging bucket rotor and re-suspended in 4°C protoplast wash solution, last both steps were repeated once.

To prepare protoplasts from suspension cells, six day old cells were pelleted by centrifugation and the supernatant was removed completely by aspiration. Then cells were diluted in fresh AS medium and centrifuged again. The pellet was re-suspended in protoplasting solution; all further steps were carried out as described for leaf material.

### 3. Cell death assay

The number of dead cells was counted by exposing the cells to Evans blue solution for 10 min at indicated time points after harpin treatment, washing three times in 0.1 mM CaCl<sub>2</sub>, pH 5.6, and following visualizing under light microscopy. Among 500 cells, the dead cells were counted in a Fuchs-Rosenthal counting cell chamber (Marienfeld, Lauda-Königshofen), and the ratio was calculated. The procedure was repeated in 4 independent experiments.

### 4. Nucleic acid based techniques

#### 4.1. DNA isolation from *Alternaria alternata* infected plants

Frozen plant material was grounded with mortar and pestle under liquid nitrogen. When 500 µl of -20°C cold chloroform and 500 µl CTAB buffer containing 1% (v/v) β-mercaptoethanol were added to 100 mg powdered tissue, the tubes were placed in a pre-cooled 4°C shaking incubator for 10 min at 1800xg. After centrifugation at 13 000xg and 4°C for 10 min, 500 µl of -20°C cold chloroform and 100 µl Nucleon PhytoPure resin were added to the supernatant. The mixture was shaken 10 min at 1800xg and 4°C, followed by centrifugation at 12 000xg and 4°C for 10 min. Washing of the resulting pellet occurred by successive adding of 70%, 80% and pure ethanol with subsequent centrifugation. The supernatant was aspirated, and the DNA air-dried and then dissolved in 100 µl TE buffer.

#### 4.2. RNA isolation

RNA was extracted using TRIzol reagent according to the supplier's instructions (Invitrogen, Karlsruhe). Frozen cell or leaf material was grounded with mortar and pestle under liquid nitrogen. After addition of 1 ml TRIzol reagent to 100 mg frozen tissue, the tubes were incubated for 10 min at room temperature under occasional agitation. Then 200 µl of chloroform were added, the mixture was incubated for further 3 min at room temperature, and centrifuged for 15 min at 12 000xg and 4°C. The upper aqueous phase was incubated with 500 µl isopropanol for 10 min, and the RNA was pelleted by centrifugation at 12 000xg. In a last purification step 1 ml of 70% ethanol was added to the pellet; after centrifugation and aspiration of the supernatant, the RNA was air-dried and then dissolved in 50 µl DEPC water. RNA preparations were checked on agarose gels, concentration was determined measuring the UV absorbance at 230 nm, 260 nm, and 280 nm using an Ultraspec spectrophotometer (Amersham Biosciences, Freiburg). Pure preparations of RNA have OD ratio values ( $A_{260}/A_{280}$ ) of between 1.8 and 2.0 and ( $A_{260}/A_{230}$ ) of  $\geq 2.0$ .

#### 4.3. Semi-quantitative RT-PCR

For semi-quantitative RT-PCR total RNA was isolated substantially as described by (Kiefer et al., 2000). Frozen plant material was grounded with mortar and pestle under liquid nitrogen. After addition of 1 ml RNA extraction buffer to 100 mg powdered tissue, the tubes were placed in a pre-heated 65°C water bath for 10 min. When 500 µl of -20°C cold chloroform and 100 µl Nucleon

PhytoPure resin were added, the mixture was shaken 10 min at 1800xg and room temperature, followed by centrifugation at 13 000xg and 4°C for 10 min. The supernatant was mixed with 500 µl of -20°C cold chloroform and again centrifuged for 5 min. Then, 2 volumes of 4°C cold isopropanol were added to the supernatant, tubes were incubated on ice for 5 min, and the nucleic acids were pelleted by centrifugation at 13 000xg and 4°C for 10 min. To digest the present DNA, the pellet was dissolved in 50 µl DNase buffer, incubated at 37°C for 20 min and washed with pure ethanol. In a last purification step 1 ml of 70% ethanol was added to the pellet; after centrifugation and aspiration of the supernatant, the RNA was air-dried and then dissolved in 50 µl DEPC water.

To prepare cDNA, 1 µl Poly-d(T)<sub>12-18</sub>-primer and 5 µg of total RNA were adjusted to a volume of 12 µl, incubated 10 min at 70°C and exactly 1 min on ice. After addition of 8.5 µl cDNA Mastermix, tubes were stepwise incubated for 60 min at 42°C, 15 min at 70°C and finally on ice. The remaining total RNA was degraded by incubation with 1 µl RNase H and 5 µl RNase A for 20 min at 37°C, the reaction was stopped by transfer on ice. Single stranded cDNA was quantified in a black 96 well microplate using the RiboGreen™ RNA quantitation kit, and a Fluostar microplate reader (Tecan, Crailsheim) with an excitation wavelength of 480 nm and an emission wavelength of 520 nm. For PCR the amplification parameters were optimized as follows:

PCR Mastermix	<i>Mlo2</i>	<i>Mlo6</i>	<i>Mlo12</i>
PCR buffer	5.0µl	5.0µl	5.0µl
dNTP Mix	1.0µl	1.0µl	1.0µl
MgCl <sub>2</sub>	5.0µl	5.0µl	5.0µl
Taq-polymerase (Goldstar)	0.2µl	0.2µl	0.2µl
Primer <i>fwd</i> (10µM)	1.0µl	1.0µl	1.0µl
Primer <i>rev</i> (10µM)	1.0µl	1.0µl	1.0µl
template cDNA	4 ng	8 ng	4 ng
<b>Adjust to 50 µl with ddH<sub>2</sub>O</b>			

**PCR program:**

	72°C	10 min
cycles	94°C	45 sec
	58°C	45 sec
	72°C	1 min
	72°C	5 min

With the *Mlo2* and *Mlo12* primer pairs the PCR was carried out for 30 cycles, with the *Mlo6* primer pair for 35 cycles. For *Arabidopsis thaliana* currently 15 *mlo* gene family members are known (Devoto et al., 2003). Due to the high sequence similarity in coding regions (*Mlo2* vs. *Mlo6* show 84.6%, *Mlo2* vs. *Mlo12* 80.7% and *Mlo6* vs. *Mlo12* 77.6% similarity), nucleotide sequences were aligned using the Vector NTI Suite 7.0 program and the region of greatest sequence diversity was chosen for the selection of the primers.

Additionally, the selected sequences were blasted with the whole *Arabidopsis* genome using the NCBI BLASTn program (<http://www.ncbi.nlm.nih.gov/BLAST/>) by comparing the nucleotide query sequence against a nucleotide sequence database. The following gene-specific forward and reverse primers were synthesized:

*Mlo2*-fwd: 5'-CGA TTG TCC TCG AAC ATT CTA TTC A-3'  
*Mlo2*-rev: 5'-CAA GAA GAA GTC TTC GAC CGG G-3'  
*Mlo6*-fwd: 5'-TTC GTA ATG CTC CTC ACA AAC GA-3'  
*Mlo6*-rev: 5'-GCT GTG TTC GTA TTT GTC CAG GTC-3'  
*Mlo12*-fwd: 5'-CGC TTC TAT TGG TTG TAT TGC AAA C-3'  
*Mlo12*-rev: 5'-CGG CGA GGA CTG TAA AAG TCG-3'

PCR products were quantified in a black 96 well microplate (Greiner Bio-One, Essen) using the PicoGreen<sup>TM</sup> dsDNA quantitation kit and a Fluostar microplate reader (Tecan, Crailsheim) with an excitation wavelength of 480 nm and an emission wavelength of 520 nm. PCR products were resolved in 2% agarose gels and visualized by ethidium bromide staining.

## 5. Microarrays

### 5.1. Microarray experiments

**Agilent Arabidopsis 1.0 microarrays:** In the early stages commercial *Arabidopsis* 1.0 Oligo Microarrays (catalog no. G4135A, Agilent Technologies) were used to compare transcription profiles of *Arabidopsis* suspension cells at different stages after elicitor treatment (Cluis et al., 2004; Shikata et al., 2004). The content on these cDNA microarrays is derived from the ATH1 v. 3 database of The Institute for Genomic Research (TIGR). Sequences and gene annotation are published on the Agilent website at ([www.agilent.com/chem/dnasupport](http://www.agilent.com/chem/dnasupport)). The 60-mer oligonucleotides are printed in a 119 row by 156 column grid layout, and represent 14,200 genes.

Three 200 ml flasks with *Arabidopsis* suspension cells (200ml) were treated with 50 µg/ml harpin protein (final concentration), and three flasks with control cells were treated with an equal volume of suitable storage buffer. Three independent biological replicates were sampled for each time point after treatment. Elicitor treated and control cells were harvested, sucked off, frozen in liquid nitrogen, and stored at -80°C until RNA isolation. Total RNA was extracted as described in chapter VI, 4.2. using TRIzol method.

**Agilent Arabidopsis 2.0 microarrays:** Later *In situ* synthesized *Arabidopsis* 2.0 Oligo Microarrays (catalog no. G4130A, Agilent Technologies) were used for transcript analysis of *Arabidopsis* suspension cells after elicitor treatment (Umezawa et al., 2004). The content on these microarrays is also derived from the ATH1 v. 3 database of The Institute for Genomic Research (TIGR) and represents 21,500 genes. The 60-mer oligonucleotides are printed in a 105 row by 215 column grid layout and constitute over 80% genome coverage of *Arabidopsis thaliana*.

## 5.2. Target synthesis and array hybridization

### 5.2.1. cDNA synthesis, aminoallyl labeling and purification

Probe-labeling protocols used for this study are essentially as described for indirect aminoallyl labeling method (see [http://atarrays.tigr.org/PDF\\_Folder/Aminoallyl.pdf](http://atarrays.tigr.org/PDF_Folder/Aminoallyl.pdf)). Equal amounts (10µg) of total RNA from three independent biological samples were pooled, and each 30µg RNA sample (one untreated and one treated) was reverse-transcribed after incubation with 4 µl Poly-d(T)<sub>12-18</sub>-primer for 10 min at 70°C and exactly 1 min on ice. After addition of 15 µl cDNA Mastermix, tubes were incubated overnight at 42°C. To hydrolyze the remaining RNA, 10 µl of 1 M NaOH and 10 µl of 500 mM EDTA were added, and the tubes were incubated at 65°C for 15 min. Then 10 µl of 1 M HCl were added to neutralize the pH. For removal of unincorporated aa-dUTP and free amines samples were purified using a commercial QIAquick PCR purification kit. Because buffers of the kit contain free amines which compete with the following dye coupling reaction, the phosphate wash buffer and the phosphate elution buffer were substituted for the supplied buffers. After elution samples were dried in a speedvac.

### 5.2.2. Coupling aminoallyl labeled cDNA to Cyanine dye ester

During all following steps up to the scan of the microarrays the dye containing samples were covered as much as possible to protect them from photobleaching. Each aminoallyl-labeled cDNA sample was re-suspended in 4.5 µl of Na<sub>2</sub>CO<sub>3</sub>, (100 mM, pH 9.0). The supplied Cyanine 3 and Cyanine 5 fluorescent dye pellets were resolved in 73 µl of DMSO, and 4.5 µl of the dye were added to the relevant cDNA sample. The reaction was incubated for at least 1 h in the dark. Every 10 min the tubes were vortexed briefly, followed by short centrifugation to spin down the liquid. Dye molecules were separated from labeled products using the Qiaquick PCR purification kit including supplied buffers. Before starting the purification procedure, 35 µl of 100 mM NaOAc (pH 5.2) were added to each reaction in order to adjust the pH of the samples to the pH optimum of column membranes.

Purified Cy3- labeled cDNA from control cells was paired with the same amount Cy5- labeled cDNA from treated cells, all hybridizations were done in duplicate with fluorophor reversal (dye swap). Probes were stored at -80°C until needed for hybridization.

### 5.2.3. Hybridization and post-washing

**Agilent Arabidopsis 1.0 microarrays:** The hybridization procedure was carried out according manufacturers (Agilent Technologies, Palo Alto, USA) protocol using recommended reagents. The Cyanine 3-/ Cyanine 5- labeled cDNA pair was dried in speedvac and dissolved into 93.75 µl of nuclease-free water. To the re-suspended sample 2.5 µl Deposition control targets, 3.75 µl Cot-1 DNA and 100 µl 2xDeposition Hybridization buffer were added. The total sample volume was adjusted to 200 µl with nuclease-free water. For denaturation the solution was mixed well and incubated at 98°C for 2 min, followed by centrifugation at 14 000 rpm for 5 min. The hybridization

chambers (catalog no. G2533A, Agilent Technologies) were assembled according suppliers instructions. Slides were placed in hybridization chambers and the hybridization solution was injected through the gasket into the chamber using a 1 ml syringe. The chambers were incubated in a hybridization oven (H.Saur, Reutlingen) for exactly 18 h at 60°C under rotation. The hybridization chamber was disassembled while it was immersed in 0.5xSSC and 0.01% (v/v) SDS containing wash solution and the slides transferred into a slide rack. This rack was placed in a wash solution containing dish on a magnetic stirrer for 5 min, and then in a 0.06xSSC containing dish for further 2 min. After spinning for 2 min at 400xg at room temperature slides were scanned on the GenePix 4000 scanner.

**Agilent Arabidopsis 2.0 microarrays:** The hybridization procedure was carried out according manufacturers (Agilent Technologies, Palo Alto, USA) protocol using recommended reagents such as the In situ Hybridization Kit Plus (catalog no. 5184-3568, Agilent Technologies). The Cyanine 3-/Cyanine 5- labeled cDNA pair was dried in speedvac and dissolved into 200 µl of nuclease-free water. For denaturation the sample was incubated at 98°C for 3 min and cooled down to room temperature. To the re-suspended sample 50 µl of 10x control targets and 250 µl of 2xHybridization buffer were added. The hybridization chambers (catalog no. G2531A, Agilent Technologies) were assembled according suppliers instructions. Slides were placed in hybridization chambers and the hybridization solution was injected through the gasket into the chamber using a 1 ml syringe. The chambers were incubated in a hybridization oven (H.Saur, Reutlingen) for exactly 18 h at 60°C under rotation. The hybridization chamber was disassembled while it was immersed in 6xSSPE and 0.005% (v/v) N-lauroylsarcosine containing wash solution and the slides transferred into a slide rack. This rack was placed in a wash solution containing dish on a magnetic stirrer for 1 min, and then in a 0.06xSSPE and 0.005% (v/v) N-lauroylsarcosine containing dish for 1 further min. Within 10 sec the slide rack was transferred into a P-Stab and Drying solution (catalog no. 5185-5979, Agilent Technologies) containing dish, placed in a fume hood on a magnetic stirrer for exactly 30 sec. Then the rack was removed very slowly at a constant speed and direction. The dried slides were scanned on the GenePix 4000 scanner.

### 5.3. Data collection, analysis and gene classification

Fluorescence intensities on scanned images were quantified, corrected for background, and normalized using the GenePix Pro 4.1 software. For subsequent analysis, the output files were transferred to the Acuity 3.1 software (AXON Instruments). The selection procedure applied to our expression data was: (i) only signals more than 2-fold above local background were considered, (ii) only a gene with a minimum change in its transcript abundance of 2.0-fold was regarded as induced or repressed and (iii) only signals present in at least two independent hybridisations were analyzed. For functional classification of regulated genes the MIPS *Arabidopsis thaliana* database was used (<http://mips.gsf.de/proj/thal/db/>). Genes of yet unknown function were categorized using TIGR

database (<http://www.tigr.org/tdb/e2k1/ath1/LocusNameSearch.shtml>). In a last step the remaining genes were classified with the aid of the TAIR database (<http://www.arabidopsis.org/servlets/Search>). Transcription factors were classified by families according to sequence similarity using the Arabidopsis Gene Regulatory Information Server (AGRIS) database (<http://arabidopsis.med.ohio-state.edu>) of *Arabidopsis* transcription factors of the Ohio State University (Davuluri et al., 2003). Protein kinases like MAP kinases and receptor-like kinases were identified and categorized by the PlantsP database of the University of California, San Diego (<http://plantsp.sdsc.edu>), on the basis of identity of the extracellular domains. Genes encoding mitochondrial proteins were categorized by function according to (Heazlewood et al., 2004).

## **6. Northern blotting**

### **6.1. Sample preparation**

*Arabidopsis* cells were harvested at indicated time points and frozen in liquid nitrogen. RNA was extracted as described in chapter V, 4.2. Each RNA sample (10 µg) was adjusted to 10 µl with water followed by addition of 8 µl RNA denaturation mix and incubation at 65°C for 10 min. After cooling on ice for 2 min, samples were loaded on 1.2% agarose gel containing 3% formaldehyde, prepared with 1xMOPS buffer. Equivalent RNA loadings were confirmed by ethidium bromide staining of the gel.

### **6.2. Gel run and RNA transfer**

RNA samples were size fractionated by gel electrophoresis in 1xMOPS buffer at 90 Volt using an OWI B2 separation system (OWI, Portsmouth, USA). The gel was washed twice in 20xSSC buffer and transferred onto a double layer of Whatman paper at the blotting apparatus. The ends of the paper were extended into 20xSSC buffer containing chambers to ensure the RNA transporting sucking process. A piece nylon membrane (Roche Diagnostics, Mannheim) was placed onto the gel surface, followed by Whatman paper, and ~20 cm of absorbent paper. After blotting, the RNA was fixed onto membrane by UV irradiation using an UV Stratalinker 2400 (Stratagene, Heidelberg).

### **6.3. Preparation of DIG labeled DNA probes**

Using the PCR Dig Probe Synthesis Kit (Roche Diagnostics, Mannheim) and the primer pair *AOX1a-fw*: 5'-CGT GTG AAG CGT ATA AAG ACG ACA A-3' and *AOX1a-rev*: 5'-TCC TCC TTC ATC GGA GTT TTC TC-3' *Arabidopsis* sequence was digoxigenin labeled. The gene-specific AOX primers were chosen as suggested by (Saisho et al., 1997). PCR amplification parameters were established as follows:

<b>PCR Mastermix</b>	<b>Positive control</b>	<b>DIG labeled probe</b>
PCR buffer	5.0µl	5.0µl
dNTP Mix	1.5µl	1.5µl
DIG Mix	-	1.5µl
Taq-polymerase	1.0µl	1.0µl
Primer AOX1a-fwd (10µM)	1.5µl	1.5µl
Primer AOX1a-rev (10µM)	1.5µl	1.5µl
template DNA	1.5µl	1.5µl
<b>ddH<sub>2</sub>O</b>	<b>38.0µl</b>	<b>36.5µl</b>

**PCR program:**

95°C 5 min

35 cycles { 95°C 45 sec  
52°C 45 sec  
72°C 2 min

72°C 5 min

Aliquots of 5 µl of each reaction were separated on 1.0% agarose gel, prepared with TAE buffer. RNA loadings were visualized by ethidium bromide staining of the gel.

**6.4. Hybridization, washing and detection**

After crosslinking, the membrane was prehybridized in a hybridization solution (Roche Diagnostics, Mannheim) containing bag by shaking in a 50°C water bath at least for 1 h. The DIG labeled probe was denatured by incubation at 95°C for 10 min, transferred on ice, and pre-diluted ~1:300 in hybridization solution (usually 3 µl in 1 ml). The DIG probe containing solution was further filled up with hybridization solution up to 10 ml and placed together with the membrane in a hybridization bag. For hybridization the incubation at 50°C was continued overnight. Then the membrane was washed twice in 2xSSC, 0.1% SDS buffer for 5 min and twice in 0.1xSSC, 0.1% SDS buffer for 15 min at 50°C. Following washing, blocking and detection steps were carried out at room temperature under agitation using appropriate solutions (Roche Diagnostics, Mannheim). After washing for 2 min, membrane was placed in blocking solution and incubated for 30 min. The blocking solution was refreshed, and the membrane was incubated with 0.01% (v/v) Anti-Digoxigenin antibody for further 30 min. After washing twice in wash buffer for 15 min, the membrane was equilibrated for 2 min in detection buffer. The ready to use chemiluminescent substrate (CSPD) was spread onto the membrane surface, followed by incubation at 37°C for 10 min. Finally, the membrane was exposed to a chemiluminescent detection film (Roche Diagnostics, Mannheim) for 15-60 min at room temperature; the film was developed using a Curix60 apparatus (AGFA, Köln).



## 7. Proteome analysis \*

### 7.1. Protein sample preparation and 2-D gel electrophoresis

Lyophilized mitochondrial extracts were diluted under agitation in 400 µl lysis buffer for 30 min, then centrifuged for 5 min at 20 000xg. Total protein concentrations of the supernatants were estimated according (Bradford, 1976). Aliquots containing 250 µg protein were used for isoelectric focusing (IEF) in a horizontal electrophoresis Multiphor II unit (Amersham Biosciences, Freiburg) under utilization of 180-mm, pH 3 to 10 nonlinear immobilized pH gradient strips. The IEF was performed overnight, reaching a total of 30 KVh. The pH gradient strips were transferred onto SDS-gels, electrophoresis was performed until reaching a total of 2 KVh in an IsoDalt Gel Electrophoresis System ID 440-230V (Amersham Biosciences, Freiburg). Protein markers were used to estimate molecular weights and the pI of the separated proteins on second dimension. For each treatment (0 h, 8 h, and 24 h) three independent runs of samples on 2D-gels were carried out. After electrophoresis, 2D-gels were fixated for 30 min in an EtOH/HAc buffer, following by incubation with a fluorescent Sypro Ruby (Molecular Probes, Eugene, USA) dye for 3 h. The gels were fixated in EtOH/HAc buffer overnight, and then scanned using a 16-bit FLA 3000 scanner (Raytest, Urdorf, CH). Changes in spot intensity were analyzed by ProteomeWeaver 3.0 software (Definiens Imaging, München) on 16-bit TIFF images. Only spots, whose intensity is regulated at least 2-fold between two treatments, were identified as significant.

### 7.2. MALDI-TOF Mass Spectrometry for peptide fingerprint analysis

Protein spots were visualized by colloidal Coomassie (G250) staining, excised from 2D-gels and completely destained by washing in 25 mM  $\text{NH}_4\text{HCO}_3$ . Gel slices were digested at 37°C in 5 mM TRIS-HCl (pH 8.0) containing 17.9 µg/ml trypsin overnight. Samples were desalted using C18-ZipTips (Millipore, Schwalbach), and eluted with an 80% acetonitrile and 1% trifluoroacetic acid containing buffer. Peptides were diluted in a 1:1 ratio in matrix solution (2.5-dihydrobenzoic acid:2-hydroxy-5-methoxybenzoic acid, 9:1), and applied directly on the MALDI target. Trypsinated protein samples were measured in a peptide mass range of 0.6-4.2 kDa with a MALDI TOF Voyager-DE STR (Applied Biosystems, Foster City, USA). Resulting peptide masses were compared with those of theoretical trypsin digestions and searched against predicted masses derived from the NCBI genomic database using ProFound software (Genomic Solutions).

\*) Proteome analysis was carried out in cooperation with the TopLab Company (Martinsried, Germany).

## 8. Western blotting

### 8.1. Cytochrome c in cytosolic fractions

Ten  $\mu\text{l}$  protein gel loading buffer were added to each sample of cytosolic extract, containing 30  $\mu\text{g}$  protein. After incubation at 95°C for 5 min, protein samples were loaded on a 12.5% SDS-polyacrylamide gel (Bio-Rad, München), additionally 0.01  $\mu\text{g}$  cytochrome c (Roche Diagnostics, Mannheim) were loaded as positive control on the gel. The proteins were size fractionated by gel electrophoresis in protein gel running buffer at 25 mA using a Mighty Small separation system (Hoefer, San Francisco, USA). Subsequently, gel, blotting papers and PVDF membrane were incubated in transfer buffer for 15 min and then stacked onto the SemiPhor blotting apparatus (Hoefer, San Francisco, USA). Via semi-dry transfer proteins were blotted at 0.9 mA and 15 Volt upon the membrane. After successful blotting, visualized by Ponceau red solution, membrane was washed in TBS-T buffer for 10 min and incubated in blocking buffer for 30 min. The membrane was probed with mouse anti-cytochrome c antibody (BD Pharmingen, Heidelberg) at a dilution of 1:2000 in blocking buffer for 1 h, followed by washing three times in TBS-T buffer for 10 min. The secondary anti-mouse antibody conjugated with alkaline phosphatase (Stressgen, San Diego, USA) was applied at a dilution of 1:10000 for 1 h. For coloring reaction 50  $\mu\text{l}$  NBT and 37.5  $\mu\text{l}$  BCIP were diluted in 10 ml alkaline phosphatase buffer, then added to the membrane.

### 8.2. Cytochrome c in nuclear fractions

To 100  $\mu\text{l}$  nuclear fraction, purified as described in chapter IV, 2.3.2., 300  $\mu\text{l}$  of urea buffer were added. The mixture was sonicated for 3 min, dissolved in 1.6 ml of acetone (-20°C), and incubated at -20°C for 1 h. After centrifugation at 1000 $\times$ g and 4°C for 20 min, the pellet was left until the acetone has completely volatilized. Proteins were resolved in PBS, pH 7.2, total protein concentration was estimated according (Bradford, 1976). Ten  $\mu\text{l}$  protein gel loading buffer were added to each sample of nuclear extract, containing 30  $\mu\text{g}$  protein. The following protein separation on SDS gel and blotting procedure were carried out as described for cytosolic fractions (chapter IV, 8.1.). As secondary antibody a horseradish peroxidase linked ECL anti-mouse antibody (Amersham Biosciences, Freiburg) was applied at a dilution of 1:20000 for 1 h. After rinsing two times and further washing in TBS-T altogether for 30 min with repeated changes of the buffer, the membrane was processed for chemiluminescence detection. Protein bands were visualized with a chemiluminescence Western blotting kit Super Signal WestDura whereas membrane was exposed onto autoradiography film, which was developed using a Curix60 apparatus (AGFA, Köln). In order to exclude a contamination of the nuclear fractions with cytochrome c containing mitochondria, the membrane was stripped and re-probed with a mitochondria specific primary antibody. After incubation in stripping buffer at 60°C with agitation for 30 min, and washing 3 times in TBS-T buffer at room temperature, membrane was blocked for 1 h, and re-probed with a mouse anti- $\beta$ -ATPase monoclonal antibody (a gift from Thomas E. Elthon) at a dilution of 1:1000. Further steps were carried out as mentioned above.

## 9. Measurement of intracellular ATP

Intracellular ATP concentrations were quantified using a commercial ATP determination kit (Molecular Probes, Eugene, USA). ATP is determined with recombinant firefly luciferase and its substrate D-luciferin, the assay is based on luciferase's requirement for ATP in producing light (emission maximum ~560 nm at pH 7.8). Harvested *Arabidopsis* suspension cells (0.3 g) were washed once in ice-cold PBS pH 7.4 and collected by centrifugation at 1500xg at 4°C for 5 min. The pellet was re-suspended in 200 µl boiling buffer, and incubated for 10 min at 100°C. After centrifugation at 13 000xg for 10 min at 4°C the supernatant was stored at -80°C until ATP measurement. Ten µl of sample were added in a black 96 well microplate (Greiner Bio-one, Essen) to 90 µl of luciferase containing solution and gently mixed. The luminescence was recorded at 560 nm using a Genios plate reader (Tecan, Crailsheim). Standard curves were prepared in all experiments with different ATP concentrations, and calculations were made against the curve.

## 10. Determination of mitochondrial transmembrane potential $\Delta\psi_m$

Changes in mitochondrial transmembrane potential  $\Delta\psi_m$  in response to harpin were monitored using the mitochondrial potential sensor JC-1 as probe according to the method of (Yao et al., 2002). This dye exhibits a potential-dependent accumulation in mitochondria, indicated by a fluorescence emission shift from green (~525 nm) to red (~590 nm). *Arabidopsis* cells were stained with the JC-1 dye (5 µg/ml, final concentration) and incubated for 20 min in the dark. After filtration cells were re-suspended in 300 µl AS medium and placed in a black 96 well microplate. Changes in fluorescence intensities in harpin-treated (50 µg/ml) and untreated cells were measured immediately after treatment. Using a Fluostar microplate reader (Tecan, Crailsheim) with an excitation wavelength of 485 nm; red (590 nm) and green (538 nm) fluorescence intensities were detected every 10 min over 4 h. To ensure aeration of the medium, the microplate reader rocked the plate every 5 min for 10 sec.

## 11. Respiratory oxygen uptake

Respiratory oxygen consumption was determined in a Clark-type oxygen electrode (Bachofer, Reutlingen) in 1ml mitochondria containing reaction buffer in the presence of ADP (0.5 mM, pH 7.4) and 20 mM succinate as substrate. In one case fresh prepared mitochondria were incubated with 1 or 10 µg harpin up to three hours prior to the measurement. In a second experiment cell cultures were pre-treated with harpin (50 µg/ml final concentration), and harvested for mitochondrial isolation. Total protein content of mitochondrial fractions was estimated according (Bradford, 1976). All experiments were repeated three times in independently treatments and organelle preparations.

## 12. Activity of tricarboxylic acid cycle enzymes

Enzyme activities of citrate synthase (Bogin and Wallace, 1969), aconitase (Jenner et al., 2001), isocitrate dehydrogenase (Bergmeyer, 1989b), fumarase (Hill and Bradshaw, 1969), and malate

dehydrogenase (Kitto, 1969) were estimated in mitochondrial fractions using a thermostated spectrophotometer or a microplate reader at 25°C (Tecan, Crailsheim). The frozen mitochondria fraction was thawed on ice. The enzyme activity of samples was calculated as follows:

$$\text{Enzyme activity} = [V_{\text{react}}(\Delta\text{abs})/t] / V_{\text{sample}} \times \epsilon \times d$$

where  $V_{\text{react}}$  is the reaction volume in ml,  $V_{\text{sample}}$  is the volume of sample in ml,  $\Delta\text{abs}$  is the observed change of absorbance over a selected period,  $t$  is the time differential in min,  $\epsilon$  is the molecular extinction coefficient in  $\text{cm}^2 \mu\text{mol}^{-1}$  at selected wavelength, and  $d$  is the thickness of utilized cuvettes (1 cm). All experiments were carried out three times with independent samples; the enzyme activity was related to the protein concentration of individual sample.

### 12.1. Citrate synthase

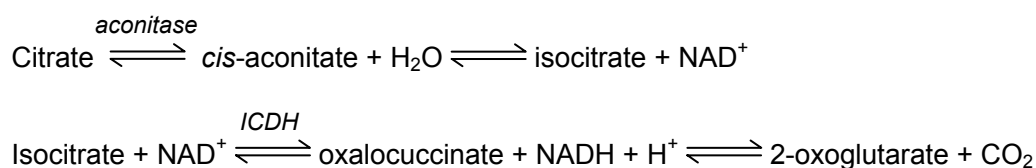
Citrate synthase activity measurement is based on the evidence of a mercaptide which absorbs light at 412 nm, and is formed by the reaction of Ellman's reagent (DTNB) with CoASH, released at the condensation of oxaloacetate and acetyl-S-CoA:



The reaction was started by the addition of 50  $\mu\text{l}$  sample to a silica cell containing 900  $\mu\text{l}$  of reaction buffer. The increase in optical density between 15 and 30 sec after starting the reaction was used to calculate the enzyme activity. The molar extinction coefficient was  $\epsilon = 13.6 \text{ cm}^2 \mu\text{mol}^{-1}$ . Readings were made against a blank containing all components with exception of acetyl-S-CoA.

### 12.2. Aconitase

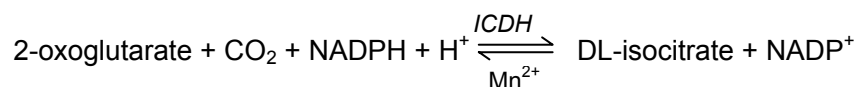
The assay utilized the coupled reaction of citrate to isocitrate and isocitrate to 2-oxoglutarate as the basis for quantitating aconitase activity by monitoring the formation of NADH at 340 nm:



The reaction was started by addition of 100  $\mu\text{l}$  of 80 mM *cis*-aconitate to a cuvette containing 900  $\mu\text{l}$  of reaction buffer including 100  $\mu\text{l}$  of sample. The molar extinction coefficient was  $\epsilon = 6.22 \text{ cm}^2 \text{mol}^{-1}$ , readings were made against a blank containing all components with exception of *cis*-aconitate.

### 12.3. Isocitrate dehydrogenase

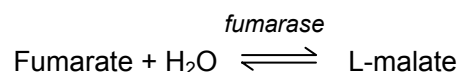
Enzyme activity of isocitrate dehydrogenase (*ICDH*) was measured as the rate of NADPH release at 340 nm in the presence of DL-isocitrate:



After incubation of 1000  $\mu\text{l}$  reaction buffer and 200  $\mu\text{l}$  of sample for 5 min at room temperature the reaction was started by addition of 100  $\mu\text{l}$  of NADP solution to the cuvette. Changes in absorbance were measured every min up to 3 min. The molar extinction coefficient was  $\epsilon = 6.22 \text{ cm}^2 \mu\text{mol}^{-1}$ .

### 12.4. Fumarase

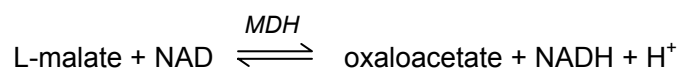
Fumarase activity was assayed by monitoring the rate of change in absorption at 280 nm after addition of enzyme containing mitochondrial extracts:



Due to the necessary wavelength of 280 nm a special UV-Star 96-well microplate (Greiner Bio-One, Essen) was used in combination with a thermostated Genios plate reader (Tecan, Crailsheim). An aliquot of 10  $\mu\text{l}$  of sample was added directly to one well containing 70  $\mu\text{l}$  of 50 mM L-malate and 50 mM sodium phosphate buffer, pH 7.3. The increase in absorbance was observed at 10 sec intervals up to 5 min. For calculation of enzyme activity a period of 3 min was selected, the molecular extinction coefficient was  $\epsilon = 1.48 \text{ cm}^2 \mu\text{mol}^{-1}$ , and the deposit thickness  $d = 0.45 \text{ cm}$ .

### 12.5. Malate dehydrogenase

Malate dehydrogenase activity was determined in 96 well microplates by measuring the initial increases in absorption at 340 nm due to NAD reduction rates in presence of L-malate:



The reaction mixture contained 135  $\mu\text{l}$  sodium glycinate buffer (90 mM), 5  $\mu\text{l}$  NAD (12.3 mM), and 5  $\mu\text{l}$  L-malate (1 M). The reaction was started by addition of 5  $\mu\text{l}$  mitochondrial fraction. Readings were made against a blank containing all assay components except NAD, at intervals of 15 sec for 3 min. For calculation of enzyme activity a period of 105 sec was selected, the molecular extinction coefficient was  $\epsilon = 6.22 \text{ cm}^2 \mu\text{mol}^{-1}$ , the deposit thickness  $d = 0.5 \text{ cm}$ .

### 13. Quantification of tricarboxylic acid cycle metabolites

Intermediates of the TCA cycle were assayed enzymatical as described by (Bergmeyer, 1989a) in the initial crude cell extract. For all measurements 96-well microplates (Greiner Bio-One, Essen) were used in combination with a thermostated Genios plate reader (Tecan, Crailsheim) at 25°C. Experiments were carried out three times with independent samples. Amounts of isocitrate, 2-oxoglutarate and citrate were estimated UV-photometrical at 340 nm; the metabolite concentration was calculated as follows:

$$C_{\text{Metabolite}} = [V_{\text{react}} \times \Delta\text{abs}] / V_{\text{sample}} \times \epsilon \times d$$

where  $V_{\text{react}}$  is the reaction volume in ml,  $V_{\text{sample}}$  is the volume of sample in ml,  $\Delta\text{abs}$  is the observed change in absorbance over a selected period,  $\epsilon$  is the molecular extinction coefficient in  $\text{cm}^2 \mu\text{mol}^{-1}$  at the selected wavelength, and  $d$  is the deposit thickness in cm.

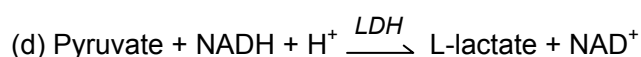
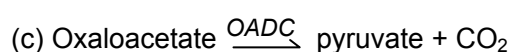
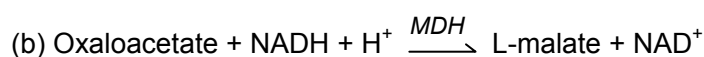
Contents of oxaloacetate and L-malate were determined fluorometrical at 360/460 nm, the metabolite concentration was calculated as follows:

$$C_{\text{Metabolite}} = [c_{\text{stand}} \times \Delta F_{\text{sample}}] / \Delta F_{\text{stand}}$$

where  $c_{\text{stand}}$  is the known concentration of a respective metabolite standard in nmol/ml,  $\Delta F_{\text{stand}}$  is the observed change in fluorescence of the standard over a selected period, and  $\Delta F_{\text{sample}}$  is the observed change in fluorescence of the sample over the same period.

#### 13.1. Citrate

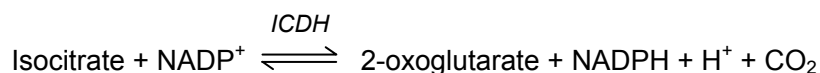
In the presence of the enzymes malate dehydrogenase (*MDH*) and lactate dehydrogenase (*LDH*), oxaloacetate and its decarboxylation product, pyruvate, are reduced by NADH to L-malate and L-lactate, respectively. The amount of NADH oxidized in reactions (b) and (d), measured by the decrease of absorbance at 340 nm is proportional and stoichiometric to the amount of citrate:



To 140  $\mu\text{l}$  of reaction buffer 6  $\mu\text{l}$  of  $\beta$ -NADH solution (10 mM) and 10  $\mu\text{l}$  of sample were added, and the absorbance was measured. The reaction was started by addition of 5  $\mu\text{l}$  LDH/MDH solution. Changes in absorbance were measured every 30 sec up to 3 min, when the reaction was complete. Then 5  $\mu\text{l}$  of citrate lyase (CL) solution were added, and the absorbance again was observed until it reached a constant value. Readings were made against a blank containing all the assay components except the sample, which was displaced by the same amount of water. The molecular extinction coefficient was  $\epsilon = 6.22 \text{ cm}^2 \mu\text{mol}^{-1}$ , and the deposit thickness  $d = 0.5 \text{ cm}$ .

### 13.2. Isocitrate

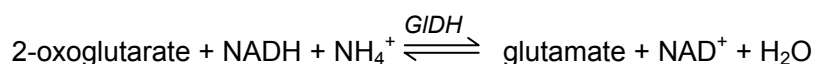
The estimation of isocitrate is based on measurement of the reduction of NADP by isocitrate dehydrogenase (ICDH); the formation of NADPH is effected stoichiometric to the amount of isocitrate:



After measuring the initial absorbance in the reaction mix, the reaction was started by addition of 10  $\mu\text{l}$  metabolite containing sample. Readings were made against air at intervals of 30 sec for 5 min. For determination of metabolite concentration a period of 2 min was selected, the molecular extinction coefficient was  $\epsilon = 6.22 \text{ cm}^2 \mu\text{mol}^{-1}$ , and the deposit thickness  $d = 0.45 \text{ cm}$ .

### 13.3. 2-oxoglutarate

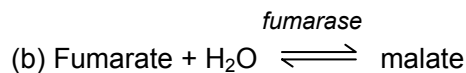
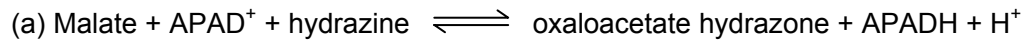
Content of 2-oxoglutarate was estimated with NADH oxidizing glutamate dehydrogenase (GIDH), the decrease of NADH is directly proportional to decrease of 2-oxoglutarate:



To 100  $\mu\text{l}$  of sample 25  $\mu\text{l}$  of  $\beta$ -NADH- $\text{Na}_2$  solution were added (0.1 mM final concentration), and the absorbance was measured. The reaction was started by addition of 10  $\mu\text{l}$  glutamate dehydrogenase (GIDH). Changes in absorbance were measured every min up to 14 min. The molar extinction coefficient was  $\epsilon = 6.22 \text{ cm}^2 \mu\text{mol}^{-1}$ , readings were made against air. For estimation of metabolite concentration a period of 10 min was selected, the deposit thickness was  $d = 0.35 \text{ cm}$ .

### 13.4. Malate

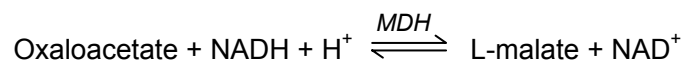
The malate assay was carried out using the 3-acetylpyridin analog of NAD (APAD) and malate dehydrogenase. The increase of APADH is proportional to the amount of malate in the cell extract:



To 200  $\mu\text{l}$  reaction mix 10  $\mu\text{l}$  of sample or standard solution were added, and the fluorescence was measured. The reaction was started by the addition of 4  $\mu\text{l}$  of *MDH* solution (1 mg/ml); changes in fluorescence were recorded until a constant value has been attained, approximate up to 30 min. For each measurement the fluorescence change in the reagent blank was determined with water as specimen. Concentrations of malate in samples were determined by reference to  $\Delta F_{\text{stand}}$  found through assay of standard solutions.

### 13.5. Oxaloacetate

Oxaloacetate was determined by monitoring the decrease of NADH concentration after addition of malate dehydrogenase:



After incubation of 60  $\mu\text{l}$  reaction buffer with 40  $\mu\text{l}$  of sample or oxaloacetate standard solution for 5 min at room temperature fluorescence was monitored. The reaction was started by the addition of 3  $\mu\text{l}$  of MDH solution; changes in fluorescence were recorded until a constant value has been attained, approximate up to 5 min. For each measurement the fluorescence change in the reagent blank was determined with water as specimen. Concentrations of oxaloacetate in samples were determined by reference to  $\Delta F_{\text{stand}}$  found through assay of standard solutions.

## 14. Fluorescence microscopy

For fluorescence staining for nitric oxide (NO), 20  $\mu\text{l}$  untreated or harpin-treated (50  $\mu\text{g/ml}$ ) *Arabidopsis* suspension cells were placed on microscope slides and stained with DAF-FM (10  $\mu\text{l}$ , 10  $\mu\text{M}$  final concentration) in the presence or absence of the NO scavenger carboxy PTIO at a final concentration of 30  $\mu\text{M}$ . Fluorescence development was observed and photographed on a Axioscop light microscope (Zeiss, Oberkochen), equipped with a standard FITC emission filter.

To visualize the mitochondrial  $\text{H}_2\text{O}_2$  burst in harpin-treated cells they were labeled with 100 nM MitoTracker Red 580 as mitochondrial specific marker and incubated for 1 h in the dark. Twenty  $\mu\text{l}$  of the stained cell suspension were placed on a microscope slide and 10  $\mu\text{M}$   $\text{H}_2\text{DCF-DA}$  was added. The samples were monitored and photographed using a BX C1 epifluorescence microscope and a black/white 12-bit (1376x1032 pixel) CCD-camera (Olympus, Hamburg). Images were analysed with Analysis 3.2 software (Soft Imaging Systems, Stuttgart). Excitation wavelength for  $\text{H}_2\text{DCF-DA}$  was



485 nm and emission wavelength 515 nm (FITC filter), MitoTracker Red 580 was excited at 577 nm and resulting fluorescence detected through a long-pass filter.

### **15. Fluorescence microscopy immunolabeling**

For immunofluorescence studies, leaves from harpin treated (12 h) and untreated *Arabidopsis* plants were harvested and rinsed 3 times for 10 min in TBS containing 0.1% Tween-20 (TBS-T). Using razor blades, thin sections were cutted and fixed in 4% paraformaldehyde / 0.2% glutaraldehyde for at least 1 h. After washing 3 times in TBS-T for 10 min, samples were incubated in blocking solution (TBS-T with 5% non-fat milk powder) for 1 hr. After incubation with the rabbit anti-harpin serum (diluted 1:500 in blocking solution) overnight at 4°C and washing 3 times with TBS-T for 30 min, samples were treated for 1 h up to 2 h in the dark with a goat anti-rabbit immunoglobulin labeled with FITC, diluted 1:100 in blocking solution. Finally, the leaf sections were washed 4 times in TBS-T in the dark for 10 min. Harpin-derived fluorescence was detected by confocal laser-scanning microscopy, settings and laser of the Zeiss Axiovert 100M inverted microscope were as described in (Huang et al., 2004).

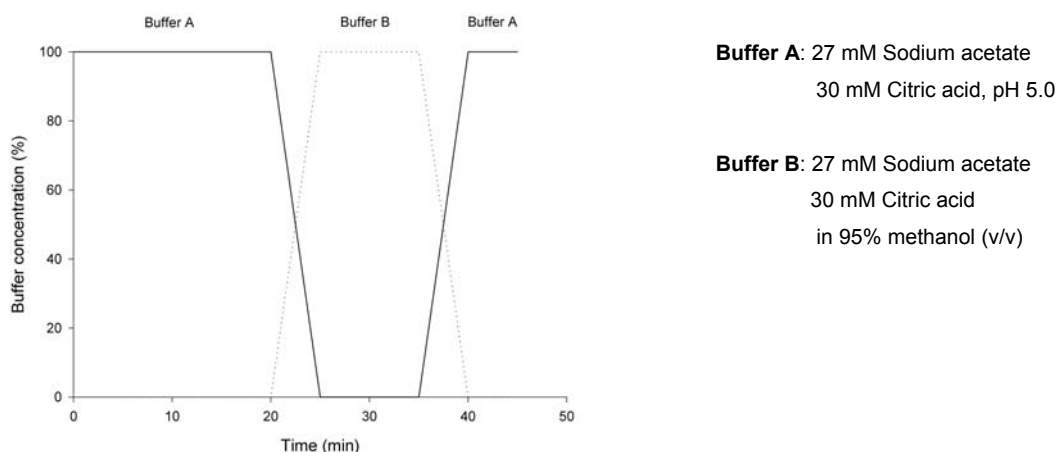
### **16. NO and ROS quantification**

An induction of NO and ROS in *Arabidopsis* suspension cells by harpin was confirmed by photometrical measurement of fluorescence intensities of DAF-FM respectively H<sub>2</sub>DCF-DA using a Genios plate reader (Tecan, Crailsheim) with usual FITC excitation and emission filters. Harpin treated cells were stained by addition of 10 µl DAF-FM or H<sub>2</sub>DCF-DA (both dyes at 10 µM) to 300 µl of cells in a black 96 well microplate (Greiner Bio-One, Essen). The fluorescence intensity was measured every min over time. The plate was rocked before measuring for 5 sec.

### **17. Determination of Salicylic acid content**

The extraction was carried out according a modified method of (Meuwly and Métraux, 1993). Determination of Salicylic acid (SA) was done in the work group headed by Dr. Günther Bahnweg in BIOP. Plant leaf material was ground with mortar and pestle under liquid nitrogen. After shaking of 100 mg frozen tissue powder with 5 ml pure methanol for 20 sec; sample was centrifuged for 10 min at 30 000xg and 4°C. The supernatant was saved and the pellet re-suspended in pure methanol, and re-centrifuged as above. Both supernatants were combined; the solvent was removed under vacuum using a RE111 rotary evaporator (Büchli, Flawil, CH) at 38°C. After resolving in 2 ml 20% formic acid and acidification to a pH below 1.5, sample was gently partitioned two times against 5 and 3 ml of a 1:1 (v/v) mixture of ethylacetate / cyclohexane. The combined organic phase was evaporated in vacuum. The aqueous phase was acidified with 8 N HCl to get a final concentration of 4N HCl and incubated for 1 h at 80°C. The hydrolysis mixture was partitioned twice as above, and the top organic layers were evaporated to dryness under vacuum, and re-suspended in 500 µl of the HPLC running

buffer (80% buffer A, 20% methanol). HPLC separation of SA was performed on RP-C-18 Nucleosil columns (150 x 4.6 mm, 5  $\mu$ m, Bischoff, Leonberg) using the below diagrammed gradient program; the flow rate was set at constant 1.5 ml/min. To 4°C temperature samples of 20  $\mu$ l were injected automatically with an Autosampler Basic Marathon (Spark, NL). On-line measurements of SA were performed fluorimetrically with a fluorescence detector RF-535 (Shimazu, München) at an excitation wavelength of 305 nm and an emission wavelength of 407 nm. The retention time for SA was 11 min.



## 18. Studies with pathogens

### 18.1. *Alternaria alternata*

These pathogen experiments were carried out as described by (Schuhegger et al., 2005) for tomato plants. The *Alternaria alternata* 2177/00 mycelium, kindly supplied by H.-P. Seidl (Technical University Munich, Institute for microbiology), was kept in ddH<sub>2</sub>O at 12°C up to 1 year. For pathogen experiments fungus mycelium was grown for about 14 days at room temperature on a malt extract agar containing petri dish. After transfer of 1cm<sup>2</sup> sized agar pieces onto oat agar plates they were stored for 1-1.5 weeks in the dark. When the plates were kept about 14 days in light, the formed spores were collected by scraping with an inoculating loop and flooding the plates with 10 ml of 62.5 mM KH<sub>2</sub>PO<sub>4</sub> solution supplemented with 5.5 mM glucose and 0.1% (v/v) Tween 20, pH 6.0. Finally the spore suspension was sieved to separate the mycelium. Concentration of spores was adjusted to 1x10<sup>5</sup> spores per ml. Elicitor treated and untreated *Arabidopsis* plants were inoculated by spraying 5 ml spore suspension onto a 5 plants containing potty. Infected plants were maintained in climate chambers (Vötsch, Balingen) under saturating humidity, chambers were provided with a 14 hours light (20°C) / 10 hours dark (18°C) cycle. At indicated time points after infection plants were photographed, harvested, frozen in liquid nitrogen and stored at -80°C until DNA isolation.

The degree of infestation of *Arabidopsis* plants by *Alternaria alternata* was acquired by monitoring the fungal DNA / plant DNA ratio in a constant amount of plant material. *Alternaria alternata* DNA from infected *Arabidopsis* plants (see chapter IV, 4.1.) was quantified by Real-Time PCR using a 7500

Real Time PCR System (Applied Biosystems, Weiterstadt). With this technology SYBR green I dye was used, which hybridize to double-stranded DNA, to detect PCR products as they accumulate during PCR cycles. Based on fluorescence emission of the dye, the amplicon synthesis, defined by the *Alternaria* specific primer pair *AaltF3*: 5'-TCT AGC TTT GCT GGA GAC TC-3' and *AaltR1,1*: 5'-AGA CCT TTG CTG ATA GAG AGT-3' (Schuhegger et al., 2005) was continuously observed during thermocycling. For each sample, a specific  $c_T$ -value is calculated, which is defined as that cycle number at which a statistically significant increase of the fluorescence can be first detected. The  $c_T$ -values are used to calculate the starting *Alternaria* DNA amount in each sample by comparing it with  $c_T$ -values of standards with known amounts of DNA. Samples without any nucleic acid substrate served as PCR controls, the so called no template controls (NTC). The PCR amplification parameters were established as follows:

	<b>Sample</b>	<b>Standard curve</b>
SYBR Green Mix	12.5 $\mu$ l	12.5 $\mu$ l
Primer <i>AaltF3</i> (5pmol/ $\mu$ l)	0.5 $\mu$ l	0.5 $\mu$ l
Primer <i>AaltR1,1</i> (5pmol/ $\mu$ l)	0.5 $\mu$ l	0.5 $\mu$ l
Sample DNA	1.0 $\mu$ l	-
<i>Alternaria</i> DNA	-	10.0 $\mu$ l
ddH <sub>2</sub> O	10.5 $\mu$ l	1.5 $\mu$ l

**PCR program:**

	50°C	2 min
	95°C	15 min
40 cycles	{	95°C 15 sec
		60°C 1 min

Starting with 20 ng *Alternaria* DNA and stepwise 1:10 dilution up to 2 pg standard curves were prepared for all experiments, and calculations were made against the curve. The damage of *Arabidopsis* plants by *Alternaria alternata* was determined for 5 independent samples each containing 5 plants, measurements were carried out threefold.

## 18.2. *Pseudomonas syringae* pv. *tomato* DC3000

The bacterial strain used in this study was *Pseudomonas syringae* pv. *tomato* DC3000 (*Pst* DC3000). Growth of bacteria, syringe injection, and bacterial pathogen enumeration were performed as described in (Katagiri et al., 2002). *Pst* DC3000 cultures were streaked out onto a plate King's medium B with appropriate antibiotics and grown for 2 days at 28°C. Bacteria were transferred to liquid King's medium B with appropriate antibiotics and grown under agitation (250rpm) at 28°C for 8-12 h until bacterial culture reached an OD<sub>600</sub> = 0.6 to 1.0. For quantification the optical density of bacterial cell suspension was measured using a spectrophotometer set at 600 nm. After centrifugation at 2500xg for 10 min in a swinging bucket rotor, pellet was re-suspended in sterile water, washed two times by repeating the centrifugation step, and the OD<sub>600</sub> was estimated again.

For *Pst* DC3000 an  $OD_{600} = 0.002$  is approximate  $1 \times 10^6$  colony forming units/ml, this level is used for syringe injection. A 1ml needleless syringe containing the bacterial suspension was used to pressure-infiltrate the leaf intracellular spaces of *Arabidopsis thaliana* plants with approximate 10  $\mu$ l liquid. When the intercellular spaces of infiltrated leaves were dry, plants were covered with a plastic dome in order to maintain the humidity. At indicated time points leaves were harvested and rinsed in 70% ethanol for 1 min under occasionally gentle agitation. Leaves were blotted briefly on paper towels, rinsed in sterile distilled water, and blotted dry on paper towels again. Leaf disks with an exactly diameter of 0.7 mm from the leaves of 3 independent replicate plants were pooled for a single tissue sample, three tissue samples were taken. Leaf disks of a single tissue sample was placed in a 1.5 ml microfuge tube with 100  $\mu$ l sterile distilled water, samples were ground with a plastic pestle by hand until pieces of intact leaf tissue were not longer visible. The pestle was rinsed with 900  $\mu$ l of sterile distilled water and the liquid was united with that in the original sample tube. Samples were thoroughly vortexed and a 100  $\mu$ l aliquot was diluted in 900  $\mu$ l sterile distilled water. A serial 1:10 dilution series was created for each sample by repeating this process. Samples were streaked out onto plates of King`s medium B with appropriate antibiotics and grown for 2 days at 28°C. Then the colony-forming units for each dilution of each sample were counted.

## V. Materials

### 1. Plant materials

Species	Ecotype	Abbreviation	Function
<i>Arabidopsis thaliana</i>	Columbia	Col-0	wild type
<i>Arabidopsis thaliana</i>	Columbia	HAT0250	mlo2 knockout mutant
<i>Arabidopsis thaliana</i>	Columbia	HAT0620	mlo6 knockout mutant
<i>Arabidopsis thaliana</i>	Columbia	HAT1210	mlo12 knockout mutant
<i>Arabidopsis thaliana</i>	Columbia	HAT0250-0620	mlo2-6 knockout mutant
<i>Arabidopsis thaliana</i>	Columbia	HAT0250-1210	mlo2-12 knockout mutant
<i>Arabidopsis thaliana</i>	Columbia	HAT0620-1210	mlo6-12 knockout mutant
<i>Arabidopsis thaliana</i>	Columbia	HAT0250-0620-1210	mlo2-6-12 knockout mutant

### 2. Bacteria and fungi

Description	Source
<i>Escherichia coli</i> DH5 $\alpha$ competent cells	Stratagene, La Jolla, California, USA
<i>Pseudomonas syringae</i> pv. <i>tomato</i> DC3000	Nikolaus Schlaich, RWTH Aachen
<i>Alternaria alternata</i> 2177/00	H.-P. Seidl, TU Munich

### 3. Chemicals

Description	Company
Acetic acid	Fluka, Buchs, CH
Acetyl-S-CoA	Sigma, Deisenhofen
Agar	Fluka, Buchs, CH
Agarose	Biozym, Hessisch Oldendorf
Ampicillin	Sigma, Deisenhofen
Bacto tryptone	Invitrogen, Karlsruhe
BCIP	Biomol, Hamburg
Betaine	Sigma, Deisenhofen
Bromphenol blue	Merck, Darmstadt
Bromphenol blue-Xylenecyanol mixture	Sigma, Deisenhofen
BSA	Sigma, Deisenhofen
$\beta$ -Mercaptoethanol	Sigma, Deisenhofen
CaCl <sub>2</sub>	Sigma, Deisenhofen
Chloroform	Merck, Darmstadt
Citric acid	Merck, Darmstadt
Complete protease inhibitor	Roche Diagnostics, Mannheim
CTAB	Sigma, Deisenhofen
Cyclohexane	Riedel-de Haën, Seelze
Cytochrome c	Sigma, Deisenhofen
Cytochrome c	Roche Diagnostics, Mannheim
2,4-Dichlorophenoxyacetic acid	Merck, Darmstadt
DL- Isocitric acid trisodium salt	Sigma, Deisenhofen

---

Diethyl pyrocarbonate	Sigma, Deisenhofen
DMSO	Sigma, Deisenhofen
DTNB	Roche Diagnostics, Mannheim
DTT	Sigma, Deisenhofen
EDTA	Bio-Rad, München
EGTA	Sigma, Deisenhofen
Ethidium bromide	Sigma, Deisenhofen
Ethylacetate	Merck, Darmstadt
Evans blue	Sigma, Deisenhofen
FeSO <sub>4</sub>	Merck, Darmstadt
Ficoll	Sigma, Deisenhofen
Formaldehyde	Sigma, Deisenhofen
Formamide	Sigma, Deisenhofen
Formic acid	Merck, Darmstadt
Glucose	Merck, Darmstadt
Glutardialdehyde	Merck, Darmstadt
Glycerol	Fluka, Buchs, CH
Glycine	Serva, Heidelberg
HCl	Fluka, Buchs, CH
HEPES	Sigma, Deisenhofen
Hexylene glycol	Sigma, Deisenhofen
H <sub>2</sub> O <sub>2</sub>	Merck, Darmstadt
H <sub>2</sub> SO <sub>4</sub>	Merck, Darmstadt
Hydrazine hydrate	Sigma, Deisenhofen
IPTG	Sigma, Deisenhofen
Isopropanol	Merck, Darmstadt
KCl	Sigma, Deisenhofen
K <sub>2</sub> HPO <sub>4</sub>	Merck, Darmstadt
KH <sub>2</sub> PO <sub>4</sub>	Merck, Darmstadt
KOH	Merck, Darmstadt
KPO <sub>4</sub>	Merck, Darmstadt
KSCN	Sigma, Deisenhofen
L-Cysteine	Sigma, Deisenhofen
L-Malate	Sigma, Deisenhofen
Malt extract	Merck, Darmstadt
Mannitol	Sigma, Deisenhofen
MES	Sigma, Deisenhofen
Methanol	Merck, Darmstadt
MgCl <sub>2</sub>	Sigma, Deisenhofen
MnSO <sub>4</sub> · H <sub>2</sub> O	Merck, Darmstadt
Mops	Sigma, Deisenhofen
Murashige and Skoog basal salt mixture	Sigma, Deisenhofen
myo-Inositol	Merck, Darmstadt
NaBH <sub>4</sub>	Sigma, Deisenhofen
NADP disodium salt	Roche Diagnostics, Mannheim
NADP isocitrate dehydrogenase	Sigma, Deisenhofen
NaOAc	Sigma, Deisenhofen
NaOH	Merck, Darmstadt
NBT	Roche Diagnostics, Mannheim
(NH <sub>4</sub> ) <sub>2</sub> SO <sub>4</sub>	Invitrogen, Karlsruhe
N-lauroylsarcosine solution	Sigma, Deisenhofen
non-fat milk powder	Roth, Karlsruhe
Oat flakes	Tagwerk
Oxaloacetic acid sodium salt	Sigma, Deisenhofen
Percoll	Sigma, Deisenhofen
Phosphoric acid	Merck, Darmstadt

---

Pipes	Sigma, Deisenhofen
PMSF	Sigma, Deisenhofen
Ponceau S	Sigma, Deisenhofen
Protease inhibitor cocktail	Roche Diagnostics, Mannheim
PVP-40	Sigma, Deisenhofen
Pyridine-3-carboxylic acid (vitamin B <sub>3</sub> )	Merck, Darmstadt
Pyridoxine hydrochloride (vitamin B <sub>6</sub> )	Merck, Darmstadt
Saccharose	Sigma, Deisenhofen
SDS	Serva, Heidelberg
Sodium acetate	Fluka, Buchs, CH
Sodium azide	Sigma, Deisenhofen
Sodium citrate	USB, Cleveland, Ohio, USA
Sodium glycinate	Sigma, Deisenhofen
Sodium succinate	Sigma, Deisenhofen
SSPE buffer	Sigma, Deisenhofen
Sucrose	Merck, Darmstadt
Tergitol NP-40	Sigma, Deisenhofen
TES	Sigma, Deisenhofen
Thiamine chloride hydrochloride (vitamin B <sub>1</sub> )	Merck, Darmstadt
Triethanolamine hydrochloride	Fluka, Buchs, CH
TRIS	Sigma, Deisenhofen
Triton X-100	Fluka, Buchs, CH
Tween 20	Sigma, Deisenhofen
Urea	Sigma, Deisenhofen
X-Gal	Sigma, Deisenhofen
Yeast extract	Fluka, Buchs, CH
ZnCl <sub>2</sub>	Merck, Darmstadt

#### 4. Molecular biological reagents, enzymes and kits

Description	Company
aa-dUTP(5-(3-aminoallyl)-2'-deoxyuridine-5'-	Sigma, Deisenhofen
Adenosine diphosphate	Sigma, Deisenhofen
ADP	Sigma, Deisenhofen
Alexa Fluor <sup>®</sup> 488 protein labeling kit	Molecular Probes, Eugene, Oregon, USA
Anti-β-ATPase monoclonal antibody	Thomas E. Elthon, Lincoln, USA
Anti-cytochrome c monoclonal antibody 7H8.2C12	BD Pharmingen, Heidelberg
Anti-Digoxigenin antibody	Roche Diagnostics, Mannheim
Anti-Mouse IgG-AP	Stressgen, Victoria, BC Canada
Anti-Mouse IgG-hrp	Amersham Biosciences, Freiburg
Anti-Rabbit IgG (whole molecule)-FITC	Sigma, Deisenhofen
APAD	Sigma, Deisenhofen
ATP Determination Kit	Molecular Probes, Eugene, Oregon, USA
β-NAD	Fluka, Buchs, CH
β-NADH	Sigma, Deisenhofen
Cellulase R10	Serva, Heidelberg
Cis-aconitate	Sigma, Deisenhofen
Citrate lyase	Roche Diagnostics, Mannheim

cPTIO	Alexis, Lausen, CH
CSPD solution	Roche Diagnostics, Mannheim
Cy3 Mono-Reactive dye	Amersham Biosciences, Freiburg
Cy5 Mono-Reactive dye	Amersham Biosciences, Freiburg
DAF-FM	Molecular Probes, Eugene, USA
DIG Easy Hyb Granules	Roche Diagnostics, Mannheim
DIG Wash and Block buffer set	Roche Diagnostics, Mannheim
DIG Mix	Roche Diagnostics, Mannheim
dATP	Fermentas, St. Leon-Rot
dCTP	Fermentas, St. Leon-Rot
dGTP	Fermentas, St. Leon-Rot
dTTP	Fermentas, St. Leon-Rot
DNase I	Amersham Biosciences, Freiburg
First strand buffer (5x)	Invitrogen, Karlsruhe
Glutamate dehydrogenase	Roche Diagnostics, Mannheim
H <sub>2</sub> DCF-DA	Molecular Probes, Eugene, USA
In situ Hybridization Kit Plus	Agilent Technologies, Palo Alto, CA, USA
Isocitrate dehydrogenase	Fluka, Buchs, CH
JC-1	Molecular Probes, Eugene, USA
L-Lactate dehydrogenase	Roche Diagnostics, Mannheim
Maceroenzyme R10	Serva, Heidelberg
Malate dehydrogenase	Roche Diagnostics, Mannheim
MitoTracker Red 580	Molecular Probes, Eugene, USA
Nucleon PhytoPure resin	Amersham Biosciences, Freiburg
PCR DIG Probe synthesis kit	Roche Diagnostics, Mannheim
PicoGreen™ dsDNA quantitation kit	Molecular Probes, Eugene, USA
Poly-d(T) <sub>12-18</sub> -primer	Invitrogen, Karlsruhe
P-Stab and Drying solution	Agilent Technologies, Palo Alto, CA, USA
QIAquick PCR purification kit	Qiagen, Hilden
RiboGreen™ RNA quantitation kit	Molecular Probes, Eugene, USA
RNase A, H	Amersham Biosciences, Freiburg
RNaseOUT	Invitrogen, Karlsruhe
Salmon sperm DNA	Amersham Pharmacia, Buckinghamshire, UK
SOC medium	Invitrogen, Karlsruhe
Spermidine	Sigma, Deisenhofen
Super Signal WestDura	Pierce, Rockford, USA
Superscript II	Invitrogen, Karlsruhe
SYBR Green ROX Mix	ABgene, Epsom, UK
Taq-polymerase	peqLab, Erlangen
Taq-polymerase (Goldstar)	Eurogentec, Köln
TRizol	Invitrogen, Karlsruhe

## 5. Consumables

Description	Company
12.5% SDS-polyacrylamide gel	Bio-Rad, München
384-well; 96-well multiscreen filter plates	Millipore, Bedford, MA, USA
96 well microplates, black; UV-Star	Greiner Bio-One, Essen
<i>Arabidopsis</i> 1.0; 2.0 Oligo Microarrays	Agilent Technologies, Palo Alto, CA, USA
Blotting paper	Amersham Biosciences, Freiburg
Centricon YM-3, YM-10	Millipore, Schwalbach
Cover slips	Roth, Karlsruhe
CSS-100 silylated Slides	CEL Associates, Houston, TX, USA



Cuvettes, silica	Brand, Wertheim
Hybridization bags	Life Technologies, Gaithersburg, USA
Hyperfilm ECL	Amersham Biosciences, Freiburg
Lumi-film chemiluminescent detection film	Roche Diagnostics, Mannheim
Microscope slides	Hecht-Assistant, Sondheim
Miracloth	Calbiochem, San Diego, USA
Nylon membrane, positively charged	Roche Diagnostics, Mannheim
Nylon mesh	Verseidag Industrietextilien, Krefeld
PD-10 desalting columns	Amersham Biosciences, Freiburg
Petri dishes	Greiner Bio-One, Essen
PVDF membrane	Amersham Biosciences, Freiburg
Razor blades	Martor, Solingen
Safe-lock caps 0.5 ml, 1.5 ml, 2.0 ml	Eppendorf, Hamburg
Syringes; needles, Sterican 0.70x30	B.Braun, Melsungen
Syringe filters 0.2 µm, 0.45 µm	Sartorius, Göttingen
Whatman paper	Whatman Biometra, Göttingen

## 6. Buffers, solutions and media

Description	Quantity
<b>Alkaline phosphatase buffer</b>	
TRIS	100 mM
NaCl	100 mM
MgCl <sub>2</sub>	5 mM
Adjust to pH 9.5.	
<b>Ammonium sulphate solution</b>	
(NH <sub>4</sub> ) <sub>2</sub> SO <sub>4</sub>	3.2 M
<b>Blocking buffer</b>	
TBS (10x)	10% (v/v)
Tween-20	0.1% (v/v)
non-fat milk powder	5% (w/v)
<b>Boiling buffer</b>	
TRIS	100 mM
EDTA	4 mM
Adjust to pH 7.75 with HCl.	
<b>cDNA mastermix for microarrays</b>	
First strand buffer (5x)	6.0 µl
10x aminoallyl-dNTP mix	3.0 µl
DTT (100 mM)	3.0 µl
RNaseOUT	1.0 µl
Superscript II (200U/µl)	2.0 µl
<b>cDNA mastermix for RT-PCR</b>	
First strand buffer (5x)	4.0 µl
dNTP mix	1.0 µl
DTT (100 mM)	2.0 µl
RNaseOUT	0.5 µl
Superscript II	1.0 µl

**CTAB buffer**

TRIS	100 mM
EDTA	20 mM
NaCl	1.4 M
CTAB	2% (w/v)

Adjust to pH 8.0 with HCl and autoclave.

**Citrate lyase solution for citrate assay**

Citrate lyase lyophilisat	21 mg
ddH <sub>2</sub> O	3.0 ml

**Cytochrome c oxidase assay buffer**

TRIS	10 mM
KCl	120 mM

Adjust to pH 7.0 with HCl.

**Cytochrome c oxidase dilution buffer**

TRIS	10 mM
Sucrose	250 mM

Adjust to pH 7.0 with HCl.

**Cytosol extraction buffer**

Sucrose	200 mM
Hepes	20 mM
KCl	20 mM
MgCl <sub>2</sub>	1.5 mM
EDTA	1 mM
DTT	1 mM

Add complete protease inhibitor prior to use.

**Denhardt's solution (100x) 1l**

Ficoll	20 g
PVP-40	20 g
BSA	20 g

Filter sterile and store at -20°C.

**DEPC water**

Diethyl pyrocarbonate	0.2% (w/v)
-----------------------	------------

Autoclave.

**DNase buffer**

TRIS	400 mM
MgCl <sub>2</sub>	60 mM
DNase I	12.5 U

Adjust to pH 7.5 with HCl.

**Evans blue solution**

Evans blue	0.05% (w/v)
CaCl <sub>2</sub>	0.1 mM

Adjust to pH 5.6.

**Gradient buffer I**

Mannitol	600 mM
TES	20 mM
BSA	0.2% (w/v)

Adjust to pH 7.5 with KOH.

**Gradient buffer II**

Sucrose	600 mM
TES	20 mM
BSA	0.2% (w/v)
Adjust to pH 7.5 with KOH.	

**Harpin storage buffer**

Tween-20	0.5% (v/v)
Tergitol NP-40	0.5% (v/v)
EDTA	10 mM
Glycerol	50% (v/v)
Protease inhibitor cocktail	1 tablet

**LDH/MDH solution for citrate assay**

L-Lactate dehydrogenase (5 mg/ml)	250 $\mu$ l
Malate dehydrogenase (10 mg/ml)	125 $\mu$ l
Ammonium sulphate solution (3.2 M)	4 ml

**Lysis buffer for IEF**

Urea	7 M
Thiourea	2 M
DTT	1% (v/v)
Pharmalyte (pH 3-10)	0.5% (v/v)
CHAPS	4% (w/v)

**Mitochondria extraction buffer**

Mannitol	450 mM
Sodium pyrophosphate	50 mM
BSA	0.5% (w/v)
PVP-40	0.5% (w/v)
EGTA	2 mM
L-Cysteine	20 mM
Adjust to pH 8.0 with phosphoric acid. Add L-Cysteine on day of use.	

**Mitochondria wash buffer**

Mannitol	300 mM
TES	10 mM
Adjust to pH 7.5 with KOH.	

**MOPS buffer (10x)**

Mops	200 mM
Sodium acetate	50 mM
EDTA	10 mM
Adjust to pH 7.0 and autoclave.	

**MS vitamins (100x)**

Pyridine-3-carboxylic acid (vitamin B <sub>3</sub> )	25 mg
Pyridoxine hydrochloride (vitamin B <sub>6</sub> )	25 mg
Thiamine chloride hydrochloride (vitamin B <sub>1</sub> )	5.3 mg
myo-Inositol	5 g
Add ddH <sub>2</sub> O to 500 ml and store at -20°C.	

**NADP solution**

NADP	10 mM
MnSO <sub>4</sub>	120 mM

**Nuclei homogenization buffer**

Hexylene glycol	1M
Pipes	10 mM
MgCl <sub>2</sub>	10 mM
Triton X-100	0.5% (v/v)
β-mercaptoethanol	5.0 mM
PMSF	0.8 mM
Adjust to pH 7.8 with KOH. Add β-mercaptoethanol	

**Nuclei wash buffer**

Hexylene glycol	500 mM
Pipes	10 mM
MgCl <sub>2</sub>	10 mM
β-mercaptoethanol	5.0 mM
PMSF	0.8 mM
Adjust to pH 7.8 with KOH. Add β-mercaptoethanol	

**PCR buffer (10x)**

TRIS	750 mM
(NH <sub>4</sub> ) <sub>2</sub> SO <sub>4</sub>	200 mM
MgCl <sub>2</sub>	15 mM
Tween-20	0.1% (v/v)
Adjust to pH 9.0 with HCl and autoclave.	

**PCR running buffer**

Glycerol	30% (w/v)
Bromophenol blue-Xylenecyanol solid mixture	0.25% (w/v)

**Percoll step gradient****Percoll 40%**

H <sub>2</sub> O	0.5 ml
Percoll	2.0 ml
Gradient buffer I	2.5 ml

**Percoll 23%**

H <sub>2</sub> O	5.4 ml
Percoll	4.6 ml
Gradient buffer I	10.0 ml

**Percoll 18%**

H <sub>2</sub> O	3.2 ml
Percoll	1.8 ml
Gradient buffer I	5.0 ml

**Percoll self forming gradient****Percoll 28%**

H <sub>2</sub> O	6.6 ml
Percoll	8.4 ml
Gradient buffer II	15.0 ml

**Phosphate buffered saline (PBS)**

NaCl	140 mM
KCl	2.7 mM
NaH <sub>2</sub> PO <sub>4</sub>	3.2 mM
KH <sub>2</sub> PO <sub>4</sub>	1.5 mM

**Phosphate elution buffer**

KPO <sub>4</sub> , pH 8.5	4 mM
---------------------------	------

**Phosphate buffer KPO<sub>4</sub> (1M)**

K <sub>2</sub> HPO <sub>4</sub> 1M	9.5ml
KH <sub>2</sub> PO <sub>4</sub> 1M	0.5ml

**Phosphate wash buffer**

KPO <sub>4</sub> , 1 M, pH 8.5	500 µl
Ethanol 95%	84.25 ml
MilliQ water	15.25 ml

**Pre-hybridization buffer for BIOP microarrays**

SSC buffer	6x
SDS	0.5% (w/v)
BSA	1% (w/v)
Salmon sperm DNA (1µg/µl)	2% (v/v)

**Protein gel loading buffer**

SDS	4% (w/v)
Glycerol	12% (v/v)
β-mercaptoethanol	2% (v/v)
Bromophenol blue	pinch

**Ponceau red solution**

Ponceau S	0.1% (w/v)
Acetic acid	5% (v/v)

**Protein gel running buffer**

TRIS	25 mM
Glycine	192 mM
SDS	0.1% (w/v)

**Protoplasting solution**

Cellulase R10	1.5% (w/v)
Maceroenzyme R10	0.4% (w/v)
Mannitol (steril filtrated)	400 mM
KCl	20 mM
MES	20 mM
Incubate for 10 min at 55°C and cool down to room	
CaCl <sub>2</sub>	10 mM
β-mercaptoethanol	5 mM
BSA	0.1% (w/v)

**Protoplast wash solution**

NaCl	154 mM
CaCl <sub>2</sub>	125 mM
KCl	5 mM
MES	2 mM
Adjust to pH 5.7.	

**Reaction buffer for aconitase assay**

HEPES	80 mM
NADP	0.5 mM
MnCl <sub>2</sub>	0.42 mM
NADP-isocitrate dehydrogenase	0.2 U

---

Triton X-100	0.05% (v/v)
Adjust to pH 7.5 with NaOH.	
<b>Reaction buffer for citrate synthase assay</b>	
TRIS	100 mM
DTNB	20 mM
Oxaloacetate	5 mM
Acetyl-S-CoA	5 $\mu$ M
Adjust to pH 8.0 with HCl.	
<b>Reaction buffer for citrate assay</b>	
Triethanolamine-hydrochloride	100 mM
ZnCl <sub>2</sub>	0.2 mM
Adjust to pH 7.6 with HCl.	
<b>Reaction buffer for isocitrate dehydrogenase</b>	
Triethanolamine-hydrochloride	100 mM
NaCl	52 mM
DL-Isocitrate	4.6 mM
Adjust to pH 7.5 with NaOH.	
<b>Reaction buffer for isocitrate assay</b>	
TRIS	71.4 mM
MnSO <sub>4</sub> · H <sub>2</sub> O	2.9 mM
NADP-Na <sub>2</sub> H	177 $\mu$ M
Isocitrate dehydrogenase	115 mU/ml
Adjust to pH 7.4 with HCl.	
<b>Reaction buffer for malate assay</b>	
Hydrazine hydrate	100 mM
EDTA	0.2 mM
APAD	60 $\mu$ M
Adjust to pH 9.0.	
<b>Reaction buffer for oxaloacetate assay</b>	
K <sub>2</sub> HPO <sub>4</sub>	100 mM
NaH <sub>2</sub> PO <sub>4</sub>	100 mM
EDTA	0.2 mM
NADH	0.5 $\mu$ M
<b>Reaction buffer for respiratory oxygen uptake</b>	
KPO <sub>4</sub>	10 mM
MgCl <sub>2</sub>	5 mM
KCl	20 mM
mannitol	250 mM
Adjust to pH 7.4.	
<b>RNA denaturation mix</b>	
MOPS buffer (10x)	500 $\mu$ l
Formaldehyde	30 $\mu$ l
Formamide	8670 $\mu$ l
Bromphenol blue	pinch

---

---

**RNA extraction buffer**

TRIS	100 mM
EDTA	25 mM
NaCl	2 M
CTAB	2% (w/v)
PVP	2% (w/v)
Spermidine	0.5% (w/v)
β-mercaptoethanol	2% (v/v)
Adjust to pH 8.0 with HCl.	

**SSC buffer (20x)**

NaCl	3 M
Sodium citrate	300 mM
Adjust to pH 7.0 with HCl and autoclave.	

**Slide blocking solution**

NaBH <sub>4</sub>	0.75 g
PBS	200 ml
Ethanol 95%	75 ml

**Stripping buffer**

β-mercaptoethanol	100 mM
SDS	2% (w/v)
TRIS	62.5 mM
Adjust to pH 6.7 with HCl.	

**TAE buffer (10x)**

TRIS	400 mM
EDTA	10 mM
Sodium acetate	200 mM
Adjust to pH 7.8 with HCl.	

**TBS-T buffer (10x)**

TRIS	10 mM
NaCl	150 mM
Tween-20	0.05% (v/v)
Adjust to pH 7.5.	

**TE buffer (10x)**

TRIS	100 mM
EDTA	10 mM
Adjust to pH 8.0 with HCl and autoclave.	

**Transfer buffer**

TRIS	50 mM
Glycine	40 mM
SDS	0.0375% (w/v)
Methanol	20% (v/v)

**Urea buffer**

Urea	4.5 M
Glycerol	16.6% (w/v)
β-Mercaptoethanol	5% (v/v)
SDS	5% (w/v)

---

Description	Quantity
<b>AS medium (1l)</b>	
Murashige and Skoog basal salt mixture (MS)	4.3 g
2,4-Dichlorophenoxyacetic acid	1.0 mg
MS vitamins (100x)	10 ml
Saccharose	30 g
Adjust to pH 5.7 with KOH, add ddH <sub>2</sub> O and autoclave.	
<b>DYT medium (agar)</b>	
Bacto tryptone	1.6% (w/v)
NaCl	1% (w/v)
Yeast extract	1% (w/v)
Agar	1.5% (w/v)
<b>King`s medium B (1l)</b>	
Peptone	20 g
Glycerol	10 g
K <sub>2</sub> HPO <sub>4</sub>	1.5 g
MgSO <sub>4</sub> · 7H <sub>2</sub> O	1.5 g
(Agar)	20 g
Adjust to pH 7.2, add ddH <sub>2</sub> O and autoclave. Add sterile antibiotics to final concentration as follows:	
<b>LB medium</b>	
Bacto tryptone	1% (w/v)
NaCl	1% (w/v)
Yeast extract	5% (w/v)
Adjust to pH 7.0 with NaOH and autoclave	
<b>Malt extract agar</b>	
Malt extract	2% (w/v)
Agar	1.5% (w/v)
<b>Oat agar</b>	
Oat flakes	2% (w/v)
Agar	1.5% (w/v)



## Citations

- Alfano, J.R., and Collmer, A.** (1997). The type III (Hrp) secretion pathway of plant pathogenic bacteria: trafficking harpins, Avr proteins, and death. *J Bacteriol* **179**, 5655-5662.
- Allwood, E.G., Smertenko, A.P., and Hussey, P.J.** (2001). Phosphorylation of plant actin-depolymerising factor by calmodulin-like domain protein kinase. *FEBS Lett* **499**, 97-100.
- Almeida, R.D., Manadas, B.J., Carvalho, A.P., and Duarte, C.B.** (2004). Intracellular signaling mechanisms in photodynamic therapy. *Biochim Biophys Acta* **1704**, 59-86.
- Al-Qsous, S., Carpentier, E., Klein-Eude, D., Burel, C., Mareck, A., Dauchel, H., Gomord, V., and Balange, A.P.** (2004). Identification and isolation of a pectin methylesterase isoform that could be involved in flax cell wall stiffening. *Planta* **219**, 369-378.
- Alvarez, M.E., Pennell, R.I., Meijer, P.-J., Ishikawa, A., Dixon, R.A., and Lamb, C.** (1998). Reactive oxygen intermediates mediate a systemic signal network in the establishment of plant immunity. *Cell* **92**, 773-784.
- Andi, S., Taguchi, F., Toyoda, K., Shiraishi, T., and Ichinose, Y.** (2001). Effect of methyl jasmonate on harpin-induced hypersensitive cell death, generation of hydrogen peroxide and expression of PAL mRNA in tobacco suspension cultured BY-2 cells. *Plant Cell Physiol* **42**, 446-449.
- Asai, T., Tena, G., Plotnikova, J., Willmann, M.R., Chiu, W.L., Gomez-Gomez, L., Boller, T., Ausubel, F.M., and Sheen, J.** (2002). MAP kinase signalling cascade in Arabidopsis innate immunity. *Nature* **415**, 977-983.
- Aubert, D., Chevillard, M., Dorne, A.M., Arlaud, G., and Herzog, M.** (1998). Expression patterns of GASA genes in *Arabidopsis thaliana*: the GASA4 gene is up-regulated by gibberellins in meristematic regions. *Plant Mol Biol* **36**, 871-883.
- Baker, C.J., Orlandi, E.W., and Mock, N.M.** (1993). Harpin an Elicitor of the Hypersensitive Response in Tobacco Caused by *Erwinia-Amylovora* Elicits Active Oxygen Production in Suspension Cells. *Plant Physiology (Rockville)* **102**, 1341-1344.
- Bal-Price, A., and Brown, G.C.** (2000). Nitric-oxide-induced necrosis and apoptosis in PC12 cells mediated by mitochondria. *J Neurochem* **75**, 1455-1464.
- Barchowsky, A., Klei, L.R., Dudek, E.J., Swartz, H.M., and James, P.E.** (1999). Stimulation of reactive oxygen, but not reactive nitrogen species in vascular endothelial cells exposed to low levels of arsenite. *Free Radic. Biol. Med.* **27**, 1405-1412.
- Beligni, M.V., Fath, A., Bethke, P.C., Lamattina, L., and Jones, R.L.** (2002). Nitric oxide acts as an antioxidant and delays programmed cell death in barley aleurone layers. *Plant Physiol* **129**, 1642-1650.
- Bergmeyer, H.U.** (1989a). *Metabolites 2: Tri- and Dicarboxylic Acids, Purines, Pyrimidines and Derivates, Coenzymes, Inorganic Compounds.* (Weinheim: VCH Publishers, P.O.Box 101161, Weinheim).
- Bergmeyer, H.U.** (1989b). *Enzymes 1: Oxidoreductases, Transferases.* (Weinheim: VCH Publishers, P.O.Box 101161, Weinheim).
- Blume, B., Nurnberger, T., Nass, N., and Scheel, D.** (2000). Receptor-mediated increase in cytoplasmic free calcium required for activation of pathogen defense in parsley. *Plant Cell* **12**, 1425-1440.
- Bogin, E., and Wallace, A.** (1969). Citrate synthase from lemon fruit. In *Citric Acid Cycle*, J.M. Lowenstein, ed (New York, London), pp. 19-22.
- Bonas, U., and Lahaye, T.** (2002). Plant disease resistance triggered by pathogen-derived molecules: refined models of specific recognition. *Curr Opin Microbiol* **5**, 44-50.

- Bossy-Wetzell, E., Newmeyer, D.D., and Green, D.R.** (1998). Mitochondrial cytochrome c release in apoptosis occurs upstream of DEVD-specific caspase activation and independently of mitochondrial transmembrane depolarization. *Embo J* **17**, 37-49.
- Botella, M.A., Xu, Y., Prabha, T.N., Zhao, Y., Narasimhan, M.L., Wilson, K.A., Nielsen, S.S., Bressan, R.A., and Hasegawa, P.M.** (1996). Differential expression of soybean cysteine proteinase inhibitor genes during development and in response to wounding and methyl jasmonate. *Plant Physiol.* **112**, 1201-1210.
- Bourquin, V., Nishikubo, N., Abe, H., Brumer, H., Denman, S., Eklund, M., Christiernin, M., Teeri, T.T., Sundberg, B., and Mellerowicz, E.J.** (2002). Xyloglucan endotransglycosylases have a function during the formation of secondary cell walls of vascular tissues. *Plant Cell* **14**, 3073-3088.
- Bradford, M.M.** (1976). A rapid and sensitive method for the quantitation of microgram quantities of protein utilizing the principle of protein-dye binding. *Anal Biochem* **77**, 248-254.
- Braun, M., Baluska, F., von Witsch, M., and Menzel, D.** (1999). Redistribution of actin, profilin and phosphatidylinositol-4, 5-bisphosphate in growing and maturing root hairs. *Planta* **209**, 435-443.
- Buttner, D., and Bonas, U.** (2002a). Getting across--bacterial type III effector proteins on their way to the plant cell. *Embo J* **21**, 5313-5322.
- Buttner, D., and Bonas, U.** (2002b). Port of entry--the type III secretion translocon. *Trends Microbiol* **10**, 186-192.
- Carrari, F., Nunes-Nesi, A., Gibon, Y., Lytovchenko, A., Loureiro, M.E., and Fernie, A.R.** (2003). Reduced expression of aconitase results in an enhanced rate of photosynthesis and marked shifts in carbon partitioning in illuminated leaves of wild species tomato. *Plant Physiol* **133**, 1322-1335.
- Carteaux, F., Thibaud, M.C., Zimmerli, L., Lessard, P., Sarrobert, C., David, P., Gerbaud, A., Robaglia, C., Somerville, S., and Nussaume, L.** (2003). Transcriptome analysis of Arabidopsis colonized by a plant-growth promoting rhizobacterium reveals a general effect on disease resistance. *Plant J* **36**, 177-188.
- Cheong, Y.H., Chang, H.S., Gupta, R., Wang, X., Zhu, T., and Luan, S.** (2002). Transcriptional profiling reveals novel interactions between wounding, pathogen, abiotic stress, and hormonal responses in Arabidopsis. *Plant Physiol* **129**, 661-677.
- Chivasa, S., and Carr, J.P.** (1998). Cyanide restores *N* gene-mediated resistance to tobacco mosaic virus in transgenic tobacco expressing salicylic acid hydroxylase. *Plant Cell* **10**, 1489-1498.
- Cluis, C.P., Mouchel, C.F., and Hardtke, C.S.** (2004). The Arabidopsis transcription factor HY5 integrates light and hormone signaling pathways. *Plant J* **38**, 332-347.
- Cohen, G., Kim, M., and Ogwu, V.** (1996). A modified catalase assay suitable for a plate reader and for the analysis of brain cell cultures. *J Neurosci Methods* **67**, 53-56.
- Cohn, J., Sessa, G., and Martin, G.B.** (2001). Innate immunity in plants. *Curr. Opin. Immunol.* **13**, 55-62.
- Dangl, J.L., and Jones, J.D.** (2001). Plant pathogens and integrated defence responses to infection. *Nature* **411**, 826-833.
- Davuluri, R.V., Sun, H., Palaniswamy, S.K., Matthews, N., Molina, C., Kurtz, M., and Grotewold, E.** (2003). AGRIS: Arabidopsis gene regulatory information server, an information resource of Arabidopsis cis-regulatory elements and transcription factors. *BMC Bioinformatics* **4**, 25.
- de Capdeville, G., Beer, S.V., Watkins, C.B., Wilson, C.L., and Aist, J.R.** (2003). Pre- and post-harvest harpin treatments of apples induce resistance to blue mold. *Plant disease* **87**, 39-44.
- Delledonne, M., Xia, Y., Dixon, R.A., and Lamb, C.** (1998). Nitric oxide functions as a signal in plant disease resistance. *Nature* **394**, 585-588.

- Delledonne, M., Zeier, J., Marocco, A., and Lamb, C.** (2001). Signal interactions between nitric oxide and reactive oxygen intermediates in the plant hypersensitive disease resistance response. *Proc Natl Acad Sci U S A* **98**, 13454-13459.
- Desikan, R., Reynolds, A., Hancock, J.T., and Neill, S.J.** (1998). Harpin and hydrogen peroxide both initiate programmed cell death but have differential effects on defence gene expression in *Arabidopsis* suspension cultures. *Biochem J* **330**, 115-120.
- Desikan, R., Hancock, J.T., Ichimura, K., Shinozaki, K., and Neill, S.J.** (2001). Harpin induces activation of the Arabidopsis mitogen-activated protein kinases AtMPK4 and AtMPK6. *Plant Physiol* **126**, 1579-1587.
- Devoto, A., Hartmann, H.A., Piffanelli, P., Elliott, C., Simmons, C., Taramino, G., Goh, C.S., Cohen, F.E., Emerson, B.C., Schulze-Lefert, P., and Panstruga, R.** (2003). Molecular phylogeny and evolution of the plant-specific seven-transmembrane MLO family. *J Mol Evol* **56**, 77-88.
- Dixon, R.A., Harrison, M.J., and Lamb, C.J.** (1994). Early Events In the Activation Of Plant Defense Responses. *Annual Review Of Phytopathology* **32**, 479-501.
- Djajanegara, I., Finnegan, P.M., Mathieu, C., McCabe, T., Whelan, J., and Day, D.A.** (2002). Regulation of alternative oxidase gene expression in soybean. *Plant Mol Biol* **50**, 735-742.
- Dong, H., Delaney, T.P., Bauer, D.W., and Beer, S.V.** (1999). Harpin induces disease resistance in Arabidopsis through the systemic acquired resistance pathway mediated by salicylic acid and the NIM1 gene. *Plant J* **20**, 207-215.
- Dong, H.P., Peng, J., Bao, Z., Meng, X., Bonasera, J.M., Chen, G., Beer, S.V., and Dong, H.** (2004). Downstream divergence of the ethylene signaling pathway for harpin-stimulated Arabidopsis growth and insect defense. *Plant Physiol* **136**, 3628-3638.
- Dong, J., Chen, C., and Chen, Z.** (2003). Expression profiles of the Arabidopsis WRKY gene superfamily during plant defense response. *Plant Mol Biol* **51**, 21-37.
- Durner, J., Shah, J., and Klessig, D.F.** (1997). Salicylic acid and disease resistance in plants. *Trends Plant Sci* **2**, 266-274.
- Durner, J., Wendehenne, D., and Klessig, D.F.** (1998). Defense gene induction in tobacco by nitric oxide, cyclic GMP, and cyclic ADP-ribose. *Proc. Natl. Acad. Sci. USA* **95**, 10328-10333.
- Eckardt, N.A.** (2002). Plant Disease Susceptibility Genes? *Plant Cell* **14**, 1983-1986.
- Elliott, C., Zhou, F., Spielmeier, W., Panstruga, R., and Schulze-Lefert, P.** (2002). Functional conservation of wheat and rice Mlo orthologs in defense modulation to the powdery mildew fungus. *Mol Plant Microbe Interact* **15**, 1069-1077.
- Felix, G., Duran, J.D., Volko, S., and Boller, T.** (1999). Plants have a sensitive perception system for the most conserved domain of bacterial flagellin. *Plant Journal* **18**, 265-276.
- Fernie, A.R., and Sweetlove, L.J.** (2003). Broad-range metabolite analysis: integration into genomic programs. In 1<sup>st</sup> Int'l Beilstein Symposium on EScEC, M.G. Hicks and C. Kettner, eds (Rüdesheim), pp. 71-86.
- Fernie, A.R., Carrari, F., and Sweetlove, L.J.** (2004). Respiratory metabolism: glycolysis, the TCA cycle and mitochondrial electron transport. *Curr Opin Plant Biol* **7**, 254-261.
- Foissner, I., Wendehenne, D., Langebartels, C., and Durner, J.** (2000). *In vivo* imaging of an elicitor-induced nitric oxide burst in tobacco. *Plant J.* **23**, 817-824.
- Gerber, I.B., Zeidler, D., Durner, J., and Dubery, I.A.** (2004). Early perception responses of *Nicotiana tabacum* cells in response to lipopolysaccharides from *Burkholderia cepacia*. *Planta* **218**, 647-657.

- Giovane, A., Servillo, L., Balestrieri, C., Raiola, A., D'Avino, R., Tamburrini, M., Ciardiello, M.A., and Camardella, L.** (2004). Pectin methylesterase inhibitor. *Biochim Biophys Acta* **1696**, 245-252.
- Glazebrook, J.** (2004). Contrasting Mechanisms of Defense Against Biotrophic and Necrotrophic Pathogens. *Annu Rev Phytopathol.*
- Goldstein, J.C., Waterhouse, N.J., Juin, P., Evan, G.I., and Green, D.R.** (2000). The coordinate release of cytochrome c during apoptosis is rapid, complete and kinetically invariant. *Nat Cell Biol* **2**, 156-162.
- Gomez-Gomez, L., and Boller, T.** (2002). Flagellin perception: a paradigm for innate immunity. *Trends Plant Sci* **7**, 251-256.
- Goodman, R.N., and Novacky, A.J.** (1994). The hypersensitive reaction in plants to pathogens: A resistance phenomenon. (St. Paul: American Phytopathological Society Press).
- Grant, J.J., Yun, B.W., and Loake, G.J.** (2000). Oxidative burst and cognate redox signalling reported by luciferase imaging: identification of a signal network that functions independently of ethylene, SA and MeJA but is dependent on MAPKK activity. *Plant J* **24**, 569-582.
- Gray, G.R., Maxwell, D.P., Villarimo, A.R., and McIntosh, L.** (2004). Mitochondria/nuclear signaling of alternative oxidase gene expression occurs through distinct pathways involving organic acids and reactive oxygen species. *Plant Cell Rep* **23**, 497 - 503.
- Green, D.R., and Reed, J.C.** (1998). Mitochondria and apoptosis. *Science* **281**, 1309-1312.
- Grisham, J.** (2000). Protein biopesticide may be next wave in pest control. *Nat Biotechnol* **18**, 595.
- Guttman, D.S.** (2004). Plants as models for the study of human pathogenesis. *Biotechnol Adv* **22**, 363-382.
- Hansen, G.** (2000). Evidence for Agrobacterium-induced apoptosis in maize cells. *Mol Plant Microbe Interact* **13**, 649-657.
- Hayashi, F., Smith, K.D., Ozinsky, A., Hawn, T.R., Yi, E.C., Goodlett, D.R., Eng, J.K., Akira, S., Underhill, D.M., and Aderem, A.** (2001). The innate immune response to bacterial flagellin is mediated by Toll-like receptor 5. *Nature* **410**, 1099-1103.
- Heazlewood, J.L., and Millar, A.H.** (2005). AMPDB: the Arabidopsis Mitochondrial Protein Database. *Nucleic Acids Res* **33 Database Issue**, D605-610.
- Heazlewood, J.L., Tonti-Filippini, J.S., Gout, A.M., Day, D.A., Whelan, J., and Millar, A.H.** (2004). Experimental analysis of the Arabidopsis mitochondrial proteome highlights signaling and regulatory components, provides assessment of targeting prediction programs, and indicates plant-specific mitochondrial proteins. *Plant Cell* **16**, 241-256.
- Heckathorn, S.A., Downs, C.A., Sharkey, T.D., and Coleman, J.S.** (1998). The small, methionine-rich chloroplast heat-shock protein protects photosystem II electron transport during heat stress. *Plant Physiol* **116**, 439-444.
- Heiskanen, K.M., Bhat, M.B., Wang, H.W., Ma, J., and Nieminen, A.L.** (1999). Mitochondrial depolarization accompanies cytochrome c release during apoptosis in PC6 cells. *J Biol Chem* **274**, 5654-5658.
- Hennig, L., GUISSEM, W., Grossniklaus, U., and Kohler, C.** (2004). Transcriptional programs of early reproductive stages in Arabidopsis. *Plant Physiol* **135**, 1765-1775.
- Hill, R.L., and Bradshaw, R.A.** (1969). Fumarase. In *Citric Acid Cycle*, J.M. Lowenstein, ed (New York, London), pp. 91-98.
- Hoeberichts, F.A., and Woltering, E.J.** (2003). Multiple mediators of plant programmed cell death: interplay of conserved cell death mechanisms and plant-specific regulators. *Bioessays* **25**, 47-57.

- Holt, B.F., 3rd, Hubert, D.A., and Dangl, J.L.** (2003). Resistance gene signaling in plants--complex similarities to animal innate immunity. *Curr Opin Immunol* **15**, 20-25.
- Huang, X., von Rad, U., and Durner, J.** (2002). Nitric oxide induces the nitric oxide-tolerant alternative oxidase in Arabidopsis suspension cells. *Planta* **215**, 914-923.
- Huang, X., Stettmaier, K., Michel, C., Hutzler, P., Mueller, M.J., and Durner, J.** (2004). Nitric oxide is induced by wounding and influences jasmonic acid signaling in Arabidopsis thaliana. *Planta* **218**, 938-946.
- Ichinose, Y., Andi, S., Doi, R., Tanaka, R., Taguchi, F., Sasebe, M., Toyoda, K., Shiraishi, T., and Yamada, T.** (2001). Generation of hydrogen peroxide is not required for harpin-induced apoptotic cell death in tobacco BY-2 cell suspension culture. *Plant Physiol. Biochem.* **39**, 771-776.
- Janska, H.** (2005). ATP-dependent proteases in plant mitochondria: What do we know about them today? *Physiologia Plantarum* **123**, 399-405.
- Jenner, H.L., Winning, B.M., Millar, A.H., Tomlinson, K.L., Leaver, C.J., and Hill, S.A.** (2001). NAD malic enzyme and the control of carbohydrate metabolism in potato tubers. *Plant Physiol* **126**, 1139-1149.
- Jiang, C.J., Weeds, A.G., and Hussey, P.J.** (1997). The maize actin-depolymerizing factor, ZmADF3, redistributes to the growing tip of elongating root hairs and can be induced to translocate into the nucleus with actin. *Plant J* **12**, 1035-1043.
- Jiang, C.M., Wu, M.C., Chang, W.H., and Chang, H.M.** (2001). Change in particle size of pectin reacted with pectinesterase isozymes from pea (*Pisum sativum* L.) sprout. *J Agric Food Chem* **49**, 4383-4387.
- Jorgensen, J.H.** (1994). Genetics of Powdery Mildew Resistance in Barley. *Critical Reviews in Plant Sciences* **13**, 97-119.
- Kalamaki, M.S., Powell, A.L., Struijs, K., Labavitch, J.M., Reid, D.S., and Bennett, A.B.** (2003). Transgenic overexpression of expansin influences particle size distribution and improves viscosity of tomato juice and paste. *J Agric Food Chem* **51**, 7465-7471.
- Kariola, T., Palomaki, T.A., Brader, G., and Palva, E.T.** (2003). *Erwinia carotovora* subsp. *carotovora* and *Erwinia*-derived elicitors HrpN and PehA trigger distinct but interacting defense responses and cell death in Arabidopsis. *Mol Plant Microbe Interact* **16**, 179-187.
- Katagiri, F., Thilmony, R., and He, S.Y.** (2002). The Arabidopsis Thaliana-Pseudomonas Syringae Interaction. In *The Arabidopsis Book*
- Kiefer, E., Heller, W., and Ernst, D.** (2000). A simple and efficient protocol for isolation of functional RNA from plant tissues rich in secondary metabolites. *Plant Mol. Biol. Reporter* **18**, 33-39.
- Kim, M.C., Panstruga, R., Elliott, C., Muller, J., Devoto, A., Yoon, H.W., Park, H.C., Cho, M.J., and Schulze-Lefert, P.** (2002a). Calmodulin interacts with MLO protein to regulate defence against mildew in barley. *Nature* **416**, 447-451.
- Kim, M.C., Lee, S.H., Kim, J.K., Chun, H.J., Choi, M.S., Chung, W.S., Moon, B.C., Kang, C.H., Park, C.Y., Yoo, J.H., Kang, Y.H., Koo, S.C., Koo, Y.D., Jung, J.C., Kim, S.T., Schulze-Lefert, P., Lee, S.Y., and Cho, M.J.** (2002b). Mlo, a modulator of plant defense and cell death, is a novel calmodulin-binding protein. Isolation and characterization of a rice Mlo homologue. *J Biol Chem* **277**, 19304-19314.
- Kinkema, M., Fan, W., and Dong, X.** (2000). Nuclear localization of NPR1 is required for activation of PR gene expression. *Plant Cell* **12**, 2339-2350.
- Kitto, G.** (1969). Intra- and extramitochondrial malate dehydrogenase from chicken and tuna heart. In *Citric Acid Cycle*, J.M. Lowenstein, ed (New York, London), pp. 107-116.
- Kliebenstein, D.J., Dietrich, R.A., Martin, A.C., Last, R.L., and Dangl, J.L.** (1999). LSD1 Regulates Salicylic Acid Induction of Copper Zinc Superoxide Dismutase in Arabidopsis thaliana. *Mol Plant-Microbe Interact* **12**, 1022-1026.

- Krause, M., and Durner, J.** (2004). Harpin inactivates mitochondria in Arabidopsis suspension cells. *Mol Plant Microbe Interact* **17**, 131-139.
- Lam, E., Pontier, D., and del Pozo, O.** (1999). Die and let live - programmed cell death in plants. *Current Opinion in Plant Biology* **2**, 502-507.
- Langebartels, C., Schraudner, M., Ernst, D., Heller, W., and Sandermann, H.** (2000). Oxidative stress and defense reactions in plants exposed to air pollutants and UV-B radiation. In *Oxidative stress in plants*, D. Inzé and M. Van Montagu, eds (Amsterdam: Harwood), pp. 105-135.
- Lee, J., Klessig, D.F., and Nurnberger, T.** (2001a). A harpin binding site in tobacco plasma membranes mediates activation of the pathogenesis-related gene HIN1 independent of extracellular calcium but dependent on mitogen-activated protein kinase activity. *Plant Cell* **13**, 1079-1093.
- Lee, J., Klusener, B., Tsiamis, G., Stevens, C., Neyt, C., Tampakaki, A.P., Panopoulos, N.J., Noller, J., Weiler, E.W., Cornelis, G.R., Mansfield, J.W., and Nurnberger, T.** (2001b). HrpZ(PspH) from the plant pathogen *Pseudomonas syringae* pv. phaseolicola binds to lipid bilayers and forms an ion-conducting pore in vitro. *Proc Natl Acad Sci U S A* **98**, 289-294.
- Lister, R., Chew, O., Lee, M.N., Heazlewood, J.L., Clifton, R., Parker, K.L., Millar, A.H., and Whelan, J.** (2004). A transcriptomic and proteomic characterization of the Arabidopsis mitochondrial protein import apparatus and its response to mitochondrial dysfunction. *Plant Physiol* **134**, 777-789.
- Liu, Y., Fiskum, G., and Schubert, D.** (2002). Generation of reactive oxygen species by the mitochondrial electron transport chain. *J Neurochem* **80**, 780-787.
- Luan, S., Kudla, J., Rodriguez-Concepcion, M., Yalovsky, S., and Grissem, W.** (2002). Calmodulins and Calcineurin B-like Proteins: Calcium Sensors for Specific Signal Response Coupling in Plants. *Plant Cell* **14**, S389-400.
- Lum, H.K., Butt, Y.K.C., and Lo, S.C.L.** (2002). Hydrogen Peroxide Induces a Rapid Production of Nitric Oxide in Mung Bean (*Phaseolus aureus*). *Nitric Oxide* **6**, 205-213.
- Maleck, K., Levine, A., Eulgem, T., Morgan, A., Schmid, J., Lawton, K.A., Dangl, J.L., and Dietrich, R.A.** (2000). The transcriptome of Arabidopsis thaliana during systemic acquired resistance. *Nat Genet* **26**, 403-410.
- Mathis, R., Van Gijsegem, F., De Rycke, R., D'Haese, W., Van Maelsaeke, E., Anthonio, E., Van Montagu, M., Holsters, M., and Vereecke, D.** (2005). Lipopolysaccharides as a communication signal for progression of legume endosymbiosis. *Proc Natl Acad Sci U S A* **102**, 2655-2660.
- Metraux, J.-P., and Durner, J.** (2004). The role of salicylic acid and nitric oxide in programmed cell death and induced resistance. In *Molecular Ecotoxicology of Plants*, H. Sandermann, ed (Berlin Heidelberg: Springer), pp. 111-150.
- Meuwly, P., and Métraux, J.-P.** (1993). Ortho-anisic acid as internal standard for the simultaneous quantitation of salicylic acid and its putative biosynthetic precursors in cucumber leaves. *Anal Biochem* **214**, 500-505.
- Meyer, A., Puhler, A., and Niehaus, K.** (2001). The lipopolysaccharides of the phytopathogen *Xanthomonas campestris* pv. *campestris* induce an oxidative burst reaction in cell cultures of *Nicotiana tabacum*. *Planta* **213**, 214-222.
- Micheli, F.** (2001). Pectin methylesterases: cell wall enzymes with important roles in plant physiology. *Trends Plant Sci* **6**, 414-419.
- Millar, A.H., and Leaver, C.J.** (2000). The cytotoxic lipid peroxidation product, 4-hydroxy-2-nonenal, specifically inhibits decarboxylating dehydrogenases in the matrix of plant mitochondria. *FEBS Lett* **481**, 117-121.
- Millar, A.H., Sweetlove, L.J., Giege, P., and Leaver, C.J.** (2001). Analysis of the Arabidopsis mitochondrial proteome. *Plant Physiol* **127**, 1711-1727.

- Miller, S.I., Ernst, R.K., and Bader, M.W.** (2005). LPS, TLR4 and infectious disease diversity. *Nat Rev Microbiol* **3**, 36-46.
- Mittler, R.** (2002). Oxidative stress, antioxidants and stress tolerance. *Trends Plant Sci* **7**, 405-410.
- Mittler, R., Vanderauwera, S., Gollery, M., and Van Breusegem, F.** (2004). Reactive oxygen gene network of plants. *Trends Plant Sci* **9**, 490-498.
- Mizoguchi, T., Ichimura, K., Yoshida, R., and Shinozaki, K.** (2000). MAP kinase cascades in Arabidopsis: their roles in stress and hormone responses. *Results Probl Cell Differ* **27**, 29-38.
- Moller, I.M.** (2001). PLANT MITOCHONDRIA AND OXIDATIVE STRESS: Electron Transport, NADPH Turnover, and Metabolism of Reactive Oxygen Species. *Annu Rev Plant Physiol Plant Mol Biol* **52**, 561-591.
- Moller, S.G., and McPherson, M.J.** (1998). Developmental expression and biochemical analysis of the Arabidopsis atao 1 gene encoding an H<sub>2</sub>O<sub>2</sub>-generating diamine oxidase. *Plant Journal* **13**, 781-791.
- Murashige, T., and Skoog, F.** (1962). A revised medium for rapid growth and bioassays with tobacco tissue cultures. *Physiol. Plant* **15**, 473-497.
- Nadimpalli, R., Yalpani, N., Johal, G.S., and Simmons, C.R.** (2000). Prohibitins, stomatins, and plant disease response genes compose a protein superfamily that controls cell proliferation, ion channel regulation, and death. *J Biol Chem* **275**, 29579-29586.
- Navarro, L., Zipfel, C., Rowland, O., Keller, I., Robatzek, S., Boller, T., and Jones, J.D.** (2004). The transcriptional innate immune response to flg22. Interplay and overlap with Avr gene-dependent defense responses and bacterial pathogenesis. *Plant Physiol* **135**, 1113-1128.
- Neuburger, M.** (1985). Preparation of plant mitochondria, criteria for assessment of mitochondrial integrity and purity, survival in vitro. In *Higher plant cell respiration*, D.A. Day, Douce, R., ed (Berlin: Springer), pp. 7-24.
- Newman, M.A., von Roepenack-Lahaye, E., Parr, A., Daniels, M.J., and Dow, J.M.** (2002). Prior exposure to lipopolysaccharide potentiates expression of plant defenses in response to bacteria. *Plant J* **29**, 487-495.
- Nimchuk, Z., Rohmer, L., Chang, J.H., and Dangl, J.L.** (2001). Knowing the dancer from the dance: R-gene products and their interactions with other proteins from host and pathogen. *Curr Opin Plant Biol* **4**, 288-294.
- Nur, E.K.A., Gross, S.R., Pan, Z., Balklava, Z., Ma, J., and Liu, L.F.** (2004). Nuclear translocation of cytochrome c during apoptosis. *J Biol Chem* **279**, 24911-24914.
- Nurnberger, T., Brunner, F., Kemmerling, B., and Piater, L.** (2004). Innate immunity in plants and animals: striking similarities and obvious differences. *Immunol Rev* **198**, 249-266.
- Odjakova, M., and Hadjiivanova, C.** (2001). The complexity of pathogen defense in plants. *Bulg. J. Plant Physiol.* **27**, 101-109.
- op den Camp, R.G., Przybyla, D., Ochsenbein, C., Laloi, C., Kim, C., Danon, A., Wagner, D., Hideg, E., Gobel, C., Feussner, I., Nater, M., and Apel, K.** (2003). Rapid induction of distinct stress responses after the release of singlet oxygen in Arabidopsis. *Plant Cell* **15**, 2320-2332.
- Osborn, A.E.** (1996). Preformed Antimicrobial Compounds and Plant Defense against Fungal Attack. *Plant Cell* **8**, 1821-1831.
- Panstruga, R.** (2005). Serpentine plant MLO proteins as entry portals for powdery mildew fungi. *Biochem Soc Trans* **33**, 389-392.
- Pearce, D.A., and Sherman, F.** (1997). Differential ubiquitin-dependent degradation of the yeast apocytochrome c isozymes. *J Biol Chem* **272**, 31829-31836.

- Pedroso, M.C., Magalhaes, J.R., and Durzan, D.** (2000). A nitric oxide burst precedes apoptosis in angiosperm and gymnosperm callus cells and foliar tissues. *J. Exp. Bot.* **51**, 1027-1036.
- Peng, J.L., Dong, H.S., Dong, H.P., Delaney, T.P., Bonasera, J.M., and Beer, S.V.** (2003). Harpin-elicited hypersensitive cell death and pathogen resistance require the NDR1 and EDS1 genes. *Physiological and Molecular Plant Pathology* **62**, 317-326.
- Piffanelli, P., Zhou, F., Casais, C., Orme, J., Jarosch, B., Schaffrath, U., Collins, N.C., Panstruga, R., and Schulze-Lefert, P.** (2002). The barley MLO modulator of defense and cell death is responsive to biotic and abiotic stress stimuli. *Plant Physiol* **129**, 1076-1085.
- Planchet, E., Jagadis Gupta, K., Sonoda, M., and Kaiser, W.M.** (2005). Nitric oxide emission from tobacco leaves and cell suspensions: rate limiting factors and evidence for the involvement of mitochondrial electron transport. *Plant J* **41**, 732-743.
- Popham, P., Pike, S., and Novacky, A.** (1995). The effect of harpin from *Erwinia amylovora* on the plasmalemma of suspension-cultured tobacco cells. *Physiological and Molecular Plant Pathology* **47**, 39-50.
- Rate, D.N., and Greenberg, J.T.** (2001). The *Arabidopsis* aberrant growth and death2 mutant shows resistance to *Pseudomonas syringae* and reveals a role for NPR1 in suppressing hypersensitive cell death. *Plant J* **27**, 203-211.
- Reuber, T.L., Plotnikova, J.M., Dewdney, J., Rogers, E.E., Wood, W., and Ausubel, F.M.** (1998). Correlation of defense gene induction defects with powdery mildew susceptibility in *Arabidopsis* enhanced disease susceptibility mutants. *Plant Journal* **16**, 473-485.
- Riechmann, J.L., and Meyerowitz, E.M.** (1998). The AP2/EREBP family of plant transcription factors. *Biol Chem* **379**, 633-646.
- Rose, J.K., and Bennett, A.B.** (1999). Cooperative disassembly of the cellulose-xyloglucan network of plant cell walls: parallels between cell expansion and fruit ripening. *Trends Plant Sci* **4**, 176-183.
- Ryerson, D.E., and Heath, M.C.** (1996). Cleavage of nuclear DNA into oligonucleosomal fragments during cell death induced by fungal infection or by abiotic treatments. *Plant Cell* **8**, 393-402.
- Saisho, D., Nambara, E., Naito, S., Tsutsumi, N., Hirai, A., and Nakazono, M.** (1997). Characterization of the gene family for alternative oxidase from *Arabidopsis thaliana*. *Plant Mol Biol* **35**, 585-596.
- Sambrook, J., Fritsch, E.F., and Maniatis, T.** (1989). *Molecular Cloning: A Laboratory Manual*. (Cold Spring Harbor: Cold Spring Harbor Laboratory Press).
- Scharf, K.D., Siddique, M., and Vierling, E.** (2001). The expanding family of *Arabidopsis thaliana* small heat stress proteins and a new family of proteins containing alpha-crystallin domains (Acd proteins). *Cell Stress Chaperones* **6**, 225-237.
- Scheel, D.** (1998). Resistance response physiology and signal transduction. *Curr. Opin Plant. Biol.* **1**, 305-310.
- Scheideler, M., Schlaich, N.L., Fellenberg, K., Beissbarth, T., Hauser, N.C., Vingron, M., Slusarenko, A.J., and Hoheisel, J.D.** (2002). Monitoring the switch from housekeeping to pathogen defense metabolism in *Arabidopsis thaliana* using cDNA arrays. *J Biol Chem* **277**, 10555-10561.
- Schenk, P.M., Kazan, K., Wilson, I., Anderson, J.P., Richmond, T., Somerville, S.C., and Manners, J.M.** (2000). Coordinated plant defense responses in *Arabidopsis* revealed by microarray analysis. *Proc Natl Acad Sci U S A* **97**, 11655-11660.
- Schuhegger, R., Knappe, C., Wenig, M., Langebartels, C., and Bahnweg, G.** (2005). Susceptibility of tomato (*Lycopersicon esculentum* Mill.) towards fungal pathogens is altered by ozone exposition and nitrogen nutrition. in preparation.



**Schulze-Lefert, P.** (2004). Knocking on the heaven's wall: pathogenesis of and resistance to biotrophic fungi at the cell wall. *Current Opinion in Plant Biology* **7**, 377-383.

**Schulze-Lefert, P., and Vogel, J.** (2000). Closing the ranks to attack by powdery mildew. *Trends Plant Sci* **5**, 343-348.

**Shah, J., Kachroo, P., and Klessig, D.F.** (1999). The Arabidopsis *ssi1* mutation restores pathogenesis-related gene expression in *npr1* plants and renders defensin gene expression salicylic acid dependent. *Plant Cell* **11**, 191-206.

**Shikata, M., Matsuda, Y., Ando, K., Nishii, A., Takemura, M., Yokota, A., and Kohchi, T.** (2004). Characterization of Arabidopsis ZIM, a member of a novel plant-specific GATA factor gene family. *J Exp Bot* **55**, 631-639.

**Siedow, J.N., and Umbach, A.L.** (1995). Plant Mitochondrial Electron Transfer and Molecular Biology. *Plant Cell* **7**, 821-831.

**Silverman, P., Seskar, M., Kanter, D., Schweizer, P., Metraux, J.P., and Raskin, I.** (1995). Salicylic acid in rice. Biosynthesis, conjugation, and possible role. *Plant Physiol.* **108**, 633-639.

**Sjogren, L.L., MacDonald, T.M., Sutinen, S., and Clarke, A.K.** (2004). Inactivation of the *clpC1* gene encoding a chloroplast Hsp100 molecular chaperone causes growth retardation, leaf chlorosis, lower photosynthetic activity, and a specific reduction in photosystem content. *Plant Physiol* **136**, 4114-4126.

**Slooten, L., Capiou, K., Van Camp, W., Van Montagu, M., Sybesma, C., and Inze, D.** (1995). Factors Affecting the Enhancement of Oxidative Stress Tolerance in Transgenic Tobacco Overexpressing Manganese Superoxide Dismutase in the Chloroplasts. *Plant Physiol* **107**, 737-750.

**Smith, A.M., Ratcliffe, R.G., and Sweetlove, L.J.** (2004). Activation and function of mitochondrial uncoupling protein in plants. *J Biol Chem* **279**, 51944-51952.

**Staskawicz, B.J., Mudgett, M.B., Dangl, J.L., and Galan, J.E.** (2001). Common and contrasting themes of plant and animal diseases. *Science* **292**, 2285-2289.

**Strobel, N.E., Ji, C., Gopalan, S., Kuc, J.A., and He, S.Y.** (1996). Induction of systemic acquired resistance in cucumber by *Pseudomonas syringae* pv. *syringae* 61 HrpZ-Pss protein. *Plant Journal* **9**, 431-439.

**Sun, Y.L., Zhao, Y., Hong, X., and Zhai, Z.H.** (1999). Cytochrome c release and caspase activation during menadione- induced apoptosis in plants. *Febs Letters* **462**, 317-321.

**Suzuki, N., Kojima, H., Urano, Y., Kikuchi, K., Hirata, Y., and Nagano, T.** (2002). Orthogonality of calcium concentration and ability of 4,5- diamino fluorescein to detect NO. *J Biol Chem* **277**, 47-49.

**Sweetlove, L.J., Mowday, B., Hebestreit, H.F., Leaver, C.J., and Millar, A.H.** (2001). Nucleoside diphosphate kinase III is localized to the inter-membrane space in plant mitochondria. *FEBS Lett* **508**, 272-276.

**Sweetlove, L.J., Heazlewood, J.L., Herald, V., Holtzapffel, R., Day, D.A., Leaver, C.J., and Millar, A.H.** (2002). The impact of oxidative stress on Arabidopsis mitochondria. *Plant J* **32**, 891-904.

**Swidzinski, J.A., Leaver, C.J., and Sweetlove, L.J.** (2004). A proteomic analysis of plant programmed cell death. *Phytochemistry* **65**, 1829-1838.

**Tao, Y., Xie, Z., Chen, W., Glazebrook, J., Chang, H.S., Han, B., Zhu, T., Zou, G., and Katagiri, F.** (2003). Quantitative nature of Arabidopsis responses during compatible and incompatible interactions with the bacterial pathogen *Pseudomonas syringae*. *Plant Cell* **15**, 317-330.

**Thornberry, N.A., and Lazebnik, Y.** (1998). Caspases: Enemies within. *Science* **281**, 1312-1316.

**Turrens, J.F., and Boveris, A.** (1980). Generation of superoxide anion by the NADH dehydrogenase of bovine heart mitochondria. *Biochem J* **191**, 421-427.

- Turrens, J.F., Alexandre, A., and Lehninger, A.L.** (1985). Ubisemiquinone is the electron donor for superoxide formation by complex III of heart mitochondria. *Arch Biochem Biophys* **237**, 408-414.
- Ulker, B., and Somssich, I.E.** (2004). WRKY transcription factors: from DNA binding towards biological function. *Curr Opin Plant Biol* **7**, 491-498.
- Umezawa, T., Yoshida, R., Maruyama, K., Yamaguchi-Shinozaki, K., and Shinozaki, K.** (2004). SRK2C, a SNF1-related protein kinase 2, improves drought tolerance by controlling stress-responsive gene expression in *Arabidopsis thaliana*. *Proc Natl Acad Sci U S A* **101**, 17306-17311.
- Van Camp, W., Bowler, C., Villarroel, R., Tsang, E.W., Van Montagu, M., and Inze, D.** (1990). Characterization of iron superoxide dismutase cDNAs from plants obtained by genetic complementation in *Escherichia coli*. *Proc Natl Acad Sci U S A* **87**, 9903-9907.
- Vanlerberghe, G.C., and McIntosh, L.** (1996). Signals regulating the expression of the nuclear gene encoding alternative oxidase of plant mitochondria. *Plant Physiol.* **111**, 589-595.
- Vanlerberghe, G.C., Robson, C.A., and Yip, J.Y.** (2002). Induction of mitochondrial alternative oxidase in response to a cell signal pathway down-regulating the cytochrome pathway prevents programmed cell death. *Plant Physiol* **129**, 1829-1842.
- Vedel, F., Lalanne, E., Sabar, M., Chetrit, P., and De Paepe, R.** (1999). The mitochondrial respiratory chain and ATP synthase complexes: Composition, structure and mutational studies. *Plant Physiology and Biochemistry* **37**, 629-643.
- Vercesi, A.E., Martins, I.S., Silva, M.A.P., and Leite, H.M.F.** (1995). PUMPing plants. *Nature* **375**, 24.
- Vranova, E., Inze, D., and Van Breusegem, F.** (2002). Signal transduction during oxidative stress. *J Exp Bot* **53**, 1227-1236.
- Wei, Y.H.** (1992). Mitochondrial Dna Alterations as Ageing-Associated Molecular Events. *Mutation Research* **275**, 145-155.
- Wei, Z.M., Laby, R.J., Zumoff, C.H., Bauer, D.W., He, S.Y., Collmer, A., and Beer, S.V.** (1992). Harpin, elicitor of the hypersensitive response produced by the plant pathogen *Erwinia amylovora*. *Science* **257**, 85-88.
- Wolter, M., Hollricher, K., Salamini, F., and Schulze-Lefert, P.** (1993). The mlo resistance alleles to powdery mildew infection in barley trigger a developmentally controlled defence mimic phenotype. *Mol Gen Genet* **239**, 122-128.
- Xie, Z.X., and Chen, Z.X.** (2000). Harpin-induced hypersensitive cell death is associated with altered mitochondrial functions in tobacco cells. *Molecular Plant-Microbe Interactions* **13**, 183-190.
- Yao, N., Tada, Y., Sakamoto, M., Nakayashiki, H., Park, P., Tosa, Y., and Mayama, S.** (2002). Mitochondrial oxidative burst involved in apoptotic response in oats. *Plant J* **30**, 567-579.
- Zeidler, D., Zähringer, U., Gerber, I., Dubery, I., Hartung, T., Bors, W., Hutzler, P., and Durner, J.** (2004). Innate immunity in *Arabidopsis thaliana*: Lipopolysaccharides activate nitric oxide synthase (NOS) and induce defense genes. *Proc Natl Acad Sci U S A* **101**, 15811-15816.
- Zhang, S., and Klessig, D.F.** (2001). MAPK cascades in plant defense signaling. *Trends Plant Sci* **6**, 520-527.
- Zhong, G.V., and Burns, J.K.** (2003). Profiling ethylene-regulated gene expression in *Arabidopsis thaliana* by microarray analysis. *Plant Mol Biol* **53**, 117-131.
- Zimmermann, I.M., Heim, M.A., Weisshaar, B., and Uhrig, J.F.** (2004). Comprehensive identification of *Arabidopsis thaliana* MYB transcription factors interacting with R/B-like BHLH proteins. *Plant J* **40**, 22-34.
- Zipfel, C., Robatzek, S., Navarro, L., Oakeley, E.J., Jones, J.D., Felix, G., and Boller, T.** (2004). Bacterial disease resistance in *Arabidopsis* through flagellin perception. *Nature* **428**, 764-767.

## Acknowledgements

There is one person above all others, who deserves my deepest thanks and respect for his continued support and patience during the period of this work: my husband, Igor Livaja.

There are many other people who contributed to this dissertation in many ways.

First, I would like to thank my supervisor and mentor PD Dr. Jörg Durner for the guidance and support that he provided over the past three years. I thank him for the possibility to realize my ideas and for the confidence.

My thanks go to all colleagues of the Institute of Biochemical Plant Pathology for their help in one or other way, especially to Elke Mattes, Claudia Knappe, Evi Bieber, Lucia Gößl, Marion Wenig and Renate Kreitmeyer.

I also want to thank some colleagues of the Institute of Pathology at the GSF. To Dr. Peter Hutzler, Dr. Axel Walch, Luise Jennen and Helga Wehnes, thanks for your kind cooperation.

I would like to acknowledge Dr. Ralph Panstruga from MPI Köln for critical reading of the mlo-part of this work.

I wish to thank Professor Heinrich Sandermann as director of the institute for giving me the possibility to make my PhD at BIOP.

Professor Gerhard Wenzel and Professor Siegfried Scherer, thanks for kindly examining this thesis.

I thank the "Deutsche Forschungsgemeinschaft" for financial support.

Last, but far from least, I would like to thank my family for emotional support.

## Lebenslauf

**Name** Maren Livaja, geb. Krause  
**Geburtsdatum** 10.04.1972  
**Geburtsort** Magdeburg

## Bildungsweg

1978-1988 Besuch und Abschluss der zehnklassigen Polytechnische Oberschule in Magdeburg

1988-1990 Unterricht am Institut zur Vorbereitung auf das Auslandsstudium an der Martin-Luther-Universität Halle-Wittenberg  
 Abschluss: Abitur

1990-1991 Studentin an der Fakultät für Biologie, Kliment Ochidsky Universität Sofia, Bulgarien

1992-1997 Studium der Bioverfahrenstechnik an der Fakultät für Maschinenwesen der Technischen Universität Dresden

1997-1998 Diplomarbeit bei ratiopharm-Merkle, Ulm

1998 Abschluss: Diplom-Ingenieurin für Bioverfahrenstechnik (TU)

1999-2002 Angestellte in den Abteilungen Genome Sequencing und Research & Development bei der MWG Biotech AG, Ebersberg

2002 bis heute Doktorandin am Institut für Biochemische Pflanzenpathologie, GSF Forschungszentrum für Umwelt und Gesundheit, Neuherberg